

# **The role of Sirt7 and Sirt1 in adipocyte differentiation and maintenance of metabolic homeostasis**

Inaugralsdissertation  
zur Erlangung des Grades eines Doktors der Medizin (Humanbiologie)  
des Fachbereichs Medizin  
der Justus-Liebig-Universität Giessen

vorgelegt von  
**Jian Fang**  
aus Zhenjiang, China  
Gießen (2013)

Gutachter: **Prof. Dr. Dr. Thomas Braun**

Gutachter: **Prof. Dr. Andreas Schäffler**

Tag der Disputation: **30. März 2015**

# Table of Contents

Table of Contents .....	III
-------------------------	-----

## 1. Introduction.....1

### 1.1 Introduction of the sirtuin family.....1

1.1.1 Discovery of sirtuins and determination of their enzymatic activity.....1

1.1.2 Sirtuins and ageing in non-mammalian species.....2

1.1.3 The mammalian sirtuin family.....3

1.1.4 Functional studies of mammalian nuclear sirtuins.....5

### 1.2 Physiological metabolic adaptation and the roles of sirtuins in liver.....9

1.2.1 Overview of liver function in metabolic adaptation.....9

1.2.2 Ribosome biogenesis and its role in liver.....12

1.2.3 Nuclear sirtuins and liver metabolism.....14

### 1.3 Molecular basis of adipocyte differentiation (adipogenesis) .....16

1.3.1 Adipose tissue and its function.....16

1.3.2 Development of obesity and adipogenesis.....17

1.3.3 Adipocyte development.....17

1.3.4 Transcription factors in adipogenesis.....18

1.3.5 The role of sirtuin proteins in adipogenesis.....20

## 2. Materials and Methods.....23

### 2.1 Materials.....23

2.1.1 Antibodies.....23

2.1.2 Primers.....24

2.1.3 DNA probes for Northern blot and Southern blot.....27

2.1.4 Plasmid vectors.....28

2.1.5 Bacterial strains.....29

2.1.6 Cell lines.....	29
2.1.7 Media for cell culture.....	30
2.1.8 Mouse strains.....	30
2.1.9 Special materials and chemicals.....	30
2.1.10 Standard buffers and solutions.....	31
2.1.11 Enzymes.....	34
2.1.12 Kits.....	34
2.1.13 Equipments.....	34
2.1.14 Software.....	35
<b>2.2 Methods.....</b>	<b>35</b>
2.2.1 Sterilization of materials and solutions.....	35
2.2.2 Cloning and constructs.....	36
2.2.3 Cell culture and transfection.....	36
2.2.3.1 Isolation of primary cells.....	36
2.2.3.2 Transient plasmid DNA transfection in HEK cells.....	37
2.2.3.3 Retrovirus production and infection.....	38
2.2.3.4 Lentiviral shRNA transduction.....	38
2.2.3.5 Adipogenesis assay and Oil red O staining.....	38
2.2.4 RNA analysis.....	39
2.2.4.1 RNA extraction.....	39
2.2.4.2 Northern blot.....	39
2.2.4.3 Reverse transcription.....	40
2.2.4.4 Polymerase chain reaction (PCR) .....	40
2.2.4.5 Quantitative real time PCR (QPCR).....	41
2.2.5 DNA and chromatin analysis.....	42
2.2.5.1 Genomic DNA extraction.....	42
2.2.5.2 Southern blot.....	42
2.2.5.3 Chromatin immunoprecipitation.....	42

2.2.6 Protein analysis.....	44
2.2.6.1 Total protein extraction.....	44
2.2.6.2 Quantification of protein concentration.....	44
2.2.6.3 SDS-PAGE and Western blot.....	44
2.2.6.4 Immunoprecipitation assay.....	45
2.2.6.5 Immunofluorescence.....	45
2.2.7 Mice experiments.....	46
2.2.7.1 Mice housing and care.....	46
2.2.7.2 Killing of the laboratory mice.....	46
<b>3. Results.....</b>	<b>47</b>
3.1 Sirt7 is required for the stimulation of hepatic rDNA transcription in response to insulin.....	47
3.1.1 Disturbed hepatic response to Fasting/Refeeding in Sirt7 KO mice.....	47
3.1.2 Higher Sirt1 expression in the liver of Sirt7 deficient mice during fasting .....	49
3.1.3 Transcription levels of pre-rRNA do not change in WT and Sirt7KO hepatocytes cultured in different glucose concentration.....	50
3.1.4 Insulin stimulates pre-rRNA transcription in WT hepatocytes, but not in the Sirt7 KO hepatocytes.....	51
3.1.5 Hypoacetylation of histones and lower PolI and UBF binding to rDNA promoter after insulin stimulation in Sirt7 deficient hepatocytes.....	52
3.2 Sirt7 is necessary for an efficient adipocyte differentiation and WAT homeostasis through repression of Sirt1, a negative regulator of PPAR $\gamma$ .....	54
3.2.1 Sirt7 is necessary for efficient adipocytes differentiation in culture.....	54
3.2.2 Sirt7 is required for PPAR $\gamma$ expression in adipogenesis.....	59

3.2.3 PPAR $\gamma$ overexpression but not Sirt7 overexpression can completely rescue the impaired adipogenesis in Sirt7 KO immortalized MEFs.....	60
3.2.4 Sirt1 expression is increased in Sirt7 deficient MEFs during adipogenesis especially at protein level.....	62
3.2.5 Sirt7 inhibits Sirt1 protein level and blocks the recruitment of Sirt1 to the PPAR $\gamma$ promoter during adipogenesis.....	64
3.2.6 Adipogenesis defects in Sirt7 deficient MEFs can be partly restored by Sirt1 knock down or Sirt1 inhibition buy NAM.....	65
3.2.7 Removal of one Sirt1 allele rescued the highly compromised adipogenic potential of Sirt7 <sup>-/-</sup> primary white preadipocytes and the abnormality of WAT in adult Sirt7 deficient mice.....	66
<b>3.3 Sirt7 can inhibit Sirt1 activity by interfering with its auto-deacetylation.....</b>	<b>69</b>
3.3.1 Sirt7 does not deacetylate Sirt1 but increases the acetylation of Sirt1.....	69
3.3.2 Sirt1 has an auto-deacetylase activity <i>in vivo</i> and <i>in vitro</i> .....	71
3.3.3 The acetyltransferase MOF acetylates and decreases the activity of Sirt1.....	72
3.3.4 A combination of acetylation and deacetylation at specific lysine residues is responsible for Sirt1 activation.....	74
<b>3.4 Generation and initial characterization of Sirt1 conditional KO mice and Sirt1/Sirt7 double knock-out mice.....</b>	<b>76</b>
3.4.1 Constructing of targeting vectors for conditional Sirt1 knockouts.....	76
3.4.2 Production of targeted ES cell clones and chimera formation.....	79
3.4.3 Generation and genotypic verification of Sirt1 conditional KO mice.....	81
3.4.4 Confirmation of embryonic lethality of Sirt1 deficiency by Sirt1 CMVKO mice.....	83
<b>4. Discussion.....</b>	<b>86</b>

4.1	The role of Sirt7 in the fasting/refeeding adaptation of liver.....	86
4.2	Sirt7 is necessary for induction of hepatic ribosomal RNA transcription by insulin.....	89
4.3	Sirt7 is required for the PPAR $\gamma$ -mediated adipogenesis through repression of Sirt1.....	92
4.4	Sirt7 regulates Sirt1 activity by interfering with its auto-deacetylation.....	100
<b>5.</b>	<b>Summary.....</b>	<b>106</b>
<b>6.</b>	<b>Zusammenfassung.....</b>	<b>107</b>
<b>7.</b>	<b>List of abbreviations.....</b>	<b>109</b>
<b>8.</b>	<b>List of figures and tables.....</b>	<b>114</b>
<b>9.</b>	<b>References.....</b>	<b>117</b>
<b>10.</b>	<b>Erklärung zur Dissertation.....</b>	<b>143</b>
<b>11.</b>	<b>Acknowledgements.....</b>	<b>144</b>
<b>12.</b>	<b>Curriculum Vitae.....</b>	<b>146</b>

# 1. Introduction

## 1.1 Introduction of the Sirtuin family

### 1.1.1 Discovery of sirtuins and determination of their enzymatic activity

Sirt7 and Sirt1 belong to a conserved family of proteins known as sirtuin and are found in all living species. Sirtuins: Sir-two-ns, derives from the name of yeast Sir2 (silent information regulator 2). It was originally isolated in a screen for silencing factors in the yeast (Rine et al., 1979). The yeast Sir2 was then characterized as an important regulator of silencing at repeated rDNA (Gottlieb and Esposito, 1989), telomeres (Aparicio et al., 1991) and at mating-type loci (Braunstein et al., 1993). Subsequently, Sir2 homologues were found in bacteria, worms, flies, plants and mammals, suggesting that the sirtuin family genes are ancient and evolutionarily conserved.

The insight into the enzyme activity of sirtuins came from the discovery that the gene silencing at mating-type loci and telomeres in yeast, is associated with hypo-acetylated histone proteins at the N-terminal lysine residues (Braunstein et al., 1993). After the initial observation that CobB, an *Escherichia coli* homolog of Sir2, could catalyze the phosphoribosyltransferase reaction in cobalamin biosynthesis (Tsang and Escalante-Semerena, 1998), researchers postulated that Sir2 possessed NAD<sup>+</sup>-dependent ADP-ribosyltransferase activity, and the ADP-ribosylation of histones by Sir2 interferes with histone acetylation, leading to hypo-acetylation in histones. However, soon it was shown that Sir2 deacetylated histones and this activity was absolutely dependent on NAD<sup>+</sup> (Imai et al., 2000; Landry et al., 2000). Later other sirtuins, including bacterial CobB, archeobacterial Sir2-AF (*Archaeoglobus fulgidus*) and human Sirt1-3 and 5 were found also to have NAD<sup>+</sup> dependent deacetylase activity *in vitro* (Smith et al., 2000). The schematic representation of sirtuins enzymatic activity as shown in figure 1.1

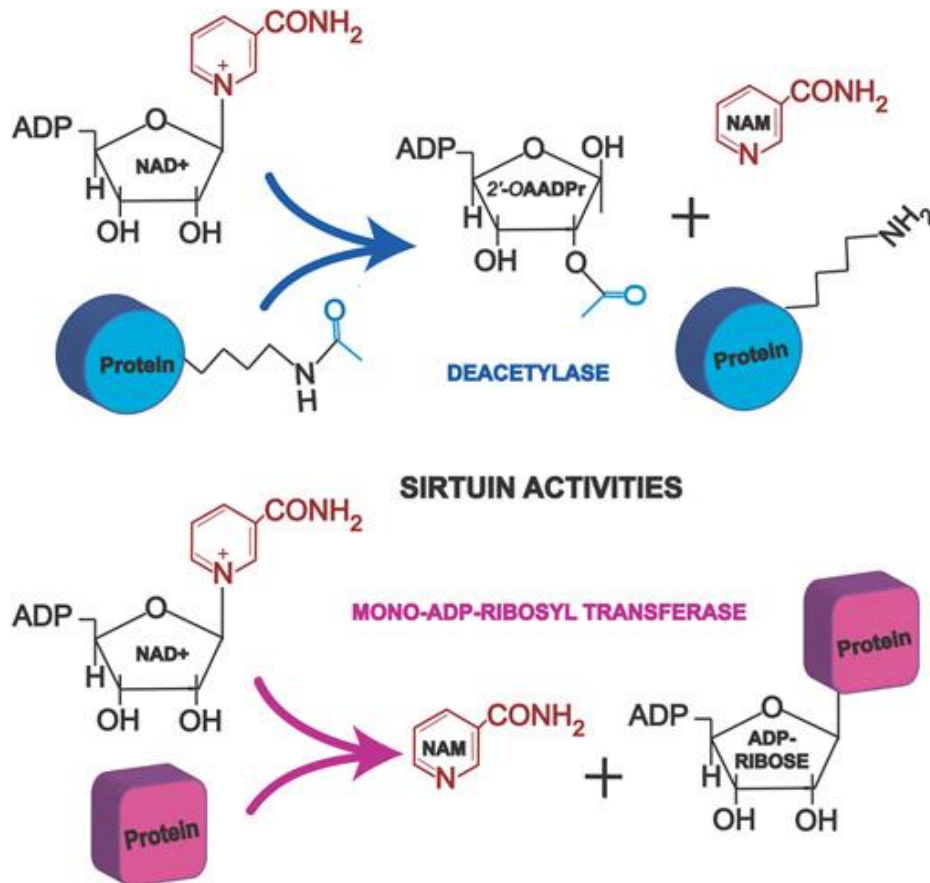


**Fig 1.1 Sirtuin enzymatic activities**

Sirtuins are  $\text{NAD}^+$ -dependent deacetylases and mono-ADP-ribosyl transferases. As deacetylases, they remove acetyl groups from proteins in the presence of  $\text{NAD}^+$ . The acetyl group is transferred to the ADP-ribose part of  $\text{NAD}^+$  to form O-acetyl-ADP-ribose (2-OAADPr) and Nicotinamide (NAM). As Mono-ADP-ribosyl transferases, they remove the mono-ADP-ribose from  $\text{NAD}^+$  and attach it to protein, also releasing NAM as a reaction product.

(Michan and Sinclair. 2007)

### 1.1.2 Sirtuins and ageing in non-mammalian species

A number of studies have suggested the role of sirtuins in aging in non-mammalian organisms. More than 14 years ago, the exponential accumulation of ERCs (extrachromosomal rDNA circles) was discovered as one of the major causes of ageing in *S. cerevisiae* (Sinclair and Guarente, 1997). ERCs are copied along with the mother cell's chromosomes prior to cell division but remain in the mother cell's nucleus afterward. Thus, a mother cell accumulates an ever increasing number of circles that eventually prevent further cell division, possibly because copying the ERCs consumes so many resources that the mother cell can no longer manage to replicate her own

genome. However, when an extra copy of the *Sir2* gene was added into yeast cells, ERCs formation was repressed and the cell's lifespan was extended by 30% (Kaeberlein et al., 1999). That finding indicated that Sir2 could act as a longevity gene in yeast, and amazingly, it was soon discovered that extra copies of the Sir2 gene also increased the lifespan of roundworms up to 50% (Tissenbaum and Guarente, 2001). Subsequently, it was found that an extra copy of the *Sir2* gene (*dSir2*) expressed ubiquitously in *Drosophila melanogaster* causes females and males to live longer (Rogina and Helfand, 2004). But, the in-depth research work by Burnett and colleagues challenged the previous publications. The new data showed that Sir2 overexpression had no effects on lifespan in worm and fruitfly (Burnett et al., 2011). These conflicting results may have been due to confounding factors in experimental design and the differences in genetic backgrounds of the organism used in the individual studies. Even without life span extension effect, Sir2 overexpression made worms more resistant to toxic protein accumulation (Burnett et al., 2011). It could be that sirtuins play their main roles in physiological homeostasis and stress responses rather than in direct lifespan regulation.

### 1.1.3 The mammalian sirtuin family

The mammalian sirtuin family consists of seven sirtuins, Sirt1-7. All of them share a highly conserved NAD<sup>+</sup>-dependent catalytic core domain, which may act preferentially as a NAD<sup>+</sup>-dependent deacetylase (DAC) and/or mono-ADP-ribosyl transferase (ART). The flanking N- and C-terminal sequences are specific for each sirtuin (Frye, 2000), and may be responsible for their variation in binding partners and subcellular localization (Haigis and Sinclair, 2010) (Figure 1.2). Three mammalian sirtuins Sirt1, Sirt6 and Sirt7 are mainly nuclear proteins, however, Sirt1 has been found to shuttle between the nucleus and the cytoplasm in various tissues (Tanno et al., 2007). In the nucleus, Sirt1 mainly associates with euchromatin, whereas Sirt6 binds to the heterochromatin and Sirt7 localizes into the nucleolus (Ford et al., 2006; Michishita et al., 2005). Sirt2 predominately resides in the cytoplasm (Frye, 1999; North et al., 2003), while Sirt3, Sirt4 and Sirt5 are mostly found in mitochondria (Michishita, Park et al. 2005).

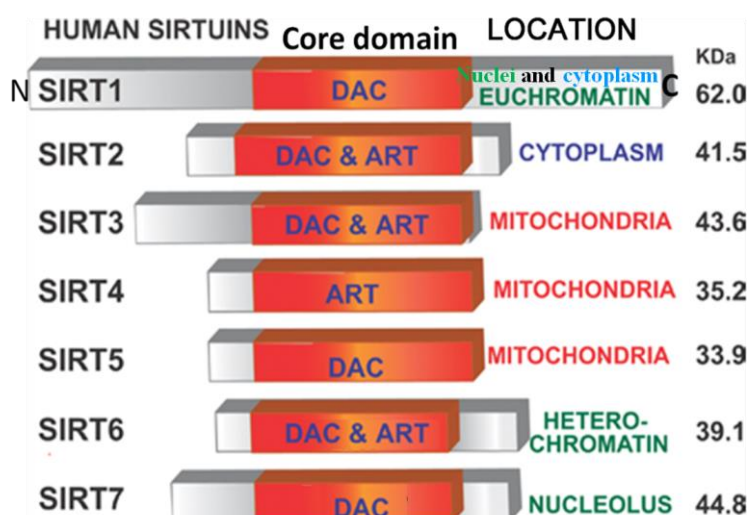


**Fig 1.2 Schematic representation of seven mammalian sirtuins**

The catalytic core domain (red) is conserved between all the seven mammalian sirtuins. The N and C-terminal flanking sequences vary in length. The seven sirtuins also show different sub-cellular localization. DAC, deacetylase; ART, mono-ADP-ribosyl transferase.

(Michan and Sinclair, 2007)

Mammalian sirtuins differ also in their enzymatic activity, Sirt1 exhibits robust deacetylase activity (Vaziri et al., 2001) and Sirt5 has weak deacetylation effect (Nakagawa and Guarente, 2009). Recently, a novel report showed that Sirt5 is an efficient protein lysine desuccinylase and demalonylase *in vitro* (Du et al., 2011). Sirt2, Sirt3 and Sirt6 possess both deacetylase and mono-ADP-ribosyl transferase activities (Frye, 1999; Liszt et al., 2005; North et al., 2003; Shi et al., 2005; Yang et al., 2009). The only reported activity so far of Sirt4 is mono-ADP-ribosyl transferase (Haigis et al., 2006). The least investigated member, Sirt7, had generally been considered to have weak or undetectable deacetylase activity (Voelter-Mahlknecht et al., 2006). However, experiments from our laboratory demonstrated that Sirt7 can deacetylate p53 *in vitro*, which corresponds to hyperacetylation of p53 in the myocardium of Sirt7 deficient mice (Vakhrusheva et al., 2008b). Recently, it was showed that Sirt7 specifically deacetylated lysine 18 in histone H3 (H3K18Ac), and displayed no activity on other lysine sites in histones (Barber et al., 2012). Like their diverse sub-cellular localization, the mammalian sirtuins are differently expressed in organs, and have different protein targets. Generally, sirtuins play critical roles in essential physiological or pathological processes.

#### 1.1.4 Functional studies of mammalian nuclear sirtuins

##### **Sirt1**

Sirt1 is the best characterized sirtuin family member in terms of its function and activity (Fig 1.3). Similar to yeast SIR2, mammalian Sirt1 was shown to be able to deacetylate histones *in vitro* at lysine residues 9 and 26 of histone H1, 9 and 14 of H3 and 16 of H4 (Imai et al., 2000; Vaquero et al., 2004). The hypoacetylation of histones facilitates heterochromatin formation and gene repression. Furthermore, Sirt1 directly binds to the histone methyltransferase Suv39h1 and enhances its methyltransferase activity on H3K9 by deacetylating lysine residue 266 in the SET domain of Suv39h1 (Vaquero et al., 2007). Several studies have indicated that Sirt1 acts as a stress sensor and mediates the cellular survival in response to various stresses, such as inflammation, hypoxic stress, heat shock and genotoxic stress (reviewed by Nakagawa and Guarente, 2011). Sirt1 improves stress resistance by deacetylating and modulating the activity of critical stress effectors such as NF- $\kappa$ B (Yeung et al., 2004), HIF1 $\alpha$  (Lim et al., 2010), HIF2 $\alpha$  (Dioum et al., 2009), HSF1 (Westerheide et al., 2009), Ku70 (Jeong et al., 2007), PARP1 (Rajamohan et al., 2009) and so on, which are thought to be the important causes of aging and aging related diseases. Furthermore, a dual role of Sirt1 in carcinogenesis was revealed. Sirt1 seems to work as both oncogenic factor and tumor suppressor (Bosch-Presegue and Vaquero, 2011). The potential tumor suppressor effect of Sirt1 is supported by its role in maintaining genome stability through the regulation of chromatin structure and improvement of DNA damage repair (Bosch-Presegue and Vaquero, 2011). Alternatively, several studies supported the roles of Sirt1 in tumor initiation and progression, which included the effects of Sirt1 on inhibition of senescence and apoptosis (mostly via deacetylation and inactivation of some tumor suppressors such as p53 (Luo et al., 2001), FOXO family (Brunet et al., 2004), E2F1 (Wang et al., 2006), Rb (Wong and Weber, 2007) and others), promotion of cellular growth and also angiogenesis (Liu et al., 2009).

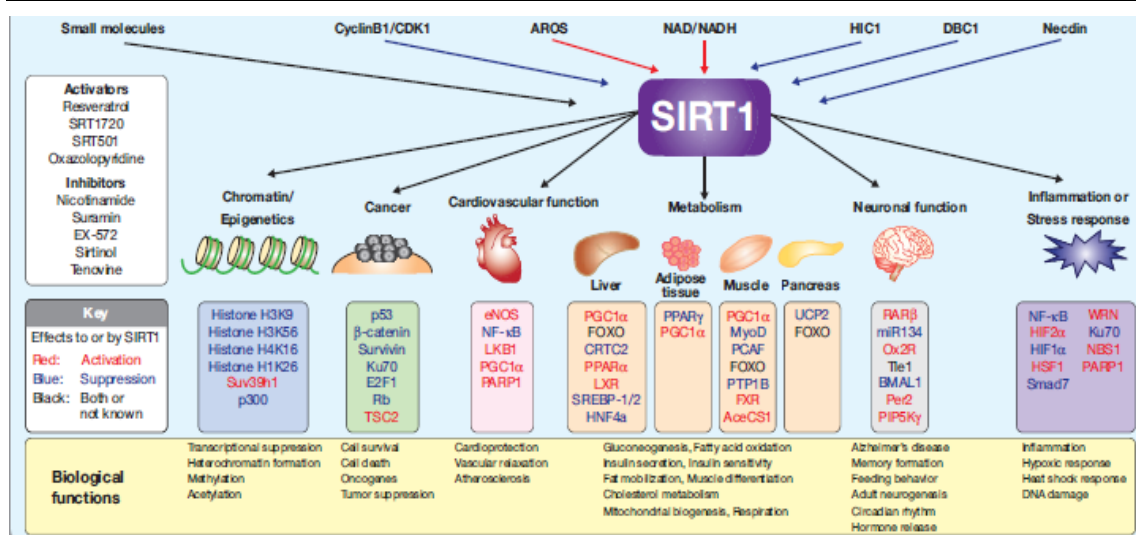


**Fig 1.3 Substrates and biological functions of Sirt1**

Adapted from (Nakagawa and Guarente, 2011)

Sirt1 has also been shown to regulate various aspects of metabolism such as glucose homeostasis (Rodgers et al., 2005), insulin secretion (Moynihan et al., 2005) and sensitivity (Bordone et al., 2006) and lipid metabolism (Kemper et al., 2009; Li et al., 2007; You et al., 2008) in different tissues. *See below.*

## Sirt6

MEFs and embryonic stem cells (ESCs) which carry Sirt6 deletion show genomic instability and impairment in base-excision repair (Mostoslavsky et al., 2006). Sirt6 forms a macromolecular complex with DNA double-strand break repair factor DNA-PK (DNA-dependent protein kinase) and stabilizes its catalytic subunit to chromatin in response to DNA damage, thereby promoting DNA DSB repair (McCord et al., 2009). Sirt6 also promotes DNA end resection through C-terminal binding protein interacting protein (CtIP) deacetylation (Kaidi et al., 2010). Furthermore, Sirt6 can associate with telomeric chromatin and Sirt6 depletion leads to telomere dysfunction with end-to-end chromosomal fusions and premature cellular senescence (Michishita et al., 2008). The critical role of Sirt6 in maintaining the genome integrity and promoting DNA repair suggests that Sirt6 may act as a tumor suppressor and prevent cancer formation.

Moreover, a pivotal role of Sirt6 in the maintenance of glucose homeostasis by inhibiting HIF1α (Zhong et al., 2010) and through the suppression of insulin signaling

and AKT activation (Xiao et al., 2010) has been demonstrated. A recent report demonstrated a role for Sirt6 in modulating the tumor metabolism: Sirt6 blocks cancer cell aerobic glycolysis (Warburg effect) and inhibits ribosome biogenesis by repressing the transcriptional activity of c-MYC, thereby preventing tumor progression (Sebastian et al., 2012).

In addition to its role in genomic stability and regulation of metabolism, Sirt6 was also shown to be involved in inflammatory processes. Sirt6 interacts with the RelA subunit of NF- $\kappa$ B and deacetylates histone H3K9 at NF- $\kappa$ B target gene promoters to attenuate NF- $\kappa$ B signaling (Kawahara et al., 2009). Thus, the hyperactive NF- $\kappa$ B signaling in Sirt6 deficient cells may contribute to premature and normal aging. Sirt6 also regulates the production of tumor necrosis factor (TNF $\alpha$ ) by acting at a post-transcriptional step in response to intracellular NAD<sup>+</sup> concentrations (Van Gool et al., 2009). It reveals the possible function of Sirt6 in the connection between metabolism and the inflammatory response.

### **Sirt7**

As the least studied mammalian sirtuin, Sirt7 has been shown to associate with rDNA and activate RNA polymerase I-dependent transcription in the nucleolus (Ford et al., 2006). Sirt7 may regulate cell growth and metabolism in response to nutritional and other signals by driving ribosome biogenesis in dividing cells. However, controversial findings were made on the possible influence on cell proliferation by Sirt7. An anti-proliferative role of Sirt7 was found in Sirt7 overexpressing cells while Sirt7 knockout cells showed higher proliferation rates; in addition, Sirt7 expression level was decreased in several murine tumorigenic cell lines (Vakhrusheva et al., 2008a; Vakhrusheva et al., 2008b). Other reports suggested that Sirt7 may act as a principle activator of proliferation. Sirt7 is abundant in highly proliferative tissues but not in lowly proliferative tissues (Michishita et al., 2005). Sirt7 was found to be up-regulated in several tumors or tumor-derived cells such as thyroid carcinoma cells (Frye R, 2002), breast cancer cells (Ashraf et al., 2006) and hepatocellular carcinoma cells (Kim et al., 2012). A recent report demonstrated that Sirt7 can promote the cancer cell proliferation

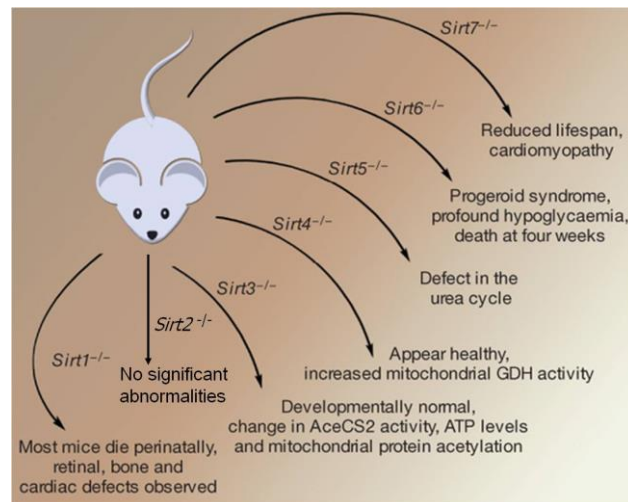
and transformation through the selective transcriptional repression of some tumor repression genes by deacetylating H3K18Ac on their promoters (Barber et al., 2012). In vivo studies using the Sirt7 knockout mice demonstrated a decreased life-span, a higher stress susceptibility and development of inflammatory cardiomyopathy with age in Sirt7 deficient mice (Vakhrusheva et al., 2008b) .

Taken together, mammalian sirtuins target multiple substrates including histones and non-histone proteins, thereby affecting a broad range of cellular functions. They are apparently connected to an ever widening circle of activities that encompass cellular stress resistance, genomic stability, tumorigenesis and energy metabolism. However, the exact biological functions of individual sirtuins still remain only partially characterized. Knockout mice are important animal models for studying new genes functions. So far, specific knockout mice for all sirtuin members have been created (Fig. 1.4). The phenotypes of these knockout mice include a reduction of their lifespan, ranging from survival of days (Sirt1) to weeks (Sirt6) or months (Sirt7) (Finkel et al., 2009). In contrast, no significant abnormalities were observed in Sirt2 KO mice (Bobrowska et al., 2012). Although Sirt3<sup>-/-</sup>, Sirt4<sup>-/-</sup> and Sirt5<sup>-/-</sup> mice appeared outwardly normal, some biochemical phenotypes have been reported (Haigis et al., 2006; Lombard et al., 2007; Nakagawa et al., 2009). In addition, the extensive efforts for screening and identification of sirtuin-modulating small molecules raised hopes for development of sirtuin targeted drugs which could have therapeutic benefits on metabolic and age-related diseases. The first Sir2-activating molecule, resveratrol, a polyphenolic compound produced by plants was identified in 2003 (Howitz et al., 2003). Since then further compounds have been discovered to activate sirtuins *in vitro*, collectively called the sirtuin activating compounds (STACs) (Milne et al., 2007). On the other hand nicotinamide (NAM), as a by-product in both sirtuin enzymatic reactions, can bind to the sirtuin/intermediate complex to promote the reverse reaction and thus inhibit the catalyzed reaction (Sauve, 2010). NAM was demonstrated to act as a noncompetitive inhibitor of sirtuins in yeast, flies and mammalian cells (Anderson et al., 2003; Sauve, 2010), Subsequently, various other sirtuin inhibitors have been discovered, including splitomicin, sirtinol, AGK2, tenovin, suramin, cambino, and Ex527 (Alcain and Villalba,

2009; Napper et al., 2005).

### Fig 1.4 Mouse knockout models as tools for exploring sirtuin function

Adapted from (Finkel et al., 2009), with modifications.



## 1.2 Physiological metabolic adaptation and the roles of sirtuins in liver

### 1.2.1 Overview of liver function in metabolic adaptation

The liver is the largest internal organ (the skin being the largest organ overall) and the largest gland in the body. Residing at the crossroads between the digestive tract and the rest of the body, the liver has a wide range of functions, the most important being the breakdown of food and its conversion into energy. Liver plays an essential role in the maintenance of the whole body's metabolic homeostasis by regulating carbohydrate, fatty acid, amino acid and cholesterol metabolism in fed and fasting conditions (Zakim and Boyer, 2003).

In fed conditions, food intake leads to an increase of blood glucose concentration (glucose is quickly absorbed from the intestine and transported via blood), which is a potent stimulus for the release of insulin from the pancreas. Insulin then binds to its receptor (a member of the tyrosine kinase receptor family) and activates the insulin signaling cascade. The hepatic action of insulin has three major targets: a) to activate glucose storage as glycogen and to shutdown glucose production and output (Bollen et al., 1998), b) to promote lipogenesis in the fed state, and c) to block all catabolic actions (Fig.1.5).

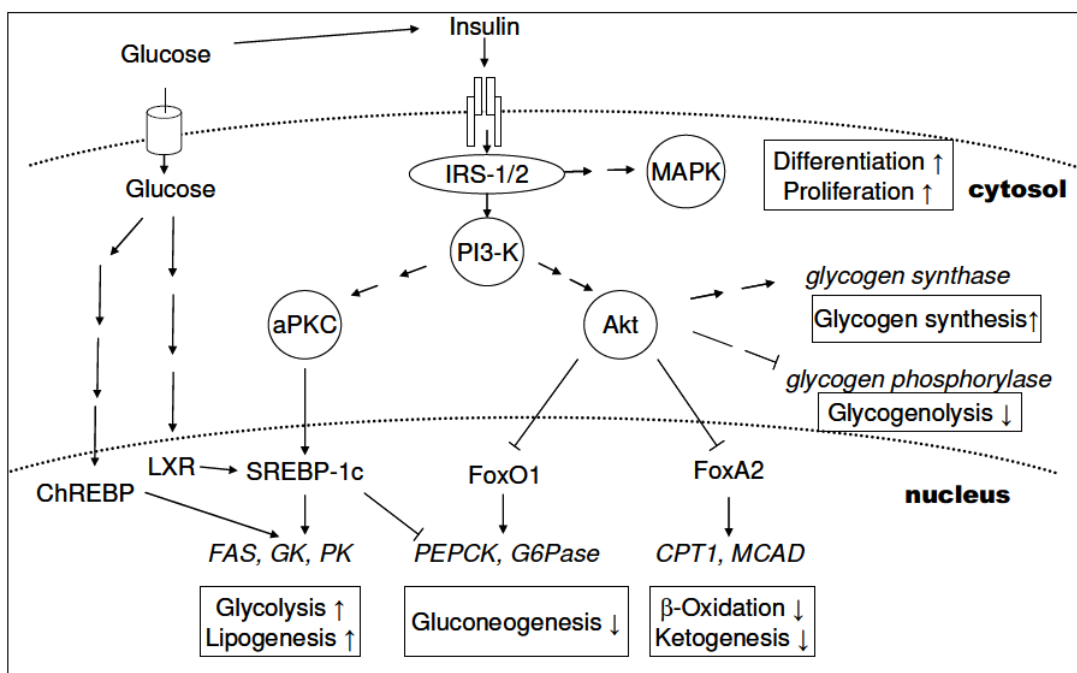


**Fig 1.5 Scheme of hepatic signaling in fed state activating anabolic pathways in the liver.** aPKC, atypical protein kinase C; ChREBP, carbohydrate response element binding protein; CPT1, carnitine palmitoyltransferase 1; FAS, fatty acid synthase; FoxO1/FoxA2, forkhead box protein O1/A2; G6Pase, glucose-6-phosphatase; GK, glucokinase; IRS, insulin receptor substrate; LXR, liver X receptor; MAPK, mitogen-activated protein kinase; MCAD, medium-chain acyl-CoA dehydrogenase; PEPCK, phosphoenolpyruvate carboxykinase; PI3-K, phosphoinositide-3 kinase; PK, pyruvate kinase; SREBP-1c, sterol regulatory element binding protein 1c. (Fritsche et al., 2008)

In fasting conditions, glucose production in the liver is responsible for maintaining the blood glucose concentration within normal range and supplying glucose to the central nervous system. During starvation the liver has the ability to provide glucose from two sources: glycogenolysis and synthesis of glucose using noncarbohydrate precursors such as lactate, glucogenic amino acids and glycerol (gluconeogenesis). Glycogenolysis occurs in the post absorptive state, 2 – 6 hours after ingestion of a meal (Suh et al., 2007) and is sufficient for short term fasting. However, gluconeogenesis, is more important during prolonged periods of fasting (18 – 24 hours) (Klover and Mooney, 2004) and it accounts for up to 90% of endogenous glucose production after 40 hours of fasting (Boden, 2004; Chandramouli et al., 1997). Both glucose production and the suppression of glycogen synthesis are regulated by glucagon, which is also secreted by the pancreas (Fig 1.6).

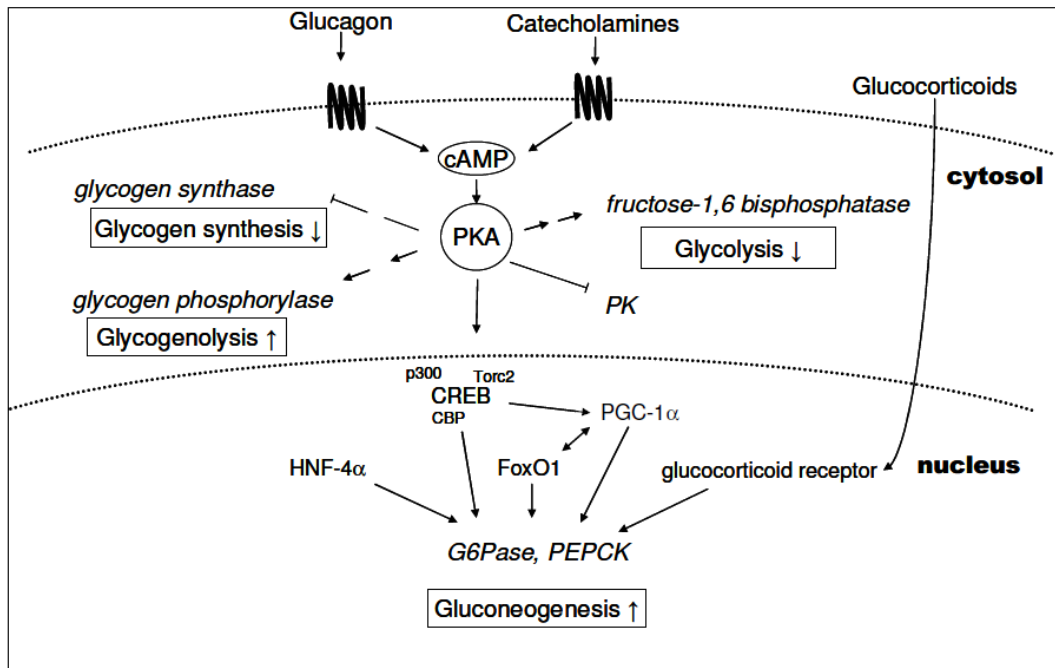


**Fig 1.6 Scheme of hepatic signalling events during fasting resulting in an increased glucose output from the liver.** cAMP, cyclic adenosine monophosphate; CBP, CREB binding protein; CREB, cAMP response element binding protein; FoxO1, forkhead box protein O1; G6Pase, glucose-6-phosphatase; HNF-4 $\alpha$ , hepatocyte nuclear factor 4 $\alpha$ ; PEPCK, phosphoenolpyruvate carboxykinase; PGC-1 $\alpha$ , peroxisome-proliferator-activated receptor- $\gamma$  co-activator 1 $\alpha$ ; PK, pyruvate kinase; PKA, protein kinase A; Torc2, transducer of regulated CREB activity 2. (Fritsche et al., 2008)

In summary, the liver is under tight control of insulin and its catabolic counterpart glucagon to maintain carbohydrate and lipid metabolic homeostasis. The regulation of the gene transcription and activity of key enzymes in the postabsorptive state and during fasting involves the same key players such as the PI-3 kinase-Akt/PKB pathway, PGC-1 $\alpha$ , HNF-4 $\alpha$ , and transcription factors of the forkhead box protein and SREBP family (Fritsche et al., 2008). They are regulated less at their transcription levels but mostly by post-translation modifications under the response to hormones, thereby quickly promoting the body's adaptation to energy alteration and maintaining homeostasis (Fritsche et al., 2008).

### 1.2.2 Ribosome biogenesis and its role in liver

Ribosome biogenesis is the process that leads to assembly of ribosomal RNA (rRNA) and ribosomal proteins into the mature 40S and 60S ribosomal subunit. In

eukaryotes, it takes place both in the cell cytoplasm and in the nucleolus of eukaryotic cells. Like most proteins, ribosomal proteins are synthesized in the cytoplasm and imported into the nucleus. 3 rRNAs (18S, 5.8S, 28S) are transcribed by RNA polymerase I while 5.8s rRNA is transcribed by RNA polymerase III in the nucleolus (Lafontaine, 2010; McStay and Grummt, 2008). In mammalian cells, rDNA transcription is a cell-cycle regulated process: transcription is absent during mitosis and gradually increases during G1, peaking in the S and G2 cell-cycle phases (Russell and Zomerdijk, 2005). The phosphorylation status of rDNA transcription factors including SL1 (Heix et al., 1998; Klein and Grummt, 1999; Sirri et al., 1999), UBF (Klein and Grummt, 1999) and TTF1 (Sirri et al., 1999) is mediated by cyclin-dependent kinases and participates in the regulation of rDNA transcription. After transcription, the rRNAs are put together with the ribosomal subunits to generate mature ribosomes in the nucleolus (Boisvert et al., 2007). A ribosome is a cellular component that synthesizes protein chains. While the liver is an important organ for protein synthesis, ribosome biogenesis has a great significance in hepatocyte cellular growth and function.

Ribosome biogenesis is an energy consuming process, so it is critical for the cell to regulate ribosome production tightly depend upon the availability of nutrients and energy sources in the extracellular environment (Rudra and Warner, 2004). Switching off the rRNA synthesis is an effective way of saving energy in an attempt to maintain cellular homeostasis during acute stress (Murayama et al., 2008; Salminen and Kaarniranta, 2009). This is illustrated by regulation of rDNA transcription and ribosome biogenesis in the liver, where starvation leads to decrease in the ribosome production while refeeding stimulates ribosome biogenesis (Conde and Franze-Fernandez, 1980; Hutson and Mortimore, 1982). Ribosome biogenesis in response to nutrient signaling (in particular amino acid) is regulated by the mammalian target of rapamycin (mTOR). After stimulation by nutrient or growth factors, mTOR phosphorylates and activates eukaryotic initiation factor 4E (e-IF4E) and S6 kinase (S6K) to enhance translation (Hay and Sonenberg, 2004). In addition, mTOR also promotes rRNA transcription through phosphorylation of TIF-IA, a subunit of SL19 (Mayer et al., 2004) and UBF

(Hannan et al., 2003). Insulin plays a key role in liver function especially in the regulation of protein synthesis. Cell culture systems have provided evidence that insulin enhances ribosome biogenesis, i.e. by stimulating the transcription of rRNA genes (rDNA) in primary chick embryo fibroblast (DePhilip et al., 1979), undifferentiated mouse myoblasts (Hammond and Bowman, 1988), and primary rat hepatocytes (Antonetti et al., 1993). The mechanism through which insulin causes these alterations was not associated with a change in the cellular content of RNA polymerase I but with the increased nuclear content of upstream binding factor (UBF) and RNA polymerase I-associated factor 53 (PAF53) (Hannan et al., 1998). Both of them are thought to be involved in recruitment of RNA Pol I to the rDNA promoter.

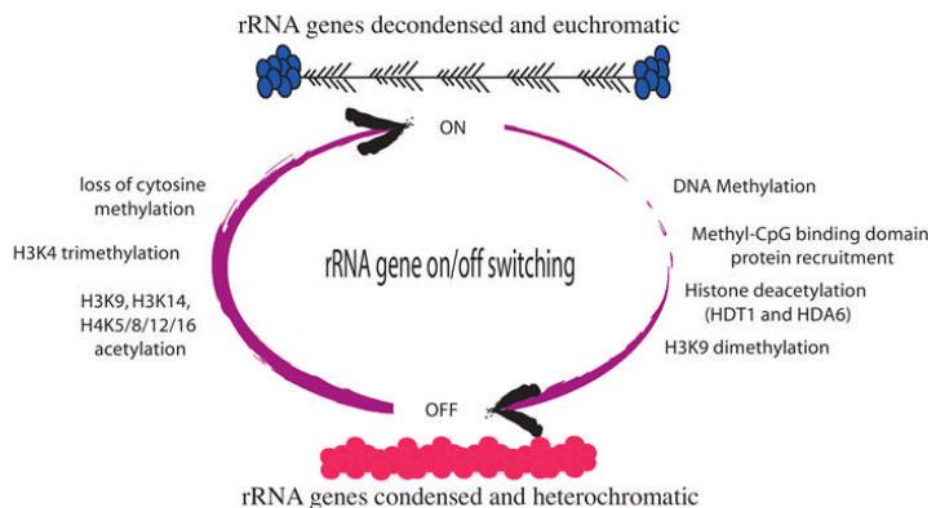


**Figure 1.7 A model for the epigenetic on/off switch regulating nucleolar dominance.** Changes in rRNA gene cytosine methylation, histone deacetylation and histone methylation occur in a concerted fashion. The “off” switch involves cytosine methylation, histone deacetylation, H3K9 dimethylation and condensation of the rRNA genes into heterochromatin. In contrast, the “on” switch involves the loss of cytosine methylation, histone H3 and H4 hyperacetylation, H3K4 trimethylation and decondensation of rRNA genes into euchromatin. Adapted from (Preuss and Pikaard, 2007)

Furthermore, the structure of chromatin is also very important in regulation of Pol I mediated rRNA transcription. The rDNA locus can be either active or silent depending on the epigenetic regulation of the chromatin structure. Epigenetic mechanisms such as DNA methylation and histone modification determine whether the chromatin structure of certain rDNA locus is open or closed for Pol I transactivation

(Grummt, 2007; Grummt and Pikaard, 2003; McStay and Grummt, 2008; Preuss and Pikaard, 2007) (Fig 1.7). The chromatin remodeling complexes such as NoRC (nucleolar remodeling complex) (Grummt and Pikaard, 2003; McStay and Grummt, 2008) and eNoSC (energy-dependent nucleolar silencing complex) (Murayama et al., 2008) interact with histone deacetylases including Sirt1 and methyltransferases, which are potent epigenetic repressors in mammalian rDNA locus and mediate the epigenetic silencing of rRNA gene expression via methylation and deacetylation of histones.

### 1.2.3 Nuclear sirtuins and liver metabolism

All members of mammalian sirtuin family have been found to be expressed in the liver with Sirt3, Sirt5 and Sirt7 showing a high mRNA expression (Dali-Youcef et al., 2007). Although Sirt1 mRNA expression is low, it is an important regulator of liver metabolism. Various reports have shown that Sirt1 regulates gluconeogenesis and glycolysis in the liver during starvation stress. For instance, Sirt1 leads to decreased gluconeogenesis during short-term fasting phase (less than 18 hrs) through its attenuation of TORC2, a key mediator of early phase gluconeogenesis (Liu et al., 2008). Prolonged fasting (24 hrs) promotes Sirt1 to deacetylate and activate PGC-1 $\alpha$ , an essential co-activator for a number of transcription factors, resulting in increased fatty acid oxidation and improved gluconeogenesis (Dominy et al., 2010; Purushotham et al., 2009; Rodgers et al., 2005). Sirt1 also increases the activity of transcriptional factor Foxo1 via deacetylation, resulting in enhanced gluconeogenesis (Rodgers and Puigserver, 2007). In addition, Sirt1 suppresses the inhibitory effect of STAT3 (signal transducer and activator of transcription 3) on gluconeogenesis by deacetylating STAT3 and decreasing its phosphorylation (Nie et al., 2009). So far, several lost of function studies of Sirt1 in knockout mice documented the essential role of Sirt1 also in maintaining hepatic lipid metabolic homeostasis. Specific deletion of the exon 4 which encodes the conserved catalytic domain of Sirt1 in mouse liver, resulted in impaired PPAR $\alpha$  signaling and fatty acid  $\beta$ -oxidation, thereby increasing the susceptibility of mice to high-fat diet induced hepatic steatosis, inflammation and endoplasmic reticulum (ER) stress (Purushotham et al., 2009). Another deletion of hepatic Sirt1 exons 5 and 6

leads to the development of liver steatosis even under normal chow diet due to the increased expression of ChREBP (Wang et al., 2010). Conversely, overexpression of Sirt1 or treatment with specific Sirt1 activators attenuates hepatic steatosis and ameliorates systemic insulin resistance especially after high-fat feeding (Banks et al., 2008; Feige et al., 2008; Li et al., 2011; Pfluger et al., 2008). Sirt1 also regulates hepatic cholesterol and bile acid homeostasis through direct modulation of the liver X receptor (LXR), farnesoid X receptor (FXR), and the sterol regulatory element binding protein (SREBP) family of transcription factors. It was previously shown that Sirt1 can directly deacetylate LXRs, resulting in increased LXR turnover and target gene expression. Systemic loss of Sirt1 in mice results in decreased expression of LXR target genes involved in HDL biogenesis (Li et al., 2007). Recently, Kemper et al. showed that downregulation of hepatic SIRT1 increases the nuclear bile acid receptor FXR acetylation and inhibits its transcription activity, causing liver steatosis and decreased bile output (Kemper et al., 2009). Further studies showed that Sirt1 may also regulate hepatic lipid metabolism through deacetylation of SREBPs (Walker et al., 2010), which promotes the expression of lipogenic and cholesterolgenic genes and facilitates lipid storage (Osborne and Espenshade, 2009). In summary, these findings imply that hepatic Sirt1 plays a critical role in hepatic metabolic regulation and the improved activity of Sirt1 in the liver may be beneficial in treating obesity-associated diseases.

Sirt6, another nuclear sirtuin, also plays an important role in hepatic metabolism. Sirt6 null mice suffer from a severe metabolic imbalance, acute onset of hypoglycemia and premature death at one month of age (Mostoslavsky et al., 2006; Zhong et al., 2010). The hypoglycemia phenotype in Sirt6 knockout mice may be caused by an enhanced glucose uptake, associated with the more abundant GLUT1 and GLUT4 expression in Sirt6 deficient mice and increased insulin signaling and activation of AKT (Xiao et al., 2010). It was reported that Sirt6 functions as a histone H3K9 deacetylase to inhibit the expression of the transcription factor Hif1 $\alpha$  and its multiple glycolytic target genes (Zhong et al., 2010). Thus, Sirt6-deficient cells or mice exhibit high Hif1 $\alpha$  activity and increased glucose uptake with upregulation of glycolysis and diminished mitochondrial respiration, providing another explanation for the

hypoglycemia phenotype of Sirt6 KO mice. Moreover, the liver-specific knock out of Sirt6 mice results in liver steatosis due to increased glycolysis and triglyceride synthesis, and reduced fatty acid oxidation (Kim et al., 2010).

So far, the function of nucleolar Sirt7 in control of the metabolic homeostasis in the liver was not analyzed.

### 1.3 Molecular basis of adipocyte differentiation (adipogenesis)

#### 1.3.1 Adipose tissue and its function

Adipose tissue or fat tissue is a loose connective tissue which is composed mainly of adipocytes and fibroblasts. Generally, two types of adipose tissue can be recognized in mammals: white adipose tissue (WAT) and brown adipose tissue (BAT). WAT is dispersed throughout the body with major intraabdominal depots around the omentum, intestines, and perirenal areas, as well as in subcutaneous depots in the buttocks, thighs, and abdomen (Gesta et al., 2007). 90% of cytoplasm in these adipocytes consists of lipids, mainly triacylglycerol, thus, WAT constitutes a primary site of energy storage. White adipose tissue functions to store energy in form of triacylglycerol. During starvation, this storage can be mobilized for energy utilization. The white adipose tissue can also act as insulator to maintain the body temperature in warm-blooded animals and protect the surrounded organ from injury. Moreover, adipose tissue has in recent years been recognized as a major endocrine organ (Kershaw and Flier, 2004), as it produces certain cytokines called adipokines such as adiponectin, leptin, resistin, TNF $\alpha$  (Rondinone, 2006) and also hormones as for example the sex hormone estrogen (Nelson and Bulun, 2001). Brown adipose tissue is especially abundant in newborns and in hibernating mammals (Gesta et al., 2007). In contrast to white adipocytes, brown adipocytes contain numerous smaller lipid droplets and a much higher number of mitochondria, which contain iron and responsible for the brown coloring (Enerback, 2009). Its primary function is to generate body heat by energy expenditure in animals or newborns (Cannon and Nedergaard, 2004).

#### 1.3.2 Development of obesity and adipogenesis

Obesity is a medical condition in which excess body fat has accumulated to the extent that it has adverse effect on health, leading to reduced life expectancy and/or various diseases such as type 2 diabetes mellitus, coronary heart disease, certain forms of cancer, asthma and osteoarthritis (Kopelman, 2000). There is a marked increase in the incidence of obesity in modern societies, especially in the western countries (Haslam and James, 2005; Woodhouse, 2008).

Obesity develops when energy intake exceeds energy expenditure (Spiegelman and Flier, 2001). Growth in adipose tissue and long-term changes in fat storage is the result of both hypertrophy (increase in size) and hyperplasia (increase in number) of adipocytes (Hausman et al., 2001). Hypertrophy is thought to be the initial event that occurs during development of obesity. The excess energy is stored in white adipocytes as triacylglycerol, the accumulation of lipids leads to the expanded size of adipocytes. However, adipocytes cannot grow and accumulate lipids indefinitely. When adipocytes exhaust their storage capacity, there is a subsequent increase in cell number (Otto and Lane, 2005). Hyperplasia is related to the generation of new adipocytes from precursor cells, called preadipocytes, which are fibroblast-like cells (Hausman et al., 2001). This process, also referred as 'adipogenesis', is the key regulatory process involved in the normal adipose tissue development and the development of obesity.

### 1.3.3 Adipocytes development

Adipose tissue develops from pluripotent mesenchymal stem cells (MSCs), which are capable of differentiating into adipocytes, osteoblasts, chondrocytes, myoblasts, and connective tissue (Gesta et al., 2007). Signaling factors responsible for the commitment to the adipocyte lineage are still not well characterized. The signals may be secreted by a mature adipocyte to recruit new cells to the adipocyte lineage (Otto and Lane, 2005; Rosen and MacDougald, 2006). BMP4 has been shown to play a role in commitment to preadipocytes *in vitro*. BMP4-treated 10T1/2 cells (multipotent stem cell line similar to mesenchymal stem cells) acquire the characteristics of preadipocytes capable for differentiating into adipocytes (Tang et al., 2004). Recently, several studies demonstrated that other multiple factors may influence the MSCs

commitment to preadipocytes, including transforming growth factor  $\beta$  (TGF $\beta$ ), insulin like growth factor 1 (IGF1), fibroblast growth factor 1 (FGF1), FGF2, activin, Wnt signaling, etc (reviewed by (Lowe et al., 2011)). Once committed, MSCs give rise to undifferentiated precursors (osteoblast, adipoblast/preadipocyte, and myoblast), which upon activation of key transcription factors enter a differentiation program to acquire their specific functions. The transition from preadipocyte to adipocyte is orchestrated by a transcriptional cascade involving the nuclear receptor PPAR $\gamma$  and members of the C/EBPs family. Adipogenesis comprises four stages: preadipocytes proliferation, contact growth arrest, mitotic clonal expansion (early differentiation), and terminal differentiation (Gesta et al., 2007).

#### 1.3.4 Transcription factors in adipogenesis

The most important transcription factors involved in the regulation of differentiation are the peroxisome proliferator-activated receptors (PPARs) family and the CCAAT/enhancer-binding proteins (C/EBPs) family, both of them belong to the nuclear receptor family similar to retinoic acid receptors and vitamin D3 receptors (Otto and Lane 2005). There are 3 members of the PPAR family:  $\alpha$ ,  $\beta$  and  $\gamma$  (Moreno et al., 2010), among which, PPAR $\gamma$  plays a critical role in adipocytes differentiation and is both necessary and sufficient for adipogenesis. No factor has been identified that can rescue adipogenesis in the absence of PPAR $\gamma$  so far (Rosen and MacDougald, 2006). Two major protein isoforms of PPAR $\gamma$  (PPAR $\gamma$ 1 and PPAR $\gamma$ 2) are generated from a differential promoter usage and an alternative first exon of the PPAR $\gamma$  gene, the latter contains an additional 30 amino acids at its N-terminus (Tontonoz and Spiegelman, 2008). In contrast to the ubiquitous expression of PPAR $\gamma$ 1 in many tissues, PPAR $\gamma$ 2 expression is restricted to adipose tissue under normal condition and can be induced in the liver of mice exposed to a high fat diet (Vidal-Puig et al., 1996). Adipogenesis of PPAR $\gamma$ 2-deficient primary preadipocytes or MEFs is severely impaired (Medina-Gomez et al., 2005; Zhang et al., 2004). In 3T3-L1 cells, in which both PPAR $\gamma$ 1 and PPAR $\gamma$ 2 were inhibited, ectopic expression of PPAR $\gamma$ 2 rescued the adipogenesis whereas ectopic expression of PPAR $\gamma$ 1 did not (Ren et al., 2002).

Although both PPAR $\gamma$ 1 and PPAR $\gamma$ 2 can enhance adipocytes differentiation in PPAR $\gamma$  deficient embryonic fibroblasts, PPAR $\gamma$ 2 is more efficient at promoting adipogenesis (Mueller et al., 2002; Ren et al., 2002).

Like most nuclear receptors, PPAR $\gamma$  forms a heterodimer with RXR prior to binding to DNA, then binds to the PPAR response element in the promoter region of the target genes and controlling their expression (Aranda and Pascual, 2001). Although the specific endogenous PPAR $\gamma$  ligands remain unclear, several dietary fat and lipid metabolites including polyunsaturated fatty acids, certain prostanoids and oxidized fatty acids have been postulated to activate PPAR $\gamma$  receptor (Tontonoz and Spiegelman, 2008). Furthermore, synthetic ligands, such as antidiabetic drugs thiazolidinedione (for example, rosiglitazone and pioglitazone) were identified as potent activators/agonist of PPAR $\gamma$  (Tontonoz and Spiegelman, 2008).

PPAR $\gamma$  is the key regulator of adipogenesis and sits at the core of the adipogenic cascade in a feedback loop with C/EBP $\alpha$ . A variety of positive signaling regulators have been identified that act upstream of PPAR $\gamma$ , including C/EBP $\beta$  and  $-\delta$ , STAT5, KLF4 and 5, early B cell factor-1 (EBF1), early growth response-2 (EGR2, also known as KROX20), brain and muscle Arnt-like protein 1 (BMAL1, also known as ARNTL1). In addition to the activators, inhibitory effects have been described for forkhead box protein O1 (FOXO1), globin transcription factors 2 and 3 (GATA2 and GATA3), C/EBP homologous protein 10 (CHOP10), KLF3, HIF1 $\alpha$ , C-terminal-binding proteins 1 and 2 (CTBP1 and CTBP2) and others (reviewed by Lowe et al., 2011). Activation of PPAR $\gamma$  promotes terminal differentiation through the induction of a variety of differentiation-dependent target genes important for triglyceride uptake and storage, including fatty-acid-binding protein (FABP4, also known as adipocyte protein 2, aP2), *sn*-1-acylglycerol-3-phosphate acyltransferase 2 (AGPAT2), lipoprotein lipase (LPL), perilipin and the secreted factors adiponectin and leptin (Lowe et al., 2011).

C/EBP family consists of 6 isoforms:  $\alpha$ ,  $\beta$ ,  $\gamma$ ,  $\delta$ ,  $\zeta$  (CHOP-10), and  $\epsilon$ . All members except the  $\epsilon$  are involved in adipogenesis (Otto and Lane, 2005). C/EBP $\beta$  and  $\delta$  are involved in the early regulation of the adipogenesis. They are rapidly induced and achieve the maximal protein levels within 4 hours after the induction of differentiation

(Tang and Lane, 1999). The early expressed C/EBP $\beta$  and  $\delta$  then induce the expression of C/EBP $\alpha$  and PPAR $\gamma$  (Farmer, 2006). C/EBP $\alpha$  is induced late in adipogenesis and it is essential for differentiation. It activates several adipogenic genes including PPAR $\gamma$ , C/EBP $\alpha$  itself and other adipocyte marker genes (Otto and Lane, 2005). Despite the fact that both C/EBP $\alpha$  and PPAR $\gamma$  are very important in adipogenesis, PPAR $\gamma$  appears to play a dominant role, since ectopic expression of PPAR $\gamma$  can rescue the differentiation of MEFs lacking C/EBP $\alpha$  to adipocytes (Wu et al., 1999), but forced expression of C/EBP $\alpha$  cannot rescue the impaired differentiation in MEFs lacking PPAR $\gamma$  (Rosen et al., 2002). Other C/EBP isoforms, CHOP10 and C/EBP  $\gamma$ , seem to be anti-adipogenic factors, presumably through the inactivation of C/EBP $\beta$  (Darlington et al., 1998).

In addition, the basic helix-loop-helix (bHLH) transcription factor ADD1/SREBP1c is also an important regulator linking lipogenesis and adipogenesis. ADD1/SREBP1c can activate a broad battery of genes involved in fatty acid and triglyceride metabolism in both fat and liver and can also accelerate adipogenesis (Kim and Spiegelman, 1996). The mechanism of how ADD1/SREBP1c promotes adipogenesis could act via direct activation of PPAR $\gamma$  (Fajas et al., 1999) or through generation of endogenous PPAR $\gamma$  ligands (Kim et al., 1998).

### 1.3.5 The role of sirtuin proteins in adipose tissue and adipogenesis

Recent studies have shown that sirtuins regulate many metabolic adaptations linked with obesity (the relations of sirtuins and metabolic adaptation have been introduced in 1.1 and 1.2.6). So far, some investigations have suggested that sirtuins control metabolic balance through the modulation of adipogenesis, as well as maturation and remodeling of adipose tissue. Sirt1 was shown to attenuate adipogenesis and increase lipolysis through the repression of PPAR- $\gamma$  transcription by docking with its cofactors NCoR (nuclear receptor co-repressor) and SMRT (silencing mediator of retinoid and thyroid hormonereceptors) to its promoter (Picard et al., 2004). Overexpression of ectopic Sirt1 blocks adipogenesis in 3T3-L1 cells, a cell culture model of adipocyte differentiation, while inhibition of endogenous Sirt1 by knockdown promotes it (Picard et al., 2004). Consistently, the specific genetic ablation of Sirt1 in

white adipose tissues leads to obesity and insulin resistance similar to the high-fat diet induced obesity in wildtype mice (Chalkiadaki and Guarente, 2012). In contrast, transgenic mice moderately overexpressing Sirt1 or mice treated with Sirt1 specific activators gain less body weight and have less WAT mass, and are protected against high-fat-diet induced obesity and metabolic damage (Baur et al., 2006; Bordone et al., 2007; Feige et al., 2008; Kim et al., 2011b; Lagouge et al., 2006). Moreover, Sirt1 represses the inflammatory gene expression in WAT, which leads to block of macrophage influx and inhibition of inflammation in adipose tissue (Gillum et al., 2011). Sirt1 also improves the insulin sensitivity in adipose tissue by deacetylating NF- $\kappa$ B (Yoshizaki et al., 2009). A recent report showed that Sirt1 can directly deacetylate PPAR $\gamma$  to recruit the brown adipose tissue program coactivator Prdm16 to PPAR $\gamma$ , leading to selective induction of BAT genes and repression of visceral WAT genes (Qiang et al., 2012).

Another sirtuin family member Sirt2, the most abundant sirtuin in adipocytes was also shown to regulate adipocyte differentiation (Jing, Gesta et al. 2007). Sirt2 overexpression inhibits adipogenesis while Sirt2 reduction promotes adipogenesis in 3T3-L1 preadipocytes. The mechanism underlying Sirt2 effects includes the deacetylation of FOXO1, which in turn represses its phosphorylation and increases FOXO1 nuclear localization to promote FOXO1's binding to PPAR $\gamma$  promoter and subsequent repression of PPAR $\gamma$  transcriptional activity (Jing et al., 2007; Wang and Tong, 2009).

Sirt3, a mitochondrial sirtuin, has been shown to regulate mitochondrial function and thermogenesis in brown adipocytes. Enforced expression of SIRT3 in the HIB1B brown adipocytes enhances expression of the uncoupling protein UCP1, and several other mitochondria-related genes. Both ADP-ribosyltransferase and deacetylase activities of Sirt3 are required for this action. It was postulated that Sirt3 stimulates CREB phosphorylation, which then directly activates PGC-1 $\alpha$  promoter, resulting in the increased UCP1 expression (Shi et al., 2005).

The nucleolar sirtuin Sirt7 interacts with RNA polymerase I and the transcription factor UBF to positively regulate rDNA transcription (Ford et al., 2006; Grob et al.,

2009). Therefore, Sirt7 seems to be a regulator linking cell growth and metabolism to nutrition response through its impact on the ribosome biogenesis. Such functions are especially important in the metabolically active tissues such as adipose tissue and liver. However, no investigations of Sirt7 role in these tissues in vivo were reported so far. The Sirt7 knockout mice generated in our laboratory exhibited various phenotypes such as smaller size, kyphosis, loss of visceral and subcutaneous fat and protection against high fat induced obesity (Vakhrusheva et al., 2008b; Yoshizawa et al., unpublished data). These preliminary data suggest that Sirt7 might play important roles in the adipogenic differentiation and in the maintenance of the adipose tissue.

## 2. Materials and Methods

### 2.1 Materials

#### 2.1.1 Antibodies

**Table 2.1 List of primary antibodies**

Name	Type	Company or other resource	Application
Sir 2 (Sirt1)	rabbit, polyclonal	Upstate (Cat.07-131)	WB (1:1000), ChIP
Sirt1	rabbit, polyclonal	Cell Signaling Techn.(Cat.2028)	WB (1:1000), IF
Sirt7	mouse, monoclonal	A. Vaquero, Barcelona, Spain	WB (1:1000)
RalA	mouse, monoclonal	BD (Cat.610221)	WB (1:5000)
GAPDH	rabbit, polyclonal	Cell Signaling Techn.(Cat.2118)	WB (1:2000)
$\beta$ -actin	mouse, monoclonal	Sigma (Cat.A-5441)	WB (1:5000)
$\beta$ -tubulin	mouse, monoclonal	Sigma (Cat.T-4026)	WB (1:5000)
aP2	Chicken, IgY	Millipore (Cat.ab3515)	WB (1:1000)
FLAG M2	mouse, monoclonal	Sigma (Cat.F-1804)	WB (1:5000), IP
p53	rabbit, polyclonal	Cell Signaling Techn.(Cat.9282)	WB (1:1000)
p53 (acetyl K373 + K382)	mouse, monoclonal	abcam (Cat.ab4276)	WB (1:1000)
Pan-actin	rabbit, polyclonal	Cell Signaling Techn.(Cat.4968)	WB (1:5000)
Histone AcH3K9	rabbit, polyclonal	abcam (Cat.ab10812)	WB (1:1000), ChIP
Histone H3K9me3	rabbit, polyclonal	abcam (Cat.ab8898)	ChIP
Histone H3	rabbit, polyclonal	abcam (Cat.ab1791)	WB (1:10000), ChIP
(CGY)FP Tag	mouse, monoclonal	Evrogen (Cat.ab122)	WB (1:5000), IP
PPAR $\gamma$	rabbit, polyclonal	Santa Cruz (Cat.sc-7196)	WB (1:1000), IF
PPAR $\gamma$ 2	goat, polyclonal	Santa Cruz (Cat.sc-22022)	WB (1:200)
RNA pol I	rabbit, polyclonal	Santa Cruz	ChIP

		(Cat.sc-28714)	
UBF	rabbit, polyclonal	Santa Cruz (Cat.sc-9131)	ChIP

**Table 2.2 List of secondary antibodies**

Name	Type	Company or other resource	Application
anti-rabbit IgG	goat, HRP-conjugated	Pierce (Cat.1858415)	WB (1:5000)
anti-mouse IgG	goat, HRP-conjugated	Pierce (Cat.1858413)	WB (1:5000)
anti-Chicken IgY	goat, HRP-conjugated	abcam(Cat.ab6877-1)	WB (1:1000)
anti-goat IgG	donkey, HRP-conjugated	rockland (Cat.600667625)	WB (1:1000)
anti-rabbit IgG	goat, Alex594-conjugated	Invitrogen (Cat.A11012)	WB (1:1000)
anti-rabbit IgG	goat, Alex488-conjugated	Invitrogen (Cat.A11070)	WB (1:1000)

**2.1.2 Primers**

All primers were synthesized and ordered from Invitrogen or Sigma-Aldrich

**Table 2.3 List of primers for quantitative real-time-PCR (QRT-PCR)**

Name	Sequence	Annealing temp.in °C
mouse rDNA (promoter)	Forward: 5'-GTTGTCAGGGTTCGACCAGTTGT-3' Reverse: 5'-GTGTCCTTTAGTGTTAATAGGG-3'	56
mouse PPAR $\gamma$ 2 (promoter)	Forward: 5'-CTGTACAGTTCACGCCCTC-3' Reverse: 5'-TCACACTGGTGTGTTTGTCTATG-3'	62
human pre-rRNA (5'ETS)	Forward: 5'-GAACGGTGGTGTGTCGTTTC-3' Reverse: 5'-GCGTCTCGTCTCGTCTCACT-3'	56
human $\beta$ -actin	Forward: 5'ATCGTCCACCGCAAATGCTTCTA-3' Reverse: 5'-AGCCATGCCAATCTCATCTTGTT-3'	60
mouse pre-rRNA (5'ETS)	Forward: 5'-TTTTTGGGGAGGTGGAGAGTC-3' Reverse: 5'-CAGAACAAGAGAACAACGAG-3'	56
mouse $\beta$ -actin	Forward: 5'-CAACGAGCGGTTCCGATG-3' Reverse: 5'-GCCACAGGATTCCATACCCA-3'	60
mouse Sirt1	Forward: 5'-AAAAGATAATAGTTCTGACTGGAGCTG-3' Reverse: 5'-GGCGAGCATAGATACCGTCT-3'	60
mouse Sirt7	Forward: 5'-CCCCGGACCGCCATCTCAG-3' Reverse: 5'-ATCTCCAGGCCAGTTCATTCAT-3'	56

mouse PPAR $\gamma$ 2	Forward: 5'-TGCGGAAGCCCTTTGGTGAC-3' Reverse: 5'-CTTGGCGAACAGCTGAGAGGAC-3'	60
mouse C/EBP $\alpha$	Forward: 5'-GGATTCTGCTTCTCTCG-3' Reverse: 5'-CGGGATCTCAGCTTCCTGTA-3'	58
mouse aP2	Forward: 5'-GAAAACGAGATGGTGACAAGC-3' Reverse: 5'-GCCCTTTCATAAACTCTTGTGG-3'	58

**Table 2.4 List of primers for semi-quantitative RT-PCR**

Name	Sequence	Annealing temp.in °C
mSirt1 Ex1-Ex56	Forward: 5'-GACGACGAGGGCGAGGAGGAGGAC-3' Reverse: 5'-TTGCAAAGGAACCATGACACTGAA-3'	62
mSirt7 Ex6-Ex9	Forward: 5'-CCCCGGACCGCCATCTCAG-3' Reverse: 5'-ATCTCCAGGCCAGTTCATTCAT-3'	62
mouse GAPDH	Forward: 5'-GACGACGAGGGCGAGGAGGAGGAC-3' Reverse: 5'-TTGCAAAGGAACCATGACACTGAA-3'	56

**Table 2.5 List of primers for genotyping**

Name	Sequence	Annealing temp.in °C
mouse SnaB loxP P1F	Forward: 5'-GGCAGTATGTGGCAGATT-3'	56
mouse SnaB loxP P2R	Reverse: 5'-CCTGAAACAGACAAGACCT-3'	56
mouse Sfi loxP P3F	Forward: 5'-CAGGCTGGTTTCCAATGTCT-3'	56
mouse Sfi loxP P4R	Reverse: 5'-AAAGGCTGCGGCTCAGACAA-3'	56
Neo loxP P5 F	Forward: 5'-CCTCCCCCGTGCCTTCCT-3'	56
Neo loxP Del P6 R	Reverse: 5'-GAACATAACAGCCAGGCAT-3'	56
Cre	Forward: 5'-GACCAGGTTCTGTTCACTCATGG-3' Reverse: 5'-AGGCTAAGTGCCTTCTCTACAC-3'	55
Flp	Forward: 5'-CTGGAGGATAACTTGTTTATTGC-3' Reverse: 5'-CTAATGTTGTGGGAAATTGGAGC-3'	54

**Table 2.6 List of primers for Northern blot probes**

Name	Sequence	Annealing temp.in °C
mSirt7 NB	Forward: 5'-CCCCGGACCGCCATCTCAG-3' Reverse: 5'-ATCTCCAGGCCAGTTCATTCAT-3'	58
mSirt1 NB	Forward: 5'-GTTCTGACTGGAGCTGGGGTTTCT-3' Reverse: 5'-TGGGCGTGGAGGTTTTTCAGTAAT-3'	62
mAceCS1 NB	Forward: 5'-TCCCAGCGCTGCCCATTTGTAGAC-3'	55

	Reverse: 5'-AGGGGCAGGATGGATGGGCAGAAA-3'	
mPEPCK NB	Forward: 5'-ATCATCTTTGGTGGCCGTAG-3' Reverse: 5'-CCTCCTTCTCCCAGAACTCC-3'	56
mFAS NB	Forward: 5'-CTGCGGCTGCGTGGCTATGATTAT-3' Reverse: 5'-TCCAGCTGCAGGTTCCCGTTGAG-3'	56

**Table 2.7 List of primers for Southern blot probes**

Name	Sequence	Annealing temp.in °C
mSirt1 SB internal probe	Forward: 5'-CCGCTCGAGTGGTATGTTTTATAATGGAC-3' Reverse: 5'-GGCCGAATTCAAATCTTGAGACAAT-3'	56
mSirt1 SB 3'probe	Forward: 5'-CGAGTGCTGGGATTAAGGTGTAT-3' Reverse: 5'-TCAGCCCCTCATCCTCACAA-3'	56

**Table 2.8 List of primers for the construction of targeting vectors**

Name	Sequence	Application
mSirt1 1RP5'	Forward: 5'-TCCCCGGGGTTTAAACAAAGATGGGC CAGACATGGT -3' Reverse: 5'-CCGAAGCTTGCACCTCAGTGTATACAGCA -3'	mSirt1 CKO target construct
mSirt1 1RP3'	Forward: 5'- GCCGAGATCTGGCATACTACTATCA -3' Reverse: 5'- GGAATTCTGCCATATGGTCTCATATAG -3'	mSirt1 CKO target construct
mSirt1 1MT5'	Forward: 5'- CGGGATCCGTCCTAGAACTTTGCAA -3' Reverse: 5'-GTTCCGCGGACCCTTACAGTTCTGAGA-3'	mSirt1 CKO target construct
mSirt1 1MT3'	Forward: 5'-CCGCTCGAGTGGTATGTTTTATAATGGAC -3' Reverse: 5'- GGCCGAATTCAAATCTTGAGACAAT -3'	mSirt1 CKO target construct
mSirt1 CKO loxP F/R	Forward: 5'-GAGGCTACGTAATAACTTCGTATAATGT ATGCTATACGAAGTTATTACGTAGATCC-3' Reverse: 5'-GGATCTACGTAATAACTTCGTATAGC ATACATTATACGAAGTTATTACGTAGCCTC-3'	loxP sequence for insertion into the SnaB I or SfiI site
mSirt7-flag	Forward: 5'-ATGGCAGCCGGTGGCGGCTGAGCC-3' Reverse: 5'-CTATCACTTGTCGTCATCGTCTTTGTAGT CTGCCACTTTCTTCCTTTTTGCACG-3'	pBabe-mSirt7 Flag construct

**Table 2.9 List of primers for mutagenesis**

These primers were designed by the "Quick Change primer design" program of

Stratagene and synthesized by Sigma-Aldrich.

Name	Sequence
mSirt7 H188Y	Forward: 5'-ACCGCCATCTCAGAGCTCTATGGGAATATGTATATTGA-3' Reverse: 5'-TCAATATACATATTCCCATAGAGCTCTGAGATGGCGGT-3'
mSirt1 K230R	Forward: 5'-GAACCACCAAAGCGGAAAAAAGAAGAGATATCAAT ACAATTGAAG-3' Reverse: 5'-CTTCAATTGTATTGATATCTTCTTTTTTTCCGC TTTGGTGGTTC-3'
mSirt1 K369R	Forward: 5'-AACAGCATCTTGCCTGATTTGTAAATACAGAGTTGA TTGTGAAGC-3' Reverse: 5'-GCTTCACAATCAACTCTGTATTACAAATCAGGCA AGATGCTGTT-3'
mSirt1 K505R	Forward: 5'-GTAAAGCTTTCAGAAATTACTGAAAGAC CTCCACGCCCA-3' Reverse: 5'-TGGGCGTGGAGGTCTTTCAGTAATTTCTGAAAGCTTTAC-3'
mSirt1 K600R	Forward: 5'-TGGTTCCAGTACTGCAGACAGAAATGAAAGAA CTTCAGTTG-3' Reverse: 5'-CAACTGAAGTTCTTTCATTTCTGTCTGCAGTAC TGGAACCA-3'

**Table 2.10 List of primers for sequencing**

Name	Sequence
T7	5'-TAATACGACTCACTATAGGG-3'
Sp6	5'-ATTTAGGTGACACTATAG-3'
CMV Forward	5'-CGCAAATGGGCGGTAGGCGTG-3'
pBABE 5'	5'-CTTTATCCAGCCCTCAC-3'
BGH Reverse	5'-TAGAAGGCACAGTCGAGG-3'
YFP Forward	5'-CAGAGCTGGTTTAGTGAACC-3'
SnaB loxP For	5'-GGCAGTATGTGGCAGATT-3'
Sfi loxP For	5'-CAGGCTGGTTTCCAATGTCT-3'

### 2.1.3 DNA probes for Northern blot and Southern blot

**Table 2.11 List of probes for Northern blot**

Name	PCR primers	Note
mSirt7	mSirt7 NB For mSirt7 NB Rev	the 456 bp PCR fragment was cloned into the pGEM-T Easy vector and excised with EcoR I, the resulting 470 bp fragment was used for hybridization at 60 °C
mSirt1	mSirt1 NB For mSirt1 NB Rev	the 678 bp PCR fragment was cloned into the pGEM-T Easy vector and excised with EcoR I, the resulting 690 bp fragment was used for hybridization at 60 °C
mAceCS1	mAceCS1 NB F	the 807 bp PCR fragment was cloned into the pGEM-T Easy

	mAceCS1 NB R	vector and excised with EcoR I, the resulting 820 bp fragment was used for hybridization at 60 °C
mPEPCK	mPEPCK NB F mPEPCK NB R	the 474 bp PCR fragment was cloned into the pGEM-T Easy vector and excised with EcoR I, the resulting 488 bp fragment was used for hybridization at 60 °C
mFAS	mFAS NB For mFAS NB Rev	the 592 bp PCR fragment was cloned into the pGEM-T Easy vector and excised with EcoR I, the resulting 606 bp fragment was used for hybridization at 60 °C

**Table 2.12 List of probes for Southern blot genotyping**

Name	PCR primers	Note
mSirt1 CKO internal probe	mSirt1 SB internal For mSirt1 SB internal Rev	the 540 bp PCR fragment was cloned into the pGEM-T Easy vector and excised with EcoR I, the resulting 554 bp fragment was used for hybridization at 65 °C
mSirt1 CKO 3'probe	mSirt1 SB 3' probe For mSirt1 SB 3' probe Rev	the 426 bp PCR fragment was cloned into the pGEM-T Easy vector and excised with EcoR I, the resulting 440 bp fragment was used for hybridization at 65 °C

## 2.1.4 Plasmid vectors

**Table 2.13 List of vectors**

Name	Description and source
pKOII-DTA	kindly provided by Nabeel Bardeesy, Boston
pL451	kindly provided by Dr. Stefan Günther (MPI Bad Nauheim)
pGEM-T-Easy	Promega, Mannheim
pTag CFP-C	BioCat (Evrogen), Heidelberg
pTag YFP-N	BioCat (Evrogen), Heidelberg
pTag-CFP-mSirt1	mSirt1 ORF was cloned into the pTag CFP-C vector for ectopic overexpression, kindly provided by Christian Smolka (MPI Bad Nauheim)
pTag-mSirt7-YFP	mSirt7 ORF was cloned into the pTag YFP-N vector for ectopic overexpression, kindly provided by Christian Smolka (MPI Bad Nauheim)
pCemmCTAP	Euroscarf (Cat. ABO 76910, Frankfurt)
pCMVTag2a-hSirt7-Flag	hSirt7 ORF was cloned into the pCMVTag2a vector for ectopic overexpression, kindly provided by Dr. Yonggang Zhou (MPI Bad Nauheim)
pCMV-sport6-mSirt1-Flag	mSirt1 ORF fused with C-terminal Flag tag was cloned into the pCMV-Sport6 vector for ectopic overexpression, kindly provided by Prof. Leo, Bruxelles
pCMV-sport6-mSirt1HY-Flag	mSirt1 H355Y mutant ORF fused with C-terminal Flag tag was cloned into the pCMV-Sport6 vector for ectopic overexpression, kindly provided by Prof. Leo, Bruxelles

pBabe	kindly provided by Prof. Grummt, Heidelberg
pQsupR-Scramble	retroviral vector for expression of the scramble shRNA, kindly provided by Prof. Grummt, Heidelberg
pQsupR-mSirt1shRNA	retroviral vector for expression of the mSirt1 shRNA to knock down mouse Sirt1, kindly provided by Prof. Grummt, Heidelberg
pBabe-Flag-HA-mPPAR $\gamma$ 2	retroviral vector for ectopic overexpression of mouse PPAR $\gamma$ 2 fused with N-terminal Flag and HA tag, Addgene, Cambridge MA
pLKO.1-puro	lentiviral vector with either scramble shRNA or target gene shRNA for transient transfection or for the production of lentiviral particles for stable expression of the specific shRNA, purchased from Sigma-Aldrich
pCMVdr8.74ps PAX2	packaging vector for the production of lentiviral particles, kindly provided by Dr. Johnny Kim (MPI Bad Nauheim)
pMD2.G	envelope vector for the production of lentiviral particles, kindly provided by Dr. Johnny Kim (MPI Bad Nauheim)

### 2.1.5 Bacterial strains

**Table 2.14 List of bacterial strains**

Name	Description
XL1-Blue	Stratagene; recA1 endA1 gyrA96 thi-1 hsdR17 supE44 relA1 lac [F' proAB lacIqZ_M15 Tn10 (Tetr)6]
DH5 $\alpha$	F- $\phi$ 80lacZ $\Delta$ M15 $\Delta$ (lacZYA-argF) U169 deoR recA1 endA1 hsdR17 (r $\kappa$ <sup>-</sup> , m $\kappa$ <sup>+</sup> ) phoA supE44 $\lambda$ - thi-1 gyrA96 relA1
BL21 (DE3)	F- ompT hsdSB(rB <sup>-</sup> , mB <sup>-</sup> ) gal dcm (DE3)

### 2.1.6 Cell lines

**Table 2.15 List of cell lines**

Name	Description
HEK 293 ATCC CRL-1573 <sup>TM</sup>	human embryonic kidney, kidney epithelial cell line
HEK 293T ATCC CRL-11268 <sup>TM</sup>	HEK 293 cells constitutively expressing the simian virus 40 (SV40) large T antigen
Phoenix-AMPHO ATCC CRL-3213 <sup>TM</sup>	variant of the 293T cell line that has been stably transfected to express the Moloney Murine Leukemia Virus (M-MLV) viral packaging proteins
Hela ATCC CRM-CCL-2 <sup>TM</sup>	human cervical adenocarcinoma cell line
3T3-L1 ATCC CL-173 <sup>TM</sup>	mouse embryonic fibroblasts, a sub strain of 3T3 cells (Swiss albino) developed through clonal isolation, preadipocytes

### 2.1.7 Media for cell culture

All media and reagents for cell culture were purchased from Invitrogen and PAA except as noted otherwise in the text.

**Table 2.16 List of media for cell culture**

Medium	composition
Proliferation medium	Dulbecco's modified Eagle's medium (DMEM, low glucose) supplemented with 10% heat-inactivated fetal calf serum (FCS, Gibco), 100 U/ml of penicillin-streptomycin and 20mM of glutamine.
Freezing medium	Proliferation medium supplemented with 10% DMSO, 20%FCS.
Hepatocytes medium	M199 medium supplemented with 10% FCS, 20mM HEPES, 5nM dexamethasone and 1nM insulin.
Adipogenesis MDI medium	Proliferation medium supplemented with 0.5 $\mu$ M isobutylmethylxanthine (IBMX), 1 $\mu$ M dexamethasone and 10 $\mu$ g/ml insulin
Adipogenesis insulin medium	Proliferation medium supplemented with 5 $\mu$ g/ml insulin

### 2.1.8 Mouse strains

**Table 2.17 List of mouse strains**

Strain Name	Description
C57BL/6J	Harlan-Winkelmann, Paderborn
CMV-Cre Tg	In this transgenic strain, deletion of <i>loxP</i> -flanked genes occurs in all tissues, including germ cells. The <i>cre</i> gene in this strain is under the transcriptional control of a human cytomegalovirus minimal promoter and is likely to be expressed before implantation during early embryogenesis. Kind gift from Klaus Rajewsky, University of Frankfurt.
TG Alb-Cre	The hepatocyte specific Cre-recombinase mediates the excision of floxed DNA regions in hepatocytes during the embryogenesis and early postnatal development. Kindly provided by Dr. Thilo Borchardt, MPI Bad Nauheim.
TG Flp deleter	The constitutively expressed Flp recombinase mediates the recombination between Flp-recognition motifs during the early embryogenesis. The <i>Flp</i> transgene in this strain is driven by a human $\beta$ -actin enhancer element. Kindly provided by S.M. Dymecki, Boston, USA
Sirt7 bKO	In this mouse strain, the deletion of the putative deacetylation domain of Sirt7 encoded by the exons 4 to 9 constitutively occurs in all tissues including germ cells. Kindly provided by Olesya Vakhrusheva, MPI Bad Nauheim

### 2.1.9 Special materials and chemicals

BSA, Fraction V	Merck (Cat.112018)
Bromophenol blue	Merck (Cat.1081220005)
Cell culture dishes	Nunc; Greiner
Chelex 100 resin	BioRad (Cat. 143-2832)

Collagenase type I	Sigma (Cat. C9891)
Collagenase type II	Invitrogen(Cat. 17101-015)
DAPI	Invitrogen (Cat.D1306)
Dexamethasone	Sigma (Cat.D4902)
Ethidium bromide	AppliChem (Cat.A1152,0100)
Ex527	Cayman (Cat. 10009798)
Falcon <sup>®</sup> cell strainer (40µM, 70µM)	BD Biosciences
Filter paper	Schleicher & Schuell, Dassel
HEPES buffer 1M	Invitrogen (Cat.15630-056)
Insulin (10 mg/mL insulin in 25 mM HEPES)	Sigma (Cat.I0516)
Isobutylmethylxanthinen (IBMX)	Sigma (Cat.I7018)
MES running buffer	Invitrogen (Cat.NP0002)
MOPS running buffer	Invitrogen (Cat.NP0001)
Mowiol	Merck (Cat.475904)
Nicotinamide (NAM)	Sigma (Cat.N0636)
NuPAGE <sup>®</sup> Novex <sup>®</sup> PAGE gel	Invitrogen
Oil red O	Sigma (Cat.O0625)
Paraformaldehyde (PFA)	Merck (Cat.1040051000)
Polybrene	Sigma (Cat.107689)
Protein Standards (Novex <sup>®</sup> Sharp)	Invitrogen (Cat.LC5800)
Proteinase inhibitor cocktail tablets	Roche (Cat.04693116001)
Protran <sup>™</sup> nitrocellulose membrane (BA85)	Whatman (Cat.1048374)
Puromycine	Sigma (Cat. P8833)
Red Alert <sup>™</sup> (Ponceau S) (10x)	Novagen (Cat. 710783)
Rosiglitazone	Enzo Life Science(Cat.ALX350-125)
Sterile Filter NML (0.2 and 0.45 µm)	Sartorius
Super Signal West <sup>™</sup> Femto	Thermo Fisher Scientific (Cat.34095)
SYBR <sup>®</sup> Green I Fluorescein qPCR Mix (2x)	Thermo Fisher Scientific (Cat.k0241)
3,3',5-Triiodo-L-thyronine (T3)	Sigma (Cat. T2877)
TRIzol <sup>®</sup> Reagent	Invitrogen (Cat.15596026)
TSA	Sigma (Cat. T8552)

### 2.1.10 Standard buffers and solutions

2x HBS	50 mM HEPES, 280 mM NaCl, 1.5 mM Na <sub>2</sub> HPO <sub>4</sub> , adjust pH to 7.05-7.1
100 mM Sodium phosphate	5.77 ml 1M Na <sub>2</sub> HPO <sub>4</sub> , 4.23 ml 1M NaH <sub>2</sub> PO <sub>4</sub> , add DEPC treated water to 100 ml and adjust pH to 7.0
Glyoxal mixture	4.5 µl 100 mM Sodium phosphate, pH7.0 22.5 µl DMSO, 6.6 µl 6M deionized glyoxal, 1 µl 10 mg/ml Ethidium bromide

---

10x MOPS buffer	400 mM MOPS, 100 mM NaAc, 10 mM EDTA, final pH 7.0, the solution was made with DEPC treated water and autoclaved
Immunoprecipitation lysis buffer	20 mM Tris-HCl, pH7.4, 200 mM NaCl, 2 mM EDTA, 2 mM EGTA, 1% Triton X-100 (v/v), protease and phosphatase inhibitor mix
Extraction buffer	100 mM Tris-HCl, pH8.0, 10% SDS (w/v), 10 mM EDTA, protease and phosphatase inhibitor mix
Protease and phosphatase inhibitor mix	0.5 µg/ml Benzamidine, 2 µg/ml Aprotinin, 2 µg/ml Leupetin, 2 mM PMSF, 1 mM Na <sub>3</sub> VO <sub>4</sub> , 20 mM NaF
2x Laemmli loading buffer	125 mM Tris-HCl, pH 6.8, 4% SDS(w/v), 20% Glycerol (v/v), 100 mM DTT, 0.004% Bromophenol blue
10x PBS (pH7.2)	137 mM NaCl, 2.7 mM KCl, 10 mM Na <sub>2</sub> HPO <sub>4</sub> , 2 mM KH <sub>2</sub> PO <sub>4</sub>
RNA loading buffer	50% Glycerol (v/v), 10 mM Sodium phosphate, pH7.0, 0.25% Bromophenol blue (w/v), 0.25% Xylene cyanol (w/v)
20x SSC	3 M NaCl, 0.3 M Na-Citrate, adjust pH to 7.0, the solution was made with DEPC treated water and autoclaved
Tail lysis buffer	10 mM Tris, pH 8.0, 100 mM NaCl, 10 mM EDTA, pH 8.0, 0.5% SDS, 200 µg/ml proteinase K
Church & Gilbert buffer	0.5 M NaH <sub>2</sub> PO <sub>4</sub> , pH 6.76, 1 mM EDTA, 7% SDS (w/v)
Washing buffer for Northern blot and Southern blot	40 mM NaH <sub>2</sub> PO <sub>4</sub> , pH 6.76 1% SDS (w/v)

---

10x TBS	500 mM Tris-HCl, 1.5 M NaCl adjust pH to 7.4
TBST	1 x TBS 0.1% Tween-20
1x TAE buffer	40 mM Tris-HCl pH 8.3, 1 mM EDTA, 20 mM Acetic acid
TE buffer	10 mM Tris-HCl pH 8.0, 1 mM EDTA
Transfer buffer for Western blot	25 mM Tris base, 192 mM Glycine, 20% Methanol
Perfusion medium I	6.3g NaCl, 0.32g KCl, 0.15gKH <sub>2</sub> PO <sub>4</sub> 0.27g MgSO <sub>4</sub> x7H <sub>2</sub> O , 1.81g NaHCO <sub>3</sub> 3.58g HEPES, 1.5g Glucose , 0.038g EGTA, add to 1000 ml with water and adjust pH to 7.4
Perfusion medium II	DMEM/Ham's F12 (1:1), 10 mM HEPES pH7.4, 500 µg/ml Collagenase type II
Washing buffer	DMEM/Ham's F12 (1:1), 10 mM HEPES pH7.4, 20% FCS
Hypotonic buffer A	10 mM HEPES, pH7.9, 10 mM KCl, 1.5 mM MgCl <sub>2</sub> , protease and phosphatase inhibitor mix
Nuclei lysis buffer	50 mM Tris-HCl, pH8.0, 10 mM EDTA, 1% SDS (w/v), 1x protease inhibitor cocktail
ChIP dilution buffer	20 mM Tris-HCl, pH8.0, 150 mM NaCl, 2 mM EDTA, 1% Triton X-100, 1x protease inhibitor cocktail
Low salt washing buffer	20 mM Tris-HCl, pH8.0,150 mM NaCl, 2 mM EDTA, 0.1% SDS (w/v), 1% Triton X-100
High salt washing buffer	20 mM Tris-HCl, pH8.0, 500 mM NaCl,

2 mM EDTA, 0.1% SDS (w/v), 1%  
Triton X-100

LiCl washing buffer

10 mM Tris-HCl, pH8.0, 250 mM LiCl, 2  
mM EDTA, 1% Na-deoxycholate, 1%  
NP-40

### 2.1.11 Enzyme

DNase I	Roche (Cat.04716728001)
Klenow-Fragment	Promega (Cat. M220A)
<i>Pfu</i> DNA Polymerase	Promega (Cat. M774A)
<i>PfuTurbo</i> DNA-Polymerase AD	Stratagene (Cat. 600255)
Proteinase K	Roth (Cat. 7528.1)
RNase A	Sigma (Cat. R4875)
Restriction endonuclease	New England Biolabs; Jena Biosciences
Shrimp Alkaline Phosphatase	Promega (Cat.M820A)
T4 DNA Ligase	Promega (Cat.M1801)
<i>Taq</i> DNA Polymerase	5 Prime (Cat.2200000)

### 2.1.12 Kits

**Table 2.18 List of used kits**

Name	Company
DC <sup>TM</sup> Protein Kit	BioRad (Cat.500-0111)
Nucleobond AX 500 Maxi Kit	Macherey-Nagel (Cat. 740414.10)
QIAEX II Gel Extraction Kit	Qiagen (Cat. 20021)
SuperScript <sup>TM</sup> II Reverse Transcriptase	Invitrogen (Cat. 18064-014)

### 2.1.13 Equipment

**Table 2.19 List of special equipment**

Equipment	Type	Company
Microscopes	Axiophot 2 Z1 fluorescence microscope	Carl Zeiss Jena
PCR machines	Thermocycler Master cycler gradient PCR iCycler iQ Multicolor Real Time PCR Machine StepOnePlus <sup>TM</sup> Real-Time PCR System	SensoQuest Eppendorf BioRad  Applied Biosystems
Spectrophotometer	NanoDrop 2000/2000c	Thermo Fisher Scientific

Ultrasonic Homogenizer	Bioruptor Sonopuls HD 2070/2200	Diagenode Bandelin
VersaDoc Image System	VersaDoc™ 3000	BioRad

### 2.1.14 Software

**Table 2.20 List of used software**

Software	Company
AxioVision® 4.8	Carl Zeiss Imaging Solutions, Jena
DNASTAR Lasergene®	DNASTAR Inc. (USA)
ImageJ	National Institutes of Health (USA)
Photoshop 8.0	Adobe Systems Incorporated (USA)
Quantity One	BioRad, München
StepOne Software v2.2.2	Applied Biosystems

## 2.2 Methods

Standard molecular biology procedures were performed according to the following books except noted otherwise in the text:

### **Current Protocols in Molecular Biology**

F.M. Ausubel, R. Brent, R.E. Kingston, D.D. Moore, J.G. Seidman, J.A. Smith, K. Struhl; Wiley Interscience, 1989

### **Molecular Cloning: A Laboratory Manual, 2nd Edition**

J. Sambrook, E.F. Fritsch, T. Maniatis; Cold Spring Harbor Laboratory Press, 1989

### 2.2.1 Sterilization of materials and solutions

Glassware was sterilized with dry heat at 180 °C. Sensitive glassware, plastic ware, solutions and media were autoclaved at 121 °C and a pressure of 2.2 bars for 30 min. Non-autoclavable solutions or media were sterilized by filtering through a 0.2 µm or a 0.45 µm cellulose acetate filter.

### 2.2.2 Cloning and constructs

All used expression constructs are listed in Table 2.13. For cloning, the desired fragments were generated by PCR using specific primers covering the whole open reading frame. With the primers, specific restriction sites were introduced, that allow the directed cloning into the target vector. The used primers are listed in Table 2.8.

### **2.2.3 Cell culture and transfection**

All cells were cultured in an incubator at 37°C and 5% CO<sub>2</sub> according to their requirements in media listed in table 2.14. For harvesting and passaging, cells were washed with 1x PBS and detached using 0.05% trypsin/0.2% EDTA. The enzyme reaction was stopped with 2 volumes of serum containing medium and a desired number of cells was seeded in fresh medium to the culture dishes. For freezing, the trypsinized cell pellets were resuspended in freezing medium and aliquoted into cryovials (about 2 x 10<sup>6</sup> cells per cryovial).

#### **2.2.3.1 Isolation of primary cells**

##### **Preparation of primary mouse hepatocytes**

Mouse primary hepatocytes were isolated from WT control and Sirt7 KO mice by a two-step collagenase perfusion technique, modified from Seglen protocol (Seglen, 1976). These preparations were done by Ms. Marion Wiesnet. The liver was perfused twice with perfusion buffer I and perfusion buffer II respectively, and resected to obtain the single cells. The single cells were filtered through 100µm nylon mesh and washed with washing buffer. Then the hepatocytes (about 6 x 10<sup>6</sup> cells per 3.5cm dish) were seeded on collagen type I coated dishes in hepatocytes medium.

##### **Preparation of primary mouse embryonic fibroblasts (MEFs)**

Mouse embryonic fibroblasts (MEF's) were prepared by Monika Euler. For embryo preparation, heterozygous mice of the Sirt7 KO mouse line were mated and the embryos were removed at embryonic day E14.5 and placed on ice. The inner organs of the embryos were removed and discarded, whereas the membranes of the embryos were used for DNA extraction and genotyping by PCR. The remaining tissues of each

embryo were minced and incubated for 10 min in 5 ml 0.25% trypsin solution at 37°C. The digestion was stopped by adding 5 ml of DMEM supplemented with 10% FCS. Afterwards, cells were pipetted up and down to obtain single cells and pelleted by centrifugation at 300xg for 5 min. The cells were then resuspended in 24 ml of DMEM with 10% FCS and seeded to 3x 10cm dishes. One cell stock was prepared from each plate after 2 days of incubation.

### **Preparation of primary white preadipocytes**

Primary white preadipocytes were isolated from *Sirt7*<sup>-/-</sup> and *Sirt7*<sup>-/-</sup> *Sirt1*<sup>+/-</sup> mice and their control littermates (*Sirt7*<sup>+/-</sup>) (the age was less than 8 weeks). Subcutaneous and visceral adipose tissue from these mice was excised, minced and incubated at 37°C with 1ml collagenase isolation buffer (100 mM HEPES pH7.5, 4.8 mM KCl, 120 mM NaCl, 1.4 mM CaCl<sub>2</sub> x 2H<sub>2</sub>O, 5mM Glucose, 2.5% BSA, 1% Per/Strep, 2 mg/ml Collagenase type I) for 1 hr. Then, the same amount of medium was added to the collagenized tissue, resuspended by pipetting and transferred to a 15 ml falcon and spun down at 300xg for 5min. The cell pellets were then resuspended in 10 ml medium, filtered through a 40 µm mesh strainer and transferred to a 15 ml falcon tube. After centrifugation at 300xg, the cell pellets were resuspended in 5 ml erythrocyte lysis buffer (154 mM NH<sub>4</sub>Cl, 10 mM KHCO<sub>3</sub>, 0.1 mM EDTA, sterile filtered), incubated for 10 min, and centrifuged again at 300xg for 5min. Upon resuspension of the pellets in an appropriate volume of fresh medium, the cells were seeded on collagen-coated plates.

### **2.2.3.2 Transient plasmid DNA transfection in HEK cells**

Transfection of HEK cells was performed according to the calcium phosphate transfection method. Approximately 24 hours before transfection, cells were seeded in 9 ml of DMEM in 10 cm dishes at a density of  $2.5 \times 10^6$  cells per plate. 5-10 µg of plasmid DNA was diluted in 450 µl ddH<sub>2</sub>O and 50 µl of 2.5 M CaCl<sub>2</sub> was added drop wise. The mixture was then added to 500 µl of 2x HBS buffer drop by drop. The calcium phosphate-DNA complex was then distributed to the cells drop wise. The next day, the medium was replaced by fresh medium and the cells were harvested usually 48 h after transfection.

### 2.2.3.3 Retrovirus production and infection

Phoenix cells were transfected with either pBabe, pBabe-mSirt7, pBabe-PPAR $\gamma$ 2-Flag, pQsupR-Scramble, pQsupR-mSirt1shRNA or pCemm, pCemm-hSirt7-Flag plasmids using the calcium phosphate transfection method. After 48 hrs of transfection, the medium containing the retroviruses was collected and filtered through a 0.45  $\mu$ m filter. After addition of 4  $\mu$ g/ml polybrene, the virus solution was transferred to the target cells (immortalized MEF's or 3T3L1 cells). Infected cells were selected with 2.5 mg/ml puromycin (the selection procedure was skipped for the pCemm retroviral vectors) for 7 days to generate stable cell lines.

### 2.2.3.4 Lentiviral shRNA transduction

HEK293T cells were cotransfected with 3 lentiviral plasmids (pLKO.1-shRNA vectors either scramble or Sirt7 knockdown; packaging vector pCMVdR8.74psPAX2; envelope vector pMD2.G) using the calcium phosphate transfection method. 18 hours after transfection, the medium was replaced by fresh high (30%) FCS medium. After additional 24 h of incubation, the medium containing the viruses was collected, filtered through a 0.45  $\mu$ M filter and 4  $\mu$ g/ml polybrene was added. The virus medium was then transferred to the 3T3L1 target cells. Infected cells were selected with 2.5 mg/ml puromycin for 7 days to generate the stable cell lines.

### 2.2.3.5 Adipogenesis assay and Oil red O staining

To induce adipogenesis in 3T3L1 and MEFs, cells were grown to 100% confluence. 2 days after cells reached confluence (day 0), adipogenesis was induced with MDI medium supplemented with or without 0.5 $\mu$ M rosiglitazone (rosiglitazone was only added to medium for MEF's differentiation, similarly hereinafter). Two days later, medium was exchanged with insulin medium containing 0.5 $\mu$ M rosiglitazone or not. The insulin medium was exchanged every second day over a time period of 7-8 days.

To induce adipogenesis in primary white preadipocytes, cells were seeded into chamber slides with a density of  $2 \times 10^4$  cells per  $\text{cm}^2$  for 4 days before induction. At day 0, cells

were treated with MDI medium supplemented with 0.2 nM T3 and 0.5  $\mu$ M rosiglitazone. Two days later, medium was changed to insulin medium containing 0.2 nM T3 and 0.5  $\mu$ M rosiglitazone. The medium was replaced every second day over a time period of 8 days.

Fat accumulation was visualized by staining of lipids with Oil red O. Therefore, cells were washed twice with 1x PBS and 4% PFA was added to each well for 20 min to fix the cells. Then, each well was washed twice with 1x PBS and rinsed twice with 60% isopropanol, 30s each time. Freshly prepared 3 mg/ml Oil red O solution in 60% isopropanol was added into each well and incubated at 56°C for 15 min. Then, the cells were rinsed twice with 60% isopropanol for 30s. Next, the cells were rinsed twice with 1x PBS and covered with 1x PBS or mounted with mowiol and a glass slide. The lipids were visualized by red colour.

## **2.2.4 RNA analysis**

### **2.2.4.1 RNA extraction**

Total RNA from cells and mouse tissues was isolated using TRIzol reagent from Invitrogen according to the manufactory's protocol. The concentration of RNA was determined with a Nano Drop 2000c spectrophotometer.

### **2.2.4.2 Northern blot**

The Northern blot analysis was performed according to Brown *et al.*, (Current Protocol in Molecular Biology, 2004) with some modifications. 30  $\mu$ g of total RNA was mixed with 35  $\mu$ l glyoxal mixture in a total volume of 48  $\mu$ l and denatured at 65°C for 1 hr and cooled down on ice for 5 min. Then 12  $\mu$ l RNA-loading buffer was added to the samples and the mixture was loaded on a 1% agarose gel prepared with 10 mM sodium phosphate buffer. The RNA was separated at a constant voltage of 5V/cm of gel in 1x MOPS running buffer for about 4 hrs. The RNA was blotted to Nylon Duralon-UV membranes (Stratagene) by capillary transfer method in 15x SSC buffer overnight. Then, the membranes were washed twice in 2x SSC buffer for 5 min. Afterwards, the

transferred RNA was cross-linked to the membrane with an UV crosslinker (Stratagene) (the energy was about 1.5 J/cm<sup>2</sup>). The ribosomal 28S and 18S RNAs could be seen under UV-light and were used as a loading control.

For hybridization, the membrane was pre-hybridized in 15 ml Church & Gilbert buffer containing 200 µg/ml denatured herring sperm DNA at 65°C for 2-3 hrs. The cDNA probes were generated by RT-PCR, purified by QIAEX II Gel Extraction Kit (Qiagen) and either subcloned into the T-vector or directly used for hybridization. The sequence of each probe was confirmed by sequencing. The <sup>32</sup>P-labeled radioactive cDNA probe was generated following the random primer labelling protocol (Feinberg and Vogelstein, 1983). 50-100 ng of cDNA probe in a total volume of 32 µl was denatured at 95°C for 10 min and cooled down on ice for 5 min, mixed with 10 µl of 5x labelling buffer (Promega), 2 µl BSA (10 mg/ml), 5 µl [ $\alpha$ -<sup>32</sup>P] dCTP (Amersham), 1 µl of Klenow enzym (2 U/µl) (Promega) and incubated for 2-3 h at 37°C. The probes were then purified by NAP-5<sup>TM</sup> Sephadex G25 columns. The radioactive labelled probes as well as the herring sperm DNA were denatured 5 min at 95°C and cooled down on ice. After pre-hybridization, new Church & Gilbert buffer containing 100 µg/ml denatured herring sperm DNA and the probe at a dilution of 3000000 counts/ml was added to the membrane. The hybridization was performed overnight at 60°C in a rotary shaker. The next day, the membrane was washed 3 times for 15 min at 60°C with washing buffer and afterwards exposed to an X-ray film at -80°C.

### **2.2.4.3 Reverse transcription**

First-strand cDNA synthesis was done by reverse transcription (RT) of 1 µg of each RNA sample using the Invitrogen SuperScriptII Reverse Transcriptase System with random primers according to the manufactory's manual. The cDNAs were stored at -20 °C or directly used as a template for the PCR (polymerase chain reaction).

### **2.2.4.4 Polymerase chain reaction (PCR)**

The PCR was applied to exponentially amplify DNA fragments *in vitro*, by using the heat-stable Taq DNA polymerase originally isolated from the bacterium *Thermus*

*aquaticus* (Saiki et al., 1988). The Taq DNA polymerase from 5 Prime was used for the RT-PCR and for genotyping, whereas the *Pfu* DNA Polymerase and the *PfuTurbo* DNA Polymerase AD were used for cloning. All used primer pairs and their respective annealing temperatures are listed in the tables of part 2.1.2. The 25  $\mu$ l standard PCR reaction was prepared as follows: 1  $\mu$ l template, 2.5  $\mu$ l 10x PCR buffer (with or without  $Mg^{2+}$ ), 1  $\mu$ l of 50 mM  $MgCl_2$  (when the 10x PCR buffer did not contain  $Mg^{2+}$ ), 1  $\mu$ l forward primer (10  $\mu$ M) and 1  $\mu$ l reverse primer (10  $\mu$ M), 0.5  $\mu$ l dNTP mix (10 mM) and 2U *Taq* DNA polymerase. The initial denaturation step (94°C, 5 min) was followed by 25-40 cycles, each with 94°C denaturation 30s, 52-65°C annealing 30s and 1min/kb elongation at 72°C. The last cycle was followed by a final extension step at 72°C for 5 min.

#### 2.2.4.5 Quantitative real time PCR (QPCR)

QPCR was performed to quantitatively determine the mRNA expression by using fluorescent dyes that incorporate into double stranded DNA. A typical QPCR setup contained 12.5  $\mu$ l 2x SYBR Green Mix (Thermo Fischer), 1  $\mu$ l of each primer (2.5 pmol) and 10  $\mu$ l of cDNA (1:100 diluted) in a total volume of 25  $\mu$ l. The PCR conditions were chosen according to the manufactory's protocol and the annealing temperatures of the primers. The PCR runs were carried out in an iCycler iQ Multicolor Real Time PCR machine (BioRad). For each gene, 5 standards (using the mixture of WT & Sirt7 KO liver or MEFs cDNA in 1:2, 1:20, 1:200, 1:2000, and 1:20000 dilutions) were carried out in triplicate to produce a standard curve. The relative amount of the target gene and endogenous housekeeping control  $\beta$ -actin was determined from the standard curve. The relative expression level of each target gene was equated to the ratio:  $SQ_{\text{target}}/SQ_{\beta\text{-actin}}$  where SQ means the starting quantity.

For the quantitation of the *Sirt7* expression, QPCR runs were performed with TaqMan assays (Applied Biosystems) on a StepOnePlus Real-Time PCR machine (Applied Biosystems) using the comparative Ct method with GAPDH as an internal control. The *Sirt7* specific FAM TaqMan probe (Mm00461899\_g1) and the GAPDH specific VIC TaqMan probe (4352339E) were purchased from Applied Biosystems.

## **2.2.5 DNA and chromatin analysis**

### **2.2.5.1 Genomic DNA extraction**

Small pieces of mice tails (0.5-1 cm), embryonic membranes or ES cells were digested in 500  $\mu$ l of the tail lysis buffer with 0.4 mg/ml proteinase K by vigorously shaking at 55°C overnight. The supernatant was transferred to a fresh 1.5 ml tube containing 500  $\mu$ l isopropanol and mixed well. The tubes were then centrifuged at 12000xg for 10 min at room temperature to precipitate the genomic DNA. The DNA pellets were washed with 75% ethanol, air dried and then dissolved in 150-200  $\mu$ l 1x TE. The genomic DNAs were stored at 4°C until use.

### **2.2.5.2 Southern blot**

After sufficient digestion by specific restriction enzymes, the genomic DNAs were separated on a 1% agarose gel with ethidium bromide in 1x TAE at 10V/cm for 4-5 hrs. The gel was photographed and the DNA was transferred to a Hybond-N membrane (Amersham) in alkaline buffer (0.4 M NaOH) by capillary blot for overnight. The transferred DNA was cross-linked to the membrane with an UV crosslinker and an energy of 1.5 J/cm<sup>2</sup>. Then, the membranes were washed briefly in 2x SSC and dried on paper. For hybridization, the membrane was first incubated in Church & Gilbert buffer containing 200  $\mu$ g/ml denatured herring sperm DNA at 65°C for 2-3 hrs. During the pre-hybridization, the internal or 3' probes were <sup>32</sup>P-labelled using the same protocol as for the Northern blot. The hybridization was performed in fresh Church & Gilbert buffer containing 100  $\mu$ g/ml herring sperm DNA and 3 000 000 counts/ml at 65°C overnight in a rotary shaker. Following hybridization, the membrane was washed 3 times for 15 min at 60°C with washing buffer and then exposed to an X-ray film at -80°C.

### **2.2.5.3 Chromatin immunoprecipitation**

After washing with 1x PBS twice, cells were cross-linked with 1% formaldehyde at room temperature for 10 min under gentle shaking directly in the culture dishes. The reaction was then quenched by adding 125 mM glycine for 5 min. Cells were washed 3

times with ice-cold 1x PBS, scraped into 1 ml 1x PBS and pelleted at 1000xg for 3 min at 4°C. The cell pellets were resuspended in hypotonic buffer A and incubated on ice for 10 min to lyse the cells and extract the crude nuclei. The nuclei were collected by brief centrifugation (1000xg, 5 min and 4°C). The nuclear pellets were then resuspended in 5 times the volume of nuclei pellet and incubated on ice for 10 min. The chromatin was then sheared into fragments with a length of 0.2-0.5 Kb by sonication, using a diagenode Bioruptor (20 min, 30 seconds on, 30 seconds off, high level, 4°C). To check the sonication efficiency, 10µl of sample were subjected to chromatin extraction using 90 µl of 10% Chelex slurry. After the addition of Chelex, the crosslinking was reversed by boiling the samples. Proteins were digested with 10 µg of proteinase K at 55°C for 30 min, and the proteinase K was inactivated by boiling the sample at 100°C for 10 min. The samples were briefly centrifuged at 12000xg for 1 min and 60 µl of the supernatant were transferred to a fresh tube. The concentration was measured using the Nano Drop 2000c Spectrophotometer. 3 µg of extracted chromatin were run on a 1.5% agarose gel to verify the sonication efficiency. 50-100 µg of sheared chromatin was diluted 10 times in ChIP dilution buffer. 10% of the chromatin was saved as the “input” sample, while the rest of the diluted chromatin was incubated with the respective primary antibody overnight at 4°C on a rotating wheel. The immuno-complexes were precipitated with protein A/G Sepharose beads (diagenode, Cat.ch-503-028) for 3 hours at 4°C. The beads were washed sequentially, once with low salt washing buffer, once with high salt washing buffer, once with LiCl washing buffer and twice with TE buffer. After the final wash, the residual buffer was aspirated with an insulin needle. 100 µl of 10% Chelex slurry were added to the beads and the chromatin was extracted as described above. Samples were centrifuged at 12000xg for 1 min and 60 µl of the supernatant were transferred to a fresh tube. Additional, 40 µl of distilled H<sub>2</sub>O were added to the Chelex resin, centrifuged at 12000xg for 1 min, and 40 µl of the supernatant were combined with the previously collected supernatant. The DNA was analysed by QPCR using an iCycler Real Time PCR machine (BioRad) and the quantification was performed by standard curve method.

## **2.2.6 Protein analysis**

### **2.2.6.1 Total protein extraction**

For isolation of whole-cell extracts, cells grown on 12 well plates or 6 cm dishes were washed twice with ice-cold 1x PBS and lysed on ice with an appropriate amount of extraction buffer. The cells were then scraped off, transferred to an eppendorf cup and homogenized by sonication on ice. For mouse samples, small pieces of tissue were lysed and homogenized in extraction buffer by sonication on ice. The lysates were then clarified by centrifugation (20000 x g, 5 min, 4°C) and supernatants were stored at -80°C or used for Western blot immediately.

### **2.2.6.2 Quantification of protein concentration**

Protein concentrations were determined using the colorimetric BioRad DC Protein Assay according to manufacturer's instructions. The whole assay is based on the Lowry method (Lowry et al., 1951) and results, dependent on the protein concentration, in the formation of a blue colour change. The absorbance was read-out at 750 nm and a standard curve was generated based on the absorbance values of different amounts of BSA. The concentrations of the protein samples were determined by comparison with the standard curve.

### **2.2.6.3 SDS-PAGE and Western blot**

20-50 µg of total protein lysate were denatured by boiling at 99°C for 5 min in 2x Laemmli loading buffer before loading on 4-12% NuPAGE Novex Bis-Tris gels (Invitrogen). Electrophoresis was performed in 1x MES SDS Running Buffer (Invitrogen) at a constant voltage of 75 volts for 30 min following 150 volts for 1.5 hrs. Separated proteins were transferred to a nitrocellulose membrane (Bio-Rad) using the XCell II Blot module (Invitrogen) and transfer buffer. The transfer was performed for 2-3 hrs at constant voltage of 30V. The transfer efficiency was verified by a water soluble staining with Ponceau S and membranes were stored dry until use. For antibody staining, membranes were shortly washed with ddH<sub>2</sub>O and blocked with 5% skim milk

in 1x TBST for 1hr at room temperature with mild agitation. Then the membranes were washed 5 times with 1x TBST for 5 min at room temperature and incubated with primary antibody diluted in 1x TBST/3% milk or 1x TBST/3% BSA for overnight with gentle shaking at 4°C. The following day, the membranes were washed 6 times for 5 min at room temperature with 1x TBST. Afterwards, the membranes were incubated for 1 hr at RT in 1x TBST/3% milk with a species specific horseradish peroxidase-conjugated secondary antibody that is directed against the primary antibody. After several washing steps for at least 2 hrs at RT with 1x TBST, the detection of the antigen-antibody reaction was monitored using “increased chemiluminescence” (SuperSignal West Femto, Pierce) in a VersaDoc 3000 gel imaging system.

#### **2.2.6.4 Immunoprecipitation assay**

For immunoprecipitation assays, cells were washed twice with ice-cold 1x PBS, harvested by scraping into 1x PBS and centrifuged at 4°C for 5 min at 600 x g. The pellet was lysed in immunoprecipitation lysis buffer (for detection of protein acetylation, the lysis buffer was supplemented with 10 µM TSA and 20 mM NAM) and incubated on ice for 10 min. Then, the sample was sonicated for 5 min at 4°C and MgCl<sub>2</sub> (final concentration of 10 mM) and 10 units of DNaseI (Roche, Cat.04716728001) were added, immediately. After 30 min of incubation at room temperature under constant rotation, the samples were centrifuged for 10 min at 20000 x g at 4°C and the supernatant was transferred to a clean tube. Then, 500 µg-1 mg of protein lysate was incubated with the desired primary antibody for overnight at 4°C under constant rotation. The following day, immunocomplexes were purified by the addition of 25 µl protein G Sepharose beads (Roth, Cat.05015952001) for 2-3 hrs at 4°C with agitation. Beads were washed 7-8 times with lysis buffer and the residual buffer was aspirated with a hypodermic needle after the last washing step. Finally, the beads were boiled in 2x Laemmli loading buffer, separated by SDS-PAGE and analysed by Western blot.

#### **2.2.6.5 Immunofluorescence**

Cells grown on 4 well, 8 well or 16 well chamber slides (Lab-Tek chamber slides, Nunc)

were fixed in 4% PFA for 20 min at room temperature, washed 3 times with 1x PBS, permeabilized with 0.1% TritonX-100 in 1x TBS for 10 min and blocked for 1 h with 3% BSA in 1x TBSTritonX at room temperature. The primary antibody was diluted in 1% BSA in 1x TBSTritonX and applied to the cells for overnight at 4°C. The next day, the cells were washed 3 times for 5 min with 1x TBSTritonX and subsequently incubated with a fluorophore-conjugated secondary antibody and DAPI (4',6'-Diamidino-2-phenylindol) diluted in 1% BSA in 1x TBSTritonX for 1 h at room temperature in the dark. Prior to mounting with mowiol, cells were washed 5 times with 1x TBSTritonX and 2 times with 1x TBST. Pictures were made using fluorescent light microscopy.

## **2.2.7 Mice experiments**

### **2.2.7.1 Mice housing and care**

All animal experiments and transgenic manipulations were performed in accordance to the applicable technological guidelines and animal welfare regulations with the approval of the regional council Giessen. All mice were kept under a 12 h light/dark cycle at 25°C in cages of the laboratory animal facility of the MPI. The mice were fed dry food and water *ad libitum*.

### **2.2.7.2 Killing of the laboratory mice**

The mice were killed by cervical dislocation (CD) according to the particular laboratory mice euthanasia protocol and approved by the Institutional Animal Care and Use Committee.

### 3. Results

#### 3.1 Sirt7 is required for the stimulation of hepatic rDNA transcription in response to insulin

##### 3.1.1 Disturbed hepatic response to fasting/refeeding in Sirt7 KO mice

Sirt7 is a least investigated sirtuin and little information is still available about the functions of Sirt7 in mammals so far. Sirt7 deficient mice were generated and analyzed in our laboratory. Sirt7  $-/-$  mice had a reduced mean and maximal lifespan and developed a progressive, age-dependent inflammatory cardiomyopathy (Vakhrusheva et al., 2008b). Another striking phenotypic feature of Sirt7  $-/-$  mice was their smaller size and leanness, which became apparent at around five months of age. Since the food consumption of Sirt7  $-/-$  mice was even slightly increased, the leanness of the animals could not be attributed to a restricted calorie intake but to a metabolic dysfunction. Because PGC-1 $\alpha$  deficient mice show similar phenotypes to the Sirt7  $-/-$  mice (Arany et al., 2005), we analyzed the expression level of PGC-1 $\alpha$  and other important metabolic genes. Interestingly, a significant reduction of the expression of both, PGC-1 $\alpha$  and PGC-1 $\beta$  was detected in the liver of Sirt7  $-/-$  mice along with a decreased expression of key enzymes of fatty acid synthesis such as ACC and ACLY (Vakhrusheva and Smolka, unpublished data, Fig 3.1).

PGC-1 $\alpha$  is a key regulator of glucose production in the liver of fasted mice through activation of the gluconeogenic pathway (Rodgers et al., 2008). To determine whether Sirt7 deficiency interferes with the gluconeogenic and lipogenic response in liver under conditions of feeding and fasting, the WT mice and Sirt7 KO mice were divided into three groups and fed a normal diet, fasted for 24hrs and re-fed for 24hrs after fasting, then the gene expression of key enzymes involved in gluconeogenesis and lipogenesis metabolism was analyzed through Northern blot.

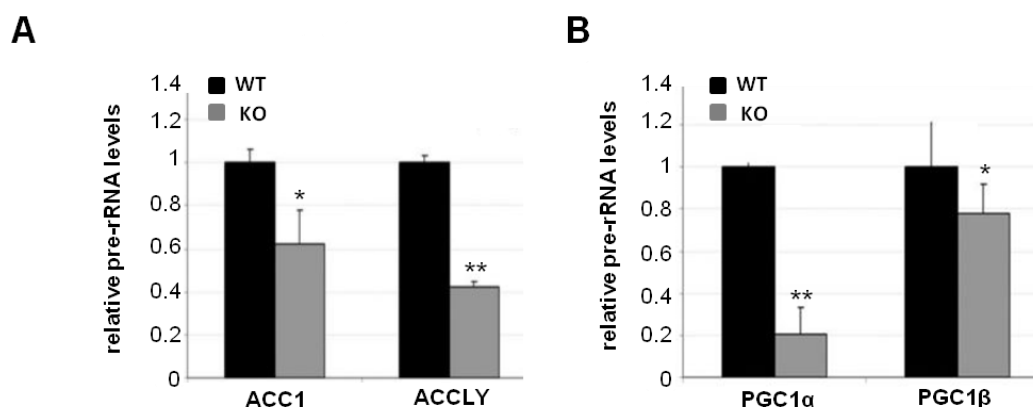


**Figure 3.1 Dysregulation of key enzymes involved in hepatic fat metabolism and of PGC1 $\alpha$  expression.** Quantitative RT-PCR analysis of the expression of acetylcarboxylase (ACC1) and ATP-citrate lyase (ACLY) (enzymes involved in fat metabolism)(A) and PGC-1 $\alpha$  and PGC-1 $\beta$ (B) in the WT and Sirt7 deficient liver. The relative mRNA levels represent means from three different animals per group and were calculated as a difference of expression between wild-type and knockout. Significance was determined by Student's *t* test. \* indicates the significance between WT and Sirt7KO: \*  $P < 0.05$ ; \*\*  $P < 0.01$ . Data from Christian Smolka.

As expected, fasting increased levels of mRNAs encoding the gluconeogenic enzyme PEPCK and down regulated the key enzymes of fatty acid synthesis FAS and AceCS1 in wild type mice, and expression of these genes was restored to normal levels upon refeeding (Fig 3.2A). The patterns of these key enzymes changes under fasting and refeeding in the liver of mice lacking Sirt7 were similar as their control wild type mice. However, the degree of these genes response to fasting and refeeding in the liver of Sirt7 KO mice was exaggerated: Expression of lipogenic genes AceCS1 and FAS was more severely reduced under fasting and showed less recovery upon refeeding than WT. Likewise, gluconeogenic enzyme PEPCK was increased much more under fasting and decreased less under refeeding (Fig 3.2A).

Sirt7 is reported as an activator of pre-rRNA transcription and is enriched in metabolically active tissues including the liver (Ford et al., 2006). Since the ribosome biogenesis is very important for liver growth and function (Chaudhuri and Lieberman, 1968), the pre-rRNA transcription levels in the liver of Sirt7KO and WT animals were examined by quantitative real-time PCR. Fig 3.2B shows that the relative levels of pre-rRNA in the liver were slightly induced upon fasting and reduced to normal levels after refeeding in WT mice. Although there was no significant change between WT and

KO in the normal diet condition, fasting caused a much stronger increase in pre-rRNA transcription in the Sirt7 deficient mice liver than in the WT controls (WT  $P_{F/ND}=0.01$  vs. S7KO  $P_{F/ND}=8.94E-05$ ). After refeeding, the pre-rRNA transcription levels remained high and did not revert to the normal levels in Sirt7 KO mice (WT  $P_{RF/F}<0.001$  vs. S7KO  $P_{RF/F}=0.07$ ). These results indicated that although the adaptive response to fasting/refeeding in the liver of Sirt7 deficient mice still exists, its regulation and fine-tuning are severely disturbed.

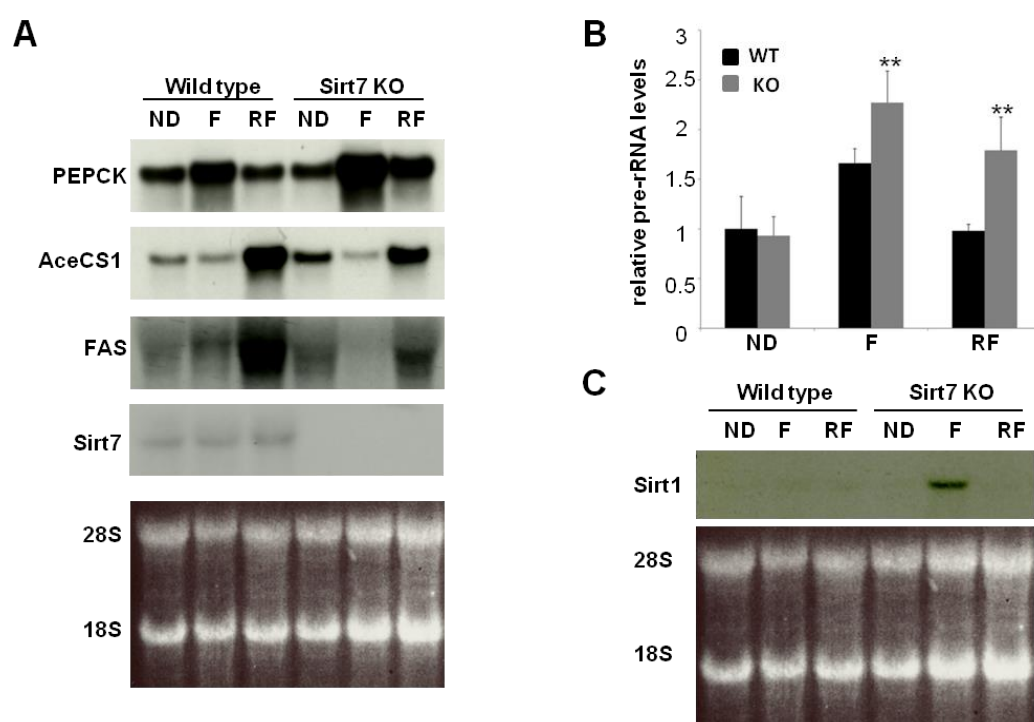


**Figure 3.2 Disturbed expression of genes encoding key enzymes involved in gluconeogenesis and lipid metabolism and of the pre-rRNA transcription in Sirt7 deficient mice liver in response to fasting/refeeding.** Wild-type (WT) (n=15) and Sirt7 KO mice (n=15) were divided into 3 groups: normal diet (ND), fasting for 24hrs (F) and refeeding for 24hrs after fasting (RF). The total liver RNA was isolated and pooled for each group. (A) Northern blot analysis of expression of phosphoenolopyruvate kinase (PEPCK), acetyl-CoA synthetase 1 (AceCS1) and fat synthase (Kralisch et al.). Ethidium bromide (Eth Br) staining of ribosomal RNA was shown as a loading control. (B) Quantitative RT-PCR analysis of pre-rRNA transcription levels. The relative pre-rRNA levels were normalized to  $\beta$ -actin. Values are average $\pm$ SD. Significance was determined by Student's *t* test. \* indicates the significance between WT and Sirt7KO; \*\*  $P < 0.01$ . (C) Northern blot analysis of expression of Sirt1 in the liver. Ethidium bromide (Eth Br) staining of ribosomal RNA as loading control.

### 3.1.2 Higher Sirt1 expression in the liver of Sirt7 deficient mice during fasting

Since recent papers had indicated that hepatic Sirt1 is an important factor in the regulation of glucose and lipid metabolism in response to fasting (Rodgers et al., 2005;

Rodgers and Puigserver, 2007), I was further interested in whether the hepatic Sirt1 expression level was changed in Sirt7 deficient mice. Although there was no change at the mRNA level of Sirt1 in the livers lacking Sirt7 under the normal diet condition, fasting enhanced the transcription of Sirt1 significantly higher in the Sirt7 KO mice (Fig 3.2C).

### 3.1.3 Transcription levels of pre-rRNA do not change in WT and Sirt7KO hepatocytes cultured in different glucose concentration

Primary cultures of hepatocytes are widely used to investigate liver function. It was shown that the rDNA transcription level was down-regulated following deprivation of glucose in HeLa cells (Murayama et al., 2008). Therefore, I wanted to check whether similar glucose-dependent regulation of rDNA transcription takes place in WT and Sirt7 KO hepatocytes. WT and Sirt7 deficient primary hepatocytes were cultured in different glucose concentration for 24hrs, and then the pre-rRNA transcription level was measured by real-time PCR. Fig 3.3A showed that there were no significant changes at low and normal glucose concentration in WT or KO hepatocytes. However, the rDNA transcription levels were significantly higher in the Sirt7 deficient hepatocytes when cultured in the high glucose medium ( $0.01 < p < 0.05$ ). To prove whether the hepatocytes responded normally to change in glucose concentration, the expression of PEPCK, a critical enzyme regulated by glucose, was analyzed by qPCR. Indeed, PEPCK expression was high in no or low glucose and was down regulated in high glucose medium (data not shown). Real time quantitative PCR analysis also confirmed the enhancement of pre-rRNA transcription in HeLa cells cultured in the high glucose medium as previously described (Murayama et al., 2008) (Fig 3.3B).

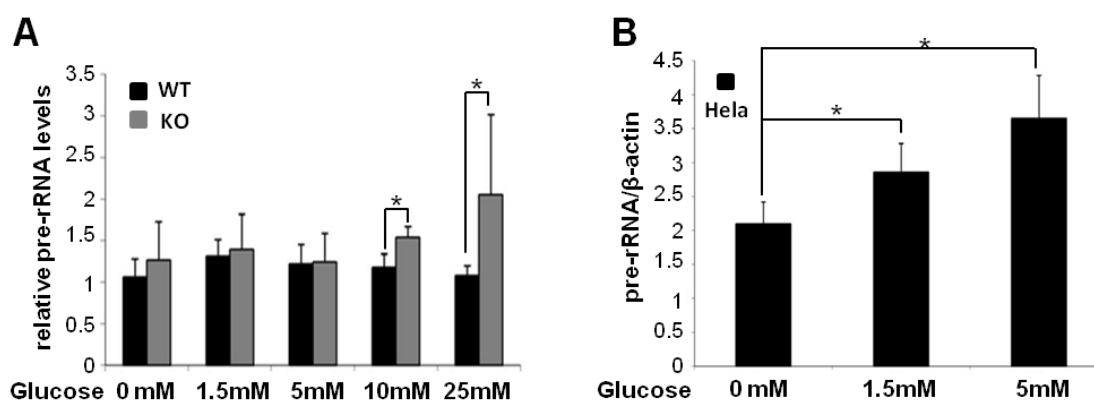


**Figure 3.3 Different glucose concentration does not affect transcription of pre-rRNA in hepatocytes but in HeLa cells.** (A) Primary hepatocytes from Wild-type (WT) (n=6) and Sirt7 KO mice (n=6) were cultured in medium containing 0, 1.5, 5, 10, 25mM glucose, and pre-rRNA transcription levels were analyzed by quantitative RT-PCR. The relative pre-rRNA levels were normalized to  $\beta$ -actin. Values are average $\pm$ SD. Significance was determined by Student's *t* test. \* indicates the significance between WT and Sirt7KO: \*  $P < 0.05$ ; \*\*  $P < 0.01$ . (B) Analysis of pre-rRNA transcription levels in HeLa cells cultured in medium containing 0mM, 1.5mM or 5mM glucose for 24hrs. Values are average $\pm$ SD for triplicate measurements. Significance was determined by Student's *t* test. \* indicates the significance between no glucose and different glucose concentration: \*  $0.01 < P < 0.05$ .

### 3.1.4 Insulin stimulates pre-rRNA transcription in WT hepatocytes, but not in the Sirt7 KO hepatocytes

Insulin is a critical hormone for regulation of glucose and lipid homeostasis in the body. It also plays a key role in the regulation of protein synthesis in a number of tissue and cell culture systems. It has been reported that insulin enhances ribosome biogenesis by stimulating the transcription of the pre-rRNA to some extent (Hannan et al., 1998). Studies in primary cultures of rat hepatocytes indicated that insulin caused an elevation in the rRNA content by stimulating the transcription of rDNA and by slowing the degradation rate of ribosome (Antonetti et al., 1993). Primary hepatocytes isolated from both WT and Sirt7 KO mice (age about 3 months) were cultured in medium with or without insulin. Interestingly, the pre-rRNA transcription level was increased following the insulin treatment in WT hepatocytes, whereas loss of Sirt7 blocked the stimulation of hepatic pre-rRNA transcription by insulin (Fig 3.4A). In contrast, PEPCK expression was significantly down-regulated by insulin in both WT and KO hepatocytes (data not shown). In experiments with hepatocytes derived from old mice (more than 18 months), insulin treatment also increased pre-rRNA transcription level in WT

hepatocytes (Fig 3.4B), although the changes were significant only when treated by 20nM insulin while in young hepatocytes significant activation of rDNA transcription was observed already after treatment with low insulin concentration (10nM) (Fig 3.4A). Interestingly, insulin failed completely to enhance the transcription of pre-rRNA in the hepatocytes from old Sirt7 KO mice (Fig 3.4B). These results suggest that Sirt7 is required for insulin stimulated hepatic ribosomal DNA transcription.

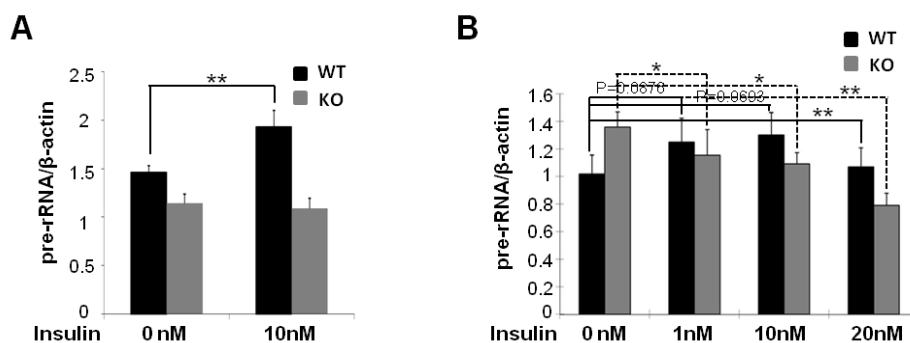


**Figure 3.4 Insulin stimulates pre-rRNA transcription in WT but not in Sirt7 deficient hepatocytes.**

(A) Primary hepatocytes from young (about 3 months) Wild-type (WT) (n=3) and Sirt7 KO mice (n=3) were cultured in medium containing 0 or 10nM insulin. Glucose concentration was kept as 5mM in all assays. The pre-rRNA transcription levels were analyzed after 24hrs by quantitative RT-PCR. The relative pre-rRNA levels were normalized to  $\beta$ -actin. Values are average $\pm$ SD. Significance was determined by Student's *t* test. \* indicates the significance after insulin treatment: \*\*  $P < 0.01$ . (B) Analysis of pre-rRNA transcription levels in primary hepatocytes from old (more than 18 months) wild-type (WT) (n=3) and Sirt7 KO mice (n=3), which were cultured in medium containing 0nm, 1nm, 10nm or 20nM insulin for 24hrs. Values are average $\pm$ SD. Significance was determined by Student's *t* test. \* indicates the significance after insulin treatment: \*  $P < 0.05$ ; \*\*  $P < 0.01$ .

### 3.1.5 Hypoacetylation of histones and lower Pol I and UBF binding to rDNA promoter after insulin stimulation in Sirt7 deficient hepatocytes

RNA polymerase I and UBF are both important components of transcription initiation complex on the rRNA gene promoter. Insulin was found to increase the nuclear content of UBF in 3T6 and H4-II E-C3 rat hepatoma cells (Antonetti et al., 1993). However, no significant changes were detected in the protein levels of UBF or Pol I with or without insulin treatment in both WT and KO mice hepatocytes on the western blot (data not shown). ChIP analysis revealed that the binding of Pol I and UBF to the rDNA promoter was both increased after insulin stimulation in WT but slightly decreased in Sirt7 deficient hepatocytes, which is consistent with the alteration

of pre-rRNA transcription observed after insulin treatment. Moreover, the occupancy of Pol I and UBF was diminished in Sirt7 lacking cells as compared to the WT cells (Fig 3.5A and 3.5B). In addition, insulin induced acetylation at Lys9 of histone H3 on rDNA promoter in WT hepatocytes, thus transforming rDNA genes into euchromatin to turn on transcription. In contrast, in the Sirt7KO hepatocytes, H3K9 was deacetylated which explains the repression of pre-rRNA transcription (Fig 3.5C). These results imply that Sirt7 is required for the stimulation of rDNA transcription by insulin in the liver via the recruitment of RNA Pol I and UBF to the rDNA promoter and the increased acetylation of histones.

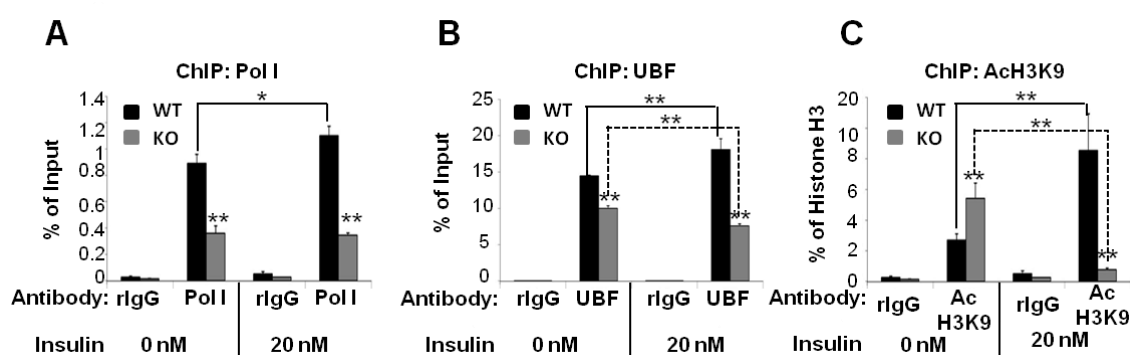


**Figure 3.5 The increased recruitment of Pol I and UBF to rDNA promoter and higher of acetylation of H3K9 at the rDNA can be seen in WT but not Sirt7 KO hepatocytes after insulin treatment.** (A-B) ChIP assay of RNA polymerase I (Pol I) (A) and upstream binding factor (UBF) (B) recruitment to the rDNA promoter in WT (n=3) and Sirt7 deficient (n=3) hepatocytes from old mice, cultured with 20nM or without (0nM) insulin for 24hrs. (C) ChIP assay of AcH3K9 enrichment on the rDNA promoter in WT and KO hepatocytes in the medium with (20nM) or without (0nM) insulin for 24hrs. The 3 different hepatocytes from the same genotype were mixed together for ChIP experiments. All values are average $\pm$ SD for triplicate. Significance was determined by Student's *t* test. \* indicates the significance after insulin treatment and between WT and Sirt7KO: \*  $P < 0.05$ ; \*\*  $P < 0.01$ .

---

## 3.2 Sirt7 is necessary for an efficient adipocyte differentiation and WAT homeostasis through repression of Sirt1, a negative regulator of PPAR $\gamma$

### 3.2.1 Sirt7 is necessary for efficient adipocytes differentiation in culture

Adult Sirt7 KO mice reveal strikingly diminished fat stores and have reduced body size and mass beginning at 5 months of age (Vakhrusheva et al., unpublished data, Fig 3.6 A, B). These changes were not caused by hypophagy since Sirt7 KO mice consumed similar amounts of food as the WT mice (data not shown). Furthermore, histological analysis of sections through the skin of mutant and normal mice showed that the subcutaneous fat layer was greatly reduced in Sirt7 KO mice, together with the significantly reduced cell size of adipocytes in the mutant mice (Vakhrusheva et al. unpublished data, Fig 3.6 C, D). In line with these observations, gene expression analysis of white adipose tissue taken from 8-month-old mice demonstrated a marked decrease in adipogenic markers PPAR $\gamma$  and aP2 in the remaining Sirt7 deficient adipose tissue (Fig 3.6 E).

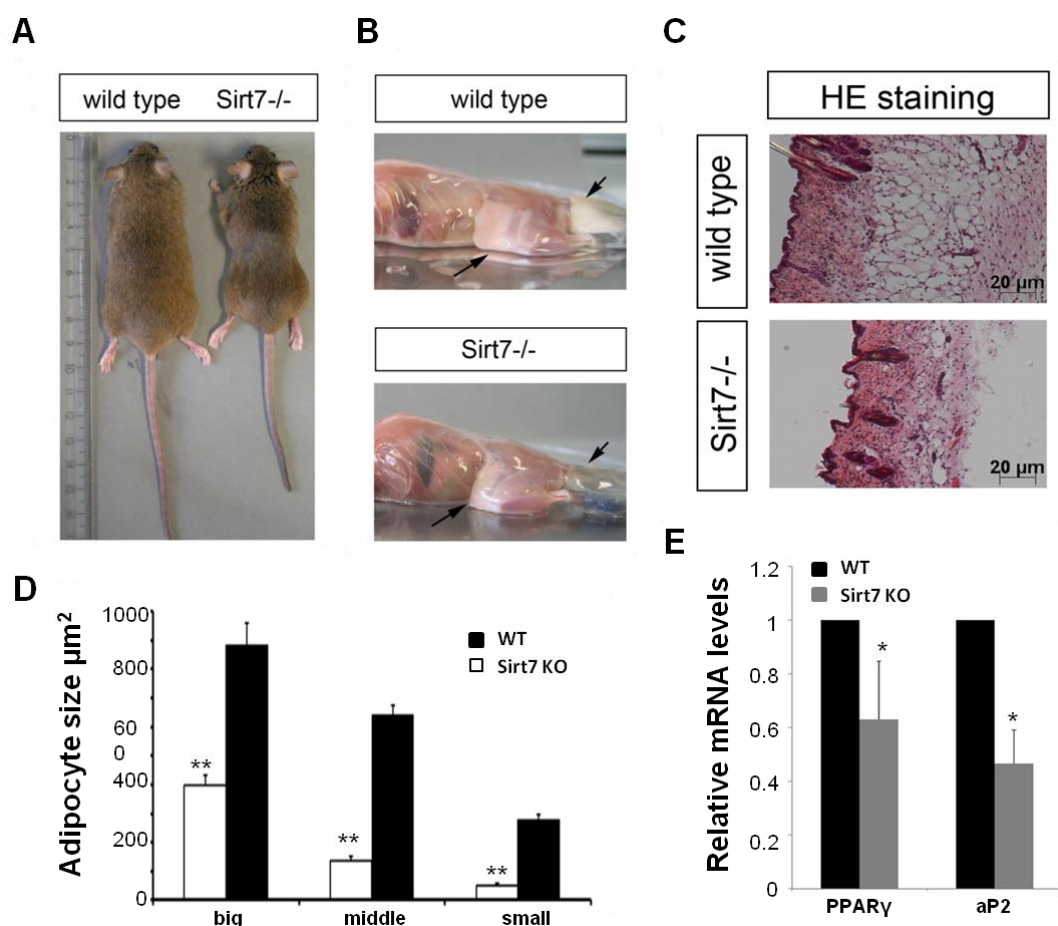


**Figure 3.6 Sirt7 knockout mice accumulate less subcutaneous and visceral fat with age.** (A) General appearance of 10 months old Sirt7 KO mice as compared to wildtype littermates. (B) Skinned wildtype and Sirt7 KO mice reveal diminished fat stores pointed out by arrows. (C) HE stained cross section through the skin of Sirt7 knockout and control mice. (D) Estimates of adipocytes sizes in WT and KO mice. (A-D) from Olesya Vakhrusheva. (E) Quantitative RT-PCR analysis of adipogenic genes PPAR $\gamma$  and aP2 in white adipose tissue of WT (n=3) and Sirt7 KO (n=3) mice (18months old). Gene expression was normalized to  $\beta$ -actin. The relative mRNA levels represent average from three different animals per group and were calculated as a difference of expression to wild-type, WT control as 1. All values are average $\pm$ SD. Significance was determined by Student's t test. \* indicates the significance between WT and Sirt7KO: \* P < 0.05; \*\* P < 0.01.

A decreased amount of adipose tissue may be caused by various factors. As we excluded hypophagy as a cause of the fat stores reduction, I wanted to investigate whether the potency to adipogenesis might be impaired in Sirt7 KO mice. Primary MEFs (mouse embryonic fibroblasts) derived from either wild type or Sirt7 KO mice were isolated and cultivated in the presence of synthetic PPAR $\gamma$  agonist rosiglitazone. A significant decrease in the abundance of Oil Red O positive lipid droplets was observed in the Sirt7 deficient MEFs compared with wild type cells differentiated for 5 days and 8 days (Fig 3.7A). Consequently, quantitative real-time PCR performed on the MEFs

during different time points of differentiation revealed a dramatic reduction of adipogenic gene markers expression, including PPAR $\gamma$ , CEBP $\alpha$ , and aP2 in Sirt7 KO MEFs as compared to WT cells (Fig 3.7B-D). In agreement with the mRNA results, protein expression of adipocytes marker aP2 was also severely reduced in Sirt7 deficient MEFs cultivated for 5 and 8 days in differentiation medium (Fig 3.7E).

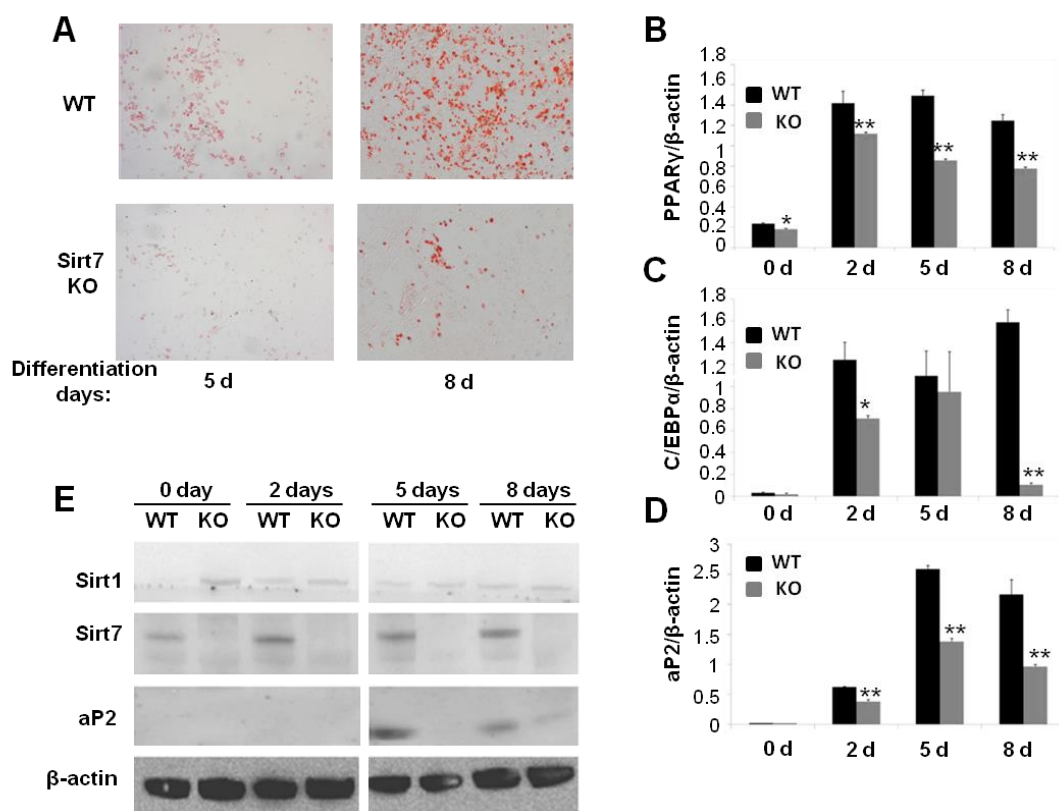


**Figure 3.7 Sirt7 is required for adipogenesis in primary MEFs.** (A) In vitro adipocytes differentiation of primary MEFs isolated from WT and Sirt7 KO mice. Morphological differentiation after 5 days (left) or 8 days (right) was visualized with oil red O staining. (B-D) The mRNA expression of adipogenic markers PPAR $\gamma$ , C/EBP $\alpha$  and aP2 at different time points after differentiation, respectively, was analyzed by quantitative RT-PCR and normalized to  $\beta$ -actin. All values are average  $\pm$  SD for triplicate measurements. Significance was determined by Student's t test. \* indicates the significance between WT and Sirt7KO: \* P < 0.05; \*\* P < 0.01. (E) Protein expression levels of Sirt1, Sirt7 and aP2 in WT and KO MEFs during adipogenesis were detected by Western blot.  $\beta$ -actin is the loading control.

The white preadipocytes cell line 3T3-L1 has been extensively used to study adipocytes differentiation *in vitro*. To further investigate the potential role of Sirt7 in adipogenesis, I therefore performed knock-down experiments using lentiviral RNAi constructs in 3T3L1 cell lines and generated five stable cell lines containing different shRNA sequences against Sirt7. The target sequences of Sirt7 were ShRNA No.1#,

5'-CCTCC CTCTT TCTAC TCCTTA-3'; ShRNA No.2#, 5'-CCTGG AGATT CCTGT CTACAA-3'; ShRNA No.3#, 5'-CGGGA TACCA TTGTG CACTTT-3'; ShRNA No.4#, 5'-TGCAT CCCTA ACAGA GAGTAT-3' and ShRNA No.5#, 5'-GTAGG AAGTC ACTAT GCAGAA-3'. The results showed that Sirt7 was strongly decreased at both the mRNA and the protein level in these stable cell lines, the most efficient one was the cell line No.5 (Fig 3.8A-B). Importantly, the results determined by Oil red O staining assay indicated that Sirt7 knockdown by RNA interference (RNAi) suppressed adipocyte differentiation, the most efficient impaired adipogenesis was in cell line No.5 (Fig 3.8C). These results confirmed the essential role of Sirt7 in adipogenesis demonstrated in the Sirt7 <sup>-/-</sup> MEFs. However, a slightly increased adipogenesis was observed in the No.3 knockdown cells. Analysis of No.3 shRNA sequence revealed that it can not only knock down Sirt7 but also other genes including EGF, kif14 and adam25. The No.5 knock down stable cell line was chosen for further investigation. After 7 days of differentiation in medium without rosiglitazone, oil red O staining showed that there were significantly fewer terminally differentiated adipocytes in cells in which Sirt7 had been silenced than in control scramble cells (Fig 3.8D). Furthermore, the mRNA expression of PPAR $\gamma$  and aP2 were decreased in Sirt7 knock down cells as demonstrated by quantitative real-time PCR. In agreement with the mRNA levels, the western blot results indicated down-regulation of adipocytes specific protein aP2 in the Sirt7 knock down cells (Fig 3.8 E-F). Taken together, these results suggest that Sirt7 is required for the efficient adipogenesis of fibroblasts and 3T3-L1 preadipocytes in culture.

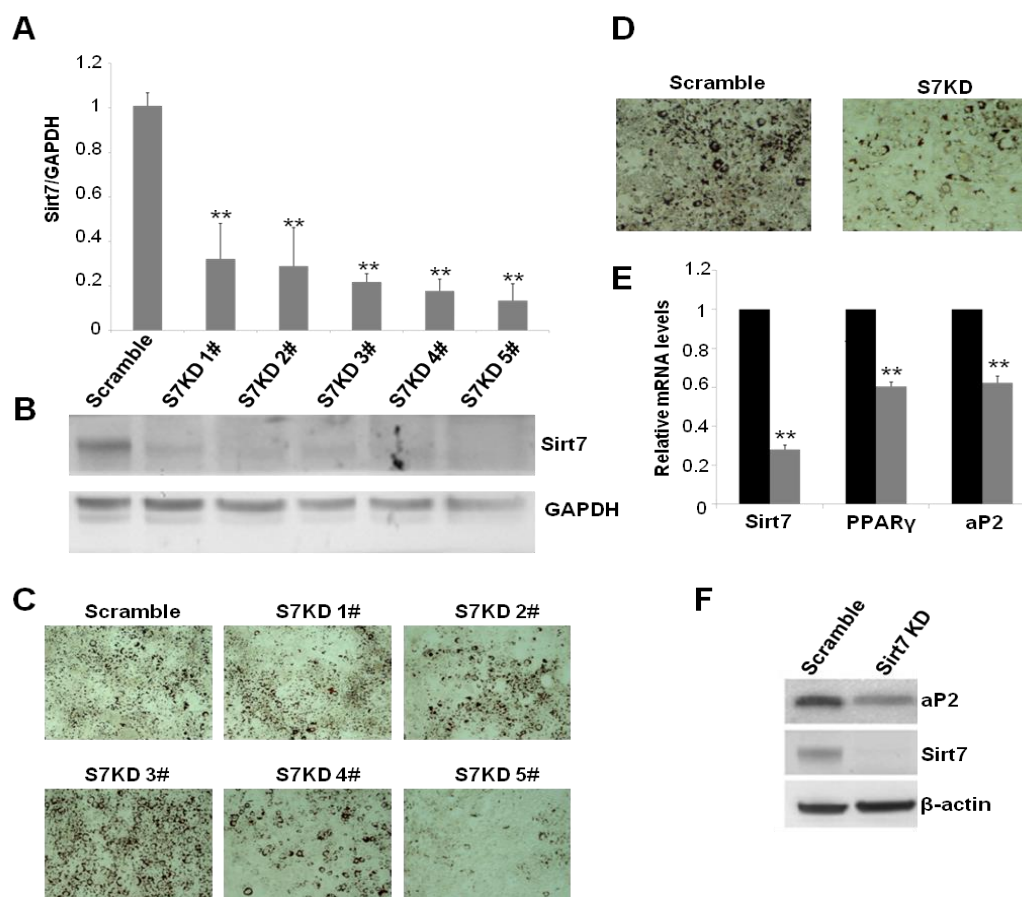


**Figure 3.8 Sirt7 is required for differentiation of 3T3-L1 preadipocytes.**

(A) The Sirt7 mRNA level in stable Sirt7-knockdown 3T3-L1 cells without adipogenesis. S7KD1#, 2#, 3#, 4# and 5# were five stable celllines generated by five different retroviral shRNA constructs. Scramble indicates control shRNA construct. Endogenous Sirt7 mRNA was determined by quantitative RT-PCR and normalized to GAPDH. Results are presented as fold expression compared to scramble. All values are average  $\pm$  SD for triplicate measurements. Significance was determined by Student's t test. \* indicates the significance compared to scramble cells: \*\*  $P < 0.01$ . (B) Sirt7 protein level in stable Sirt7-knockdown 3T3-L1 cells without differentiation was detected by Western blot. GAPDH was blotted as loading control. (C) The inhibited adipocyte differentiation in Sirt7-knockdown 3T3-L1 cells (2#, 4# and 5#). The cells were induced with standard differentiation medium without rosiglitazone. On day 8, the cells were stained with Oil-red-O. (D) The stable 3T3-L1 cells infected with S7KD5# or scramble were induced to adipogenesis for 7 days. Oil red O staining showed the blocked differentiation in Sirt7 knockdown cells. (E) The mRNA levels of Sirt7, PPAR $\gamma$  and aP2 in S7KD 5# or scramble stable cells after 7 days differentiation were detected by QRT-PCR and normalized to  $\beta$ -actin. Results are presented as fold expression compared to scramble. All values are average  $\pm$  SD for triplicate measurements. Significance was determined by Student's t test. \* indicates the significance compared to scramble cells: \*\*  $P < 0.01$ . (F) Protein expression levels of Sirt7 and aP2 in knock down cells after adipogenesis were detected by Western blot.  $\beta$ -actin is the loading control .

### 3.2.2 Sirt7 is required for PPAR $\gamma$ expression during adipogenesis

Immortalized MEFs obviate the need to isolate new cells repeatedly and allow more sustained manipulation (such as multiple viral transductions) compared with primary MEFs. Moreover the immortalized MEFs do not easily undergo replicative senescence after repeated divisions. Thus, immortalized WT and Sirt7 KO MEFs were generated and cultured in adipocyte differentiation inducing medium containing rosiglitazone. Subsequently, gene expression of PPAR $\gamma$  and the adipocyte differentiation marker aP2 was analyzed by qRT-PCR during different time points of differentiation. Again, a significantly decreased expression of PPAR $\gamma$ , C/EBP $\alpha$  and aP2 was detected in Sirt7 mutant cells (Fig 3.9A-C). The immunofluorescence staining confirmed the drastic decrease of PPAR $\gamma$  expression also at the protein level in Sirt7 KO immortalized MEFs, which was correlated with the dramatic decrease in lipid accumulation as assessed by Oil red O staining (Fig 3.9D). A similar result was observed in Sirt7 knock down 3T3-L1 cells via immunostaining (Fig 3.9E). To investigate how Sirt7 influences PPAR expression, I further analyzed the epigenetic markers on the promoter. Chromatin immunoprecipitation assays were performed in differentiating immortalized MEFs to reveal the epigenetic status of the PPAR $\gamma$  promoter during adipogenesis in WT and Sirt7 KO MEFs. As expected, a lower acetylation of lysine 9 of histone 3 (AcH3K9), indicating gene inactivation was detected at the PPAR $\gamma$  promoter in Sirt7 KO MEFs after 5 days of differentiation. Interestingly, Sirt7 deletion also led to significant increase of H3K9 trimethylation (H3K9me3), another epigenetic mark for repressed genes at the PPAR $\gamma$  promoter (Fig 3.9F). Similarly, Sirt7 knock down also caused lower acetylation of H3K9 and H4K16 on PPAR $\gamma$  promoter in the differentiating 3T3-L1 cells (Fig 3.9G). These data indicate that Sirt7 is required for the robust transcription of PPAR $\gamma$  during adipogenesis by maintaining high H3K9 acetylation and low H3K9 trimethylation.

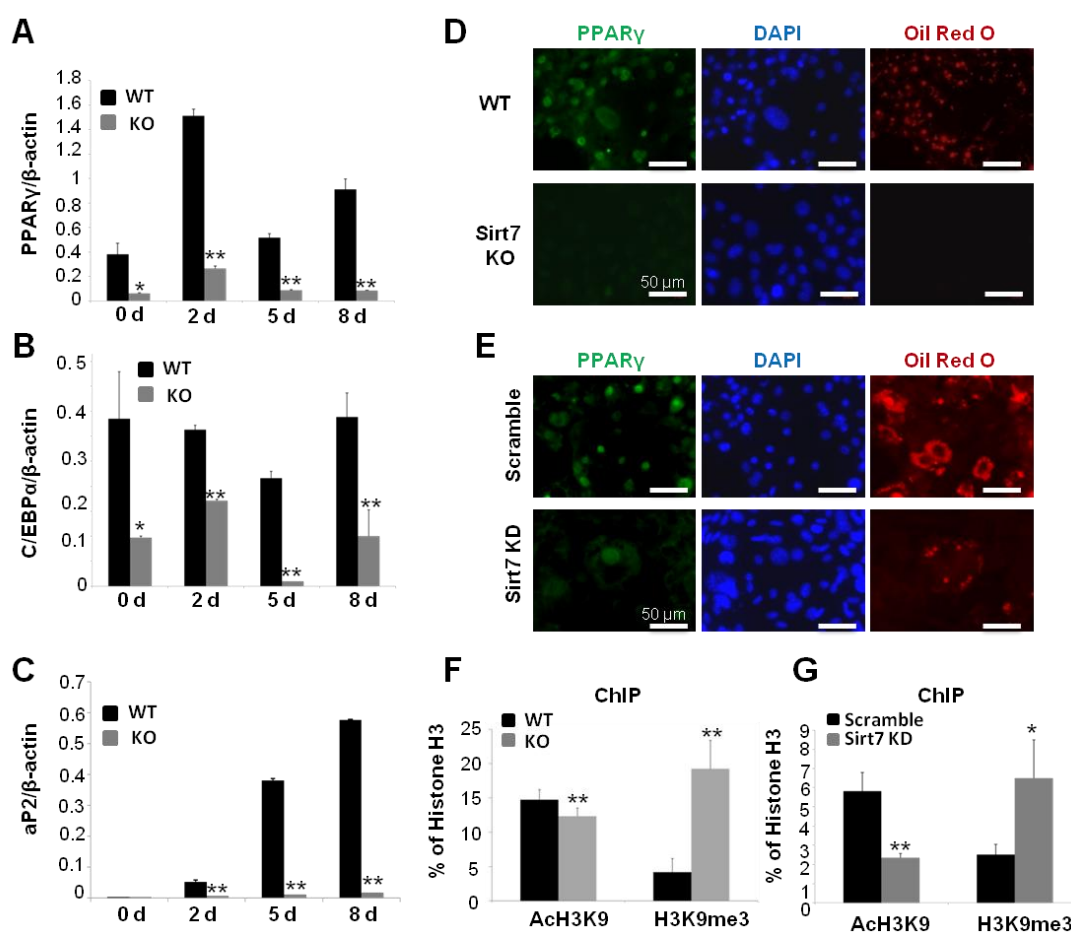


**Figure 3.9 Sirt7 is required for PPAR $\gamma$  expression in MEFs.** (A-C) mRNA expression levels of adipogenic markers PPAR $\gamma$ , C/EBP $\alpha$  and aP2 in WT and Sirt7 KO immortalized MEFs during different differentiation time were determined by quantitative RT-PCR and normalized to  $\beta$ -actin. All values are average  $\pm$  SD for triplicate. Significance was determined by Student's t test. \* indicates the significance between WT and Sirt7KO: \* P < 0.05; \*\* P < 0.01. (D-E) Micrographs of Oil red O staining (red) of the WT and KO immortalized MEFs (D) or scramble and S7KD stable 3T3-L1 cells (E) after 8 days of adipogenesis. The endogenous PPAR $\gamma$  (green) was stained with anti-PPAR $\gamma$  antibody by immunofluorescence assay. Nuclei were stained with DAPI (blue). (F-G) ChIP assay of histone acetylation (Ach3K9) and methylation (H3K9me3) on PPAR $\gamma$ 2 promoter in WT&KO MEFs (F) or scramble&S7KD 3T3-L1 preadipocytes (G). The immunoprecipitated DNA was analyzed by quantitative PCR and normalized to the histone H3. All values are average  $\pm$  SD for triplicate measurements. Significance was determined by Student's t test. \* indicates the significance between WT and Sirt7KO: \*\* P < 0.01.

### 3.2.3 PPAR $\gamma$ overexpression but not Sirt7 overexpression can completely rescue the impaired adipogenesis in Sirt7 KO immortalized MEFs

Ectopic PPAR $\gamma$  is sufficient to stimulate immortalized wild-type MEFs to differentiate into adipocytes even in the absence of synthetic PPAR $\gamma$  ligand (Ge et al.,

2002) and PPAR $\gamma$  can rescue the differentiation of MEFs lacking C/EBP $\alpha$  to mature adipocytes (Rosen et al., 2002). I further asked whether overexpression of PPAR $\gamma$  could rescue the impaired adipogenesis in the Sirt7 knock out MEFs. To investigate whether the severe adipogenesis defects in Sirt7-deficient cells were solely due to the defective expression of endogenous PPAR $\gamma$ , the immortalized MEFs derived from WT or Sirt7 KO mice were infected with either retroviral expression vector for PPAR $\gamma$ -flag or empty vector to create stable cell lines. In these cells, ectopic PPAR $\gamma$  overexpression significantly stimulated the differentiation in wildtype cells as expected, and its overexpression could completely rescue the impaired adipogenesis in Sirt7 deficient MEFs (Fig 3.10A and B), even reaching the differentiation level of WT cells overexpressing PPAR $\gamma$ . However, ectopic overexpression of Sirt7 was not able to fully restore the adipogenic potential in these cells despite the fact that Sirt7 overexpression inhibited Sirt1 protein levels in Sirt7 KO cells to a similar extent as did the PPAR $\gamma$  overexpression (Fig 3.10B). Interestingly, when Sirt7 knock down 3T3L1 cells were infected with retrovirus overexpressing human Sirt7, the expression levels of PPAR $\gamma$  were increased both at mRNA level and protein levels (Fig 3.10C and D). However, no significant changes in the expression level of adipocyte marker gene aP2 (Fig 3.10C) and in lipid droplets accumulation (data not shown) were detected.

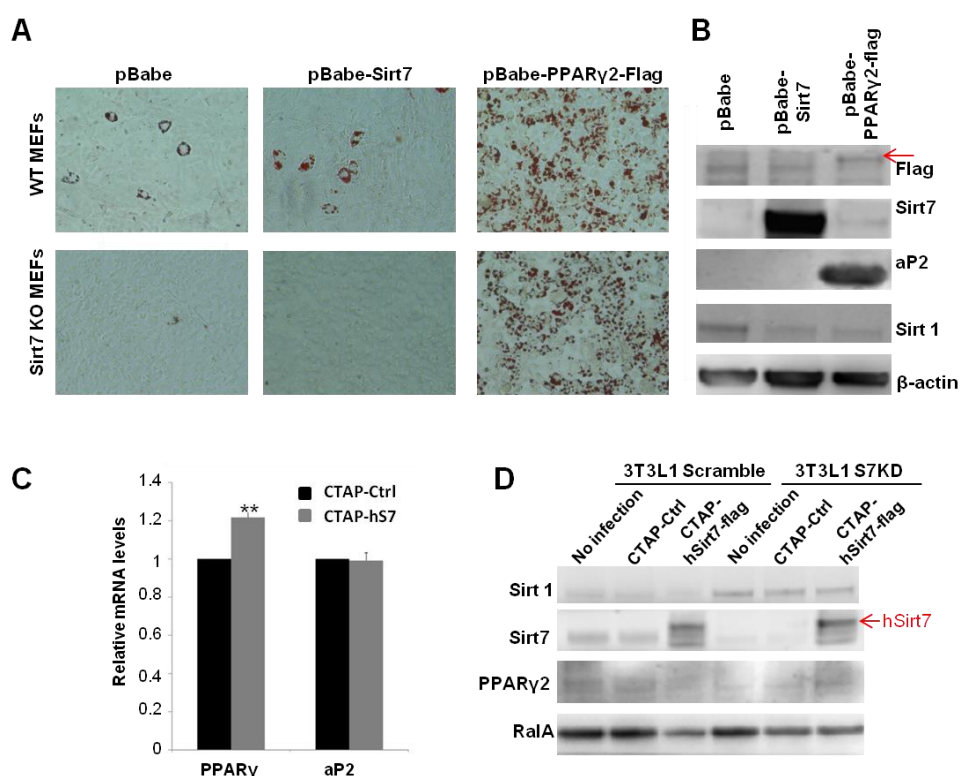


**Figure 3.10 Ectopic PPAR $\gamma$  but not Sirt7 overexpression rescues the adipogenesis defect in Sirt7 deficient cells.** (A-B) Sirt7 deficient immortalized MEFs were infected with retroviral pBabe vector expressing ectopic Sirt7 or PPAR $\gamma$ 2-Flag, and induced to adipocytes differentiation. WT MEFs were also infected to overexpress ectopic Sirt7 or PPAR $\gamma$ 2 as controls. Cells were stained with oil red O after 8 days of differentiation (A). Western blot analysis of ectopic Sirt7 and PPAR $\gamma$ 2 (with anti-Flag antibody) and the endogenous protein expression of Sirt1 and aP2 in the Sirt7 KO cells infected with ectopic Sirt7 or PPAR $\gamma$ 2 after 8 days of differentiation (B). (C-D) Scramble and S7KD 3T3-L1 preadipocytes were infected with retroviral CTAP vector expressing ectopic human Sirt7 or empty control. (C) After 8 days of adipogenesis, the mRNA expression levels of adipogenic markers PPAR $\gamma$  and aP2 were determined by quantitative RT-PCR and normalized to  $\beta$ -actin. Results are presented as fold expression compared to scramble. All values are average  $\pm$  SD for triplicate measurements. Significance was determined by Student's t test. \* indicates the significance between control and hSirt7 OE: \*\* P < 0.01. (D) Protein expression of ectopic Sirt7 and endogenous Sirt1, Sirt7 and PPAR $\gamma$  was detected by Western blot, RalA was blotted as loading control.

### 3.2.4 Sirt1 expression is increased in Sirt7 deficient MEFs during adipogenesis especially at protein level

Sirt1 was reported to inhibit adipogenesis and promote fat mobilization by repressing the activity of PPAR $\gamma$  (Picard et al., 2004). Thus, it was of interest to determine whether Sirt1 expression or activity was affected in Sirt7 knockout cells. Although no significant changes in the expression level of Sirt1 transcripts were detected in wild-type and knockout adipose tissues (Fig 3.11A) and MEFs (Fig 3.11B),

the Sirt1 protein expression was indeed elevated in Sirt7 KO MEFs, especially in the early stage of differentiation (less than 5 days) (Fig 3.6E and 3.11C). Similar increase of Sirt1 protein expression was observed in the Sirt7 knock down 3T3L1 cells (Fig 3.10D).

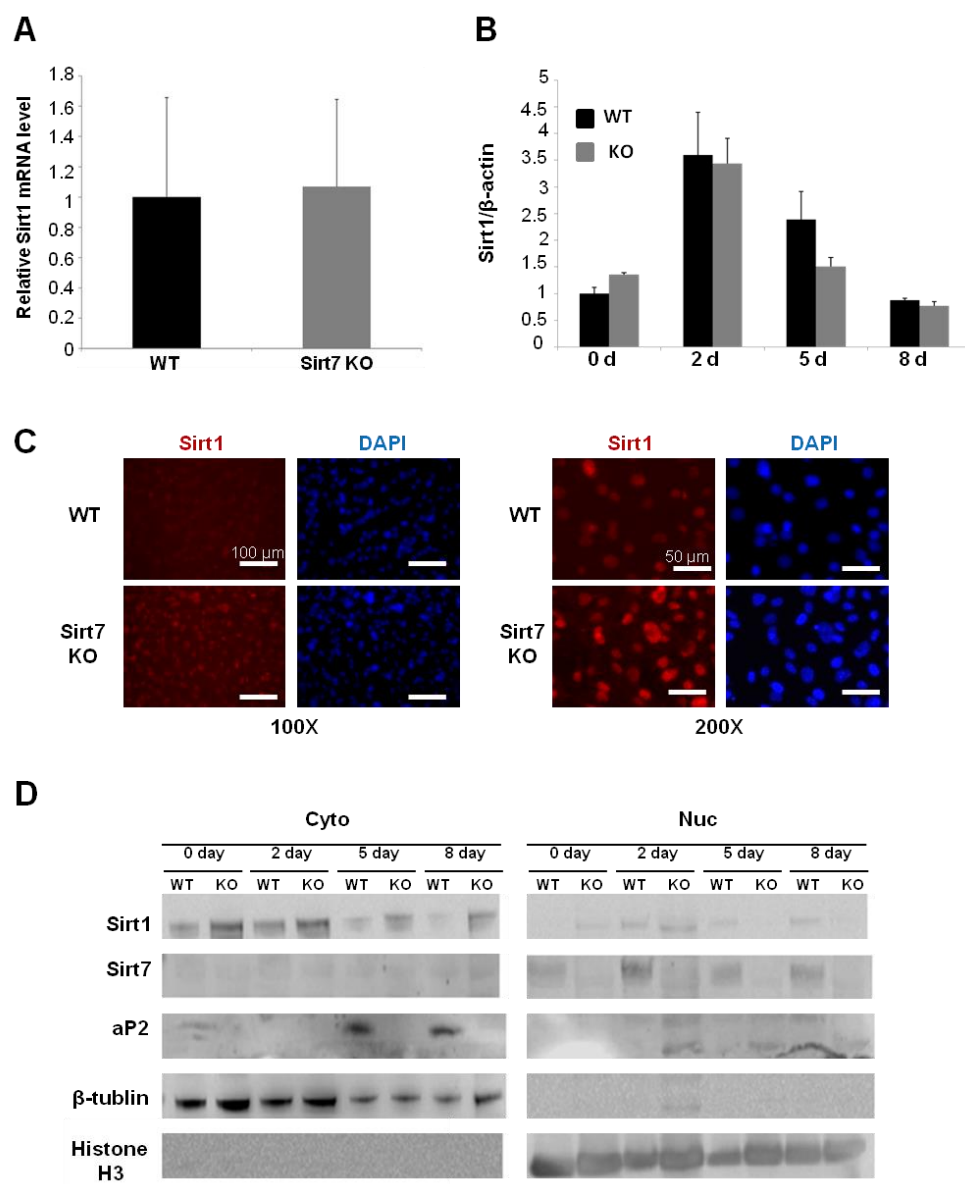


**Figure 3.11 Higher accumulation of Sirt1 protein in Sirt7 deficient cells.** (A-B) No significant changes were detected in Sirt1 mRNA levels in Sirt7 deficient mice WAT (A) or primary MEFs during differentiation (B) by QRT-PCR and normalized to  $\beta$ -actin. In (A) mRNA was isolated from 3 WT and 3 Sirt7 KO mice, results are presented as fold expression compared to WT mice. (C) Detection of Sirt1 protein by immunofluorescence in WT and Sirt7 KO immortalized MEFs pre-induced to differentiation (day 0). (D) Western blot of cytoplasmic (Cyto) or nuclear proteins (Nuc) fractionated from WT and Sirt7KO MEFs at different days of differentiation. aP2 expression indicated adipogenic differentiation; cytosolic fraction  $\beta$ -tubulin and nuclear marker histone H3 were blotted as loading control and cell fraction purity control.

Interestingly, the subcellular localization of Sirt1 seems also to be affected in Sirt7 deficient cells during adipogenesis: While in wild type cells Sirt1 predominantly resides in the cytoplasm of undifferentiated cells (day0), in the knockout cells Sirt1 is not only present in higher amounts in the cytoplasm but also is already detectable in the nucleus (Fig 3.11D). After induction to differentiation, Sirt1 gradually accumulates in the nucleus during adipogenesis in wild type cells and is present in the nucleus and in cytoplasm in all phases of differentiation (Fig 3.11D). In contrast, in Sirt7 knockout cells, Sirt1 is present in the nucleus at early stage of differentiation (day0 and day2) and is no more detectable in the nucleus after prolonged adipogenesis induction (day5 and day8), whereas, Sirt1 is present at higher level in the cytoplasm of Sirt7 KO cells at all investigated time points (Fig 3.11D).

### 3.2.5 Sirt7 inhibits Sirt1 protein level and blocks the recruitment of Sirt1 to the PPAR $\gamma$ promoter during adipogenesis

Sirt1 has been demonstrated to represses PPAR $\gamma$  by docking with its cofactors NCoR (nuclear receptor co-repressor) and SMRT (silencing mediator of retinoid and thyroid hormone receptors) to PPAR $\gamma$  promoter and inhibiting its transcription (Picard et al., 2004). Sirt1 binding to PPAR $\gamma$  promoter was then analyzed in WT&Sirt7 KO MEFs during adipogenesis. CHIP assays showed that Sirt1 binding was increased in Sirt7 KO MEFs after 5 days of differentiation (Fig 3.12A) in consistence with the lower acetylation of H3K9 on PPAR $\gamma$  promoter (Fig 3.8E). The significant increase of Sirt1 occupancy at the PPAR $\gamma$  promoter was observed in the differentiating Sirt7 knock down 3T3-L1 preadipocytes as well (Fig 3.12B). Together, these data suggested that the increased nuclear accumulation of Sirt1 and its increased recruitment at PPAR $\gamma$  promoter might directly contribute to higher deacetylation and hypermethylation of histone 3 on the PPAR $\gamma$  promoter leading to repression of PPAR $\gamma$  transcription in Sirt7 KO cells and thus being, at least in part, responsible for the reduced adipogenesis in Sirt7 deficient cells.

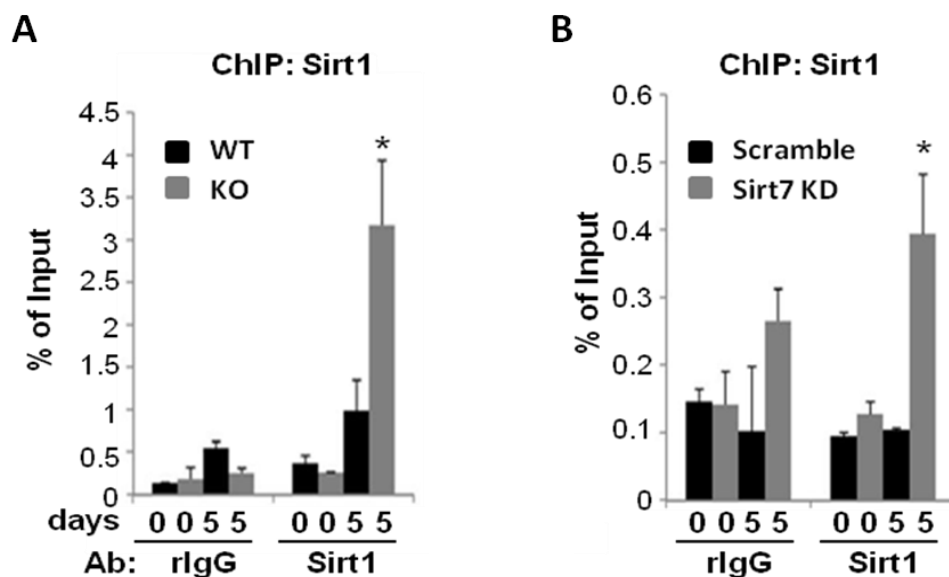


**Figure 3.12 Increased occupancy of Sirt1 at the PPAR $\gamma$  promoter in Sirt7 deficient cells during adipogenesis.** (A-B) ChIP assays of Sirt1 binding at the PPAR $\gamma$ 2 promoter in pre- (day0) and post-induced differentiation (day5) WT and Sirt7 KO immortalized MEFs (A) and Scramble and Sirt7KD

3T3-L1 cells (B). The immunoprecipitated DNA was analyzed by quantitative PCR and normalized to the input DNA. All values are average  $\pm$  SD for triplicate measurements. Significance was determined by Student's t test.

\* indicates the significance between WT and Sirt7KO or Scramble and Sirt7 KD: \* 0.01 < P < 0.05.

### 3.2.6 Adipogenesis defects in Sirt7 deficient MEFs can be partly restored by Sirt1 knock down or Sirt1 inhibition by NAM

It was indicated previously that Sirt1 inhibition by RNA interference enhances the adipogenesis potency in 3T3L1 cell lines (Picard et al., 2004). Thus, we wanted to know, whether Sirt1 knock down would improve the adipocytes differentiation of Sirt7 KO MEFs. Sirt1 expression was silenced through retroviral infection with pQsup-Sirt1 RNAi in the immortalized Sirt7 KO MEFs. The knock down efficiency was evaluated by qRT-PCR and Western Blot (Fig. 3.13A and B). After 7 days of differentiation PPAR $\gamma$  and aP2 mRNA expression was significantly increased upon Sirt1 knockdown (Fig. 3.13A). In addition, Sirt1 knockdown cells had slightly increased PPAR $\gamma$  protein and lipid droplets accumulation as compared to control cells (Fig. 3.13C). Similar effect was achieved when Sirt7 KO cells were incubated with Sirt1 inhibitor nicotinamide during the differentiation process (Fig 3.13E). In consistence with the increased number of oil red o positive cells, NAM treatment significantly enhanced the mRNA expression of PPAR $\gamma$  and aP2 in Sirt7 KO MEFs. Thus, inhibition of Sirt1 partially rescues the

impairment of adipocyte differentiation in Sirt7 deficient MEFs (Fig 3.13D).

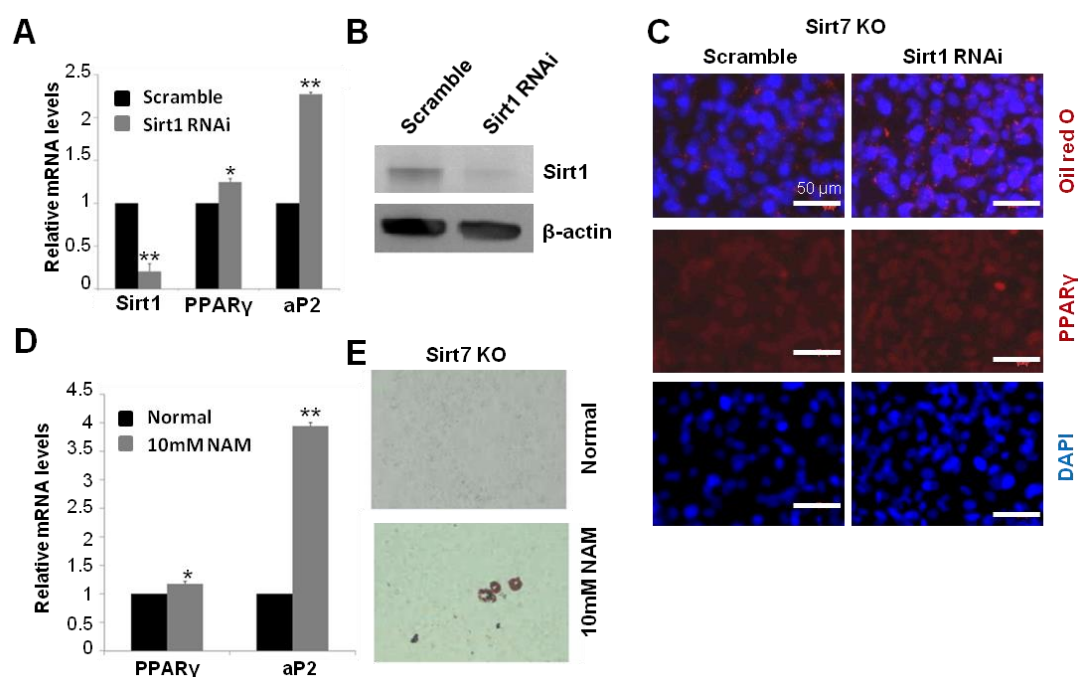


**Figure 3.13 Sirt1 knock down or inhibition of Sirt1 activity can partly rescue the impaired adipogenesis in Sirt7 KO immortalized MEFs.** (A-C) Sirt7 deficient MEFs were

infected with retroviral pSuper scramble shRNA or pSuper-Sirt1 shRNA constructs, then the cells were induced to differentiation for 8 days. (A) mRNA levels of Sirt1 and adipogenic proteins PPAR $\gamma$  and aP2 were determined by quantitative RT-PCR and normalized to  $\beta$ -actin. Results are presented as fold expression compared to Scramble controls. All values are average  $\pm$  SD for triplicate measurements. Significance was determined by Student's t test. \* indicates the significance between Scramble and Sirt1 RNAi: \* P < 0.05; \*\* P < 0.01. (B) Western blot analysis of Sirt1 protein level,  $\beta$ -actin was the loading control. (C) Cells after 8 days of differentiation were stained with Oil red O and with anti-PPAR $\gamma$  antibody. Nuclei were stained in blue (DAPI). (D-E) Sirt7 deficient MEFs were cultured with or without 10mM nicotinamide (NAM) and induced to differentiation for 8 days. (D) mRNA levels of PPAR $\gamma$  and aP2 were determined by quantitative RT-PCR and normalized to  $\beta$ -actin. Results are presented as fold expression compared to WT controls. All values are average  $\pm$  SD for triplicate measurements. Significance was determined by Student's t test. \* indicates the significance between Normal medium and 10mM NAM: \* P < 0.05; \*\* P < 0.01. (E) Oil red O stained cells after 8 days of adipogenesis in normal medium or in medium containing 10mM NAM.

### 3.2.7 Removal of one Sirt1 allele rescued the highly compromised adipogenic potential of Sirt7<sup>-/-</sup> primary white preadipocytes and the abnormality of WAT in adult Sirt7 deficient mice

To investigate whether Sirt7 is required for differentiation in primary preadipocytes, primary white preadipocytes were isolated from WT and Sirt7 KO mice and induced to differentiation for 8 days, followed by adipogenesis assay using Oil red

O staining. Sirt7 deletion led to a nearly complete block of adipogenesis in white preadipocytes (Fig 3.14A). Interestingly, the primary white preadipocytes from Sirt7<sup>-/-</sup>/Sirt1<sup>+/-</sup> mice showed increased mature adipocytes accumulation after 8 days of differentiation in contrast to the preadipocytes from Sirt7<sup>-/-</sup>/Sirt1<sup>+/+</sup> mice (Fig 3.14A). Furthermore, in contrast to the phenotype of the significant decrease of WAT weight and the lower mRNA expression of PPAR $\gamma$  in adult Sirt7 KO mice (10-12 months) (Fig 3.14B and C), Sirt7<sup>-/-</sup>/Sirt1<sup>+/-</sup> mice of the same age showed no significant changes as compared to the WT mice or Sirt1<sup>+/-</sup> mice (Fig 3.14B and C). It should be noted that one Sirt7KO mouse (no. 5584) showed even a higher white adipose tissue weight than the average weight of WAT in control mice; however, the PPAR $\gamma$  expression level was still significantly decreased. These findings indicate that Sirt7 is required for adipogenesis in primary preadipocytes and maintains the white adipose mass balance in organismal metabolic homeostasis through the inhibition of the anti-adipogenic factor Sirt1.

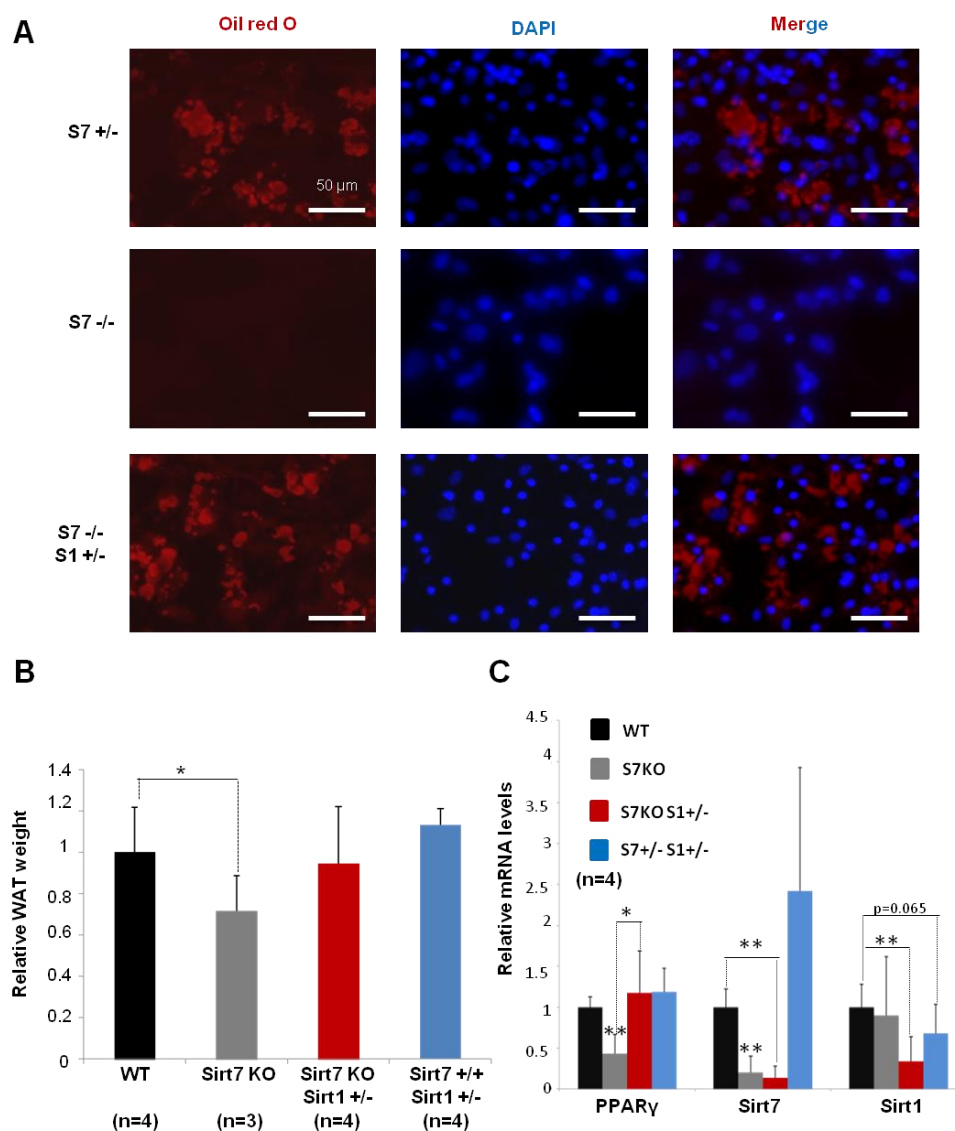


**Figure 3.14 Removal of a single Sirt1 allele improves the adipogenesis of primary Sirt7 deficient preadipocytes and increases the WAT mass and PPAR $\gamma$  expression of Sirt7 KO mice.** (A) Oil red O staining of primary white preadipocytes isolated from Sirt7<sup>+/-</sup>, Sirt7<sup>-/-</sup> and Sirt7<sup>-/-</sup>/Sirt1<sup>+/-</sup> mice cultured in adipocytes differentiation medium for 8 days. Nuclei are stained with DAPI (blue). Note the impaired differentiation of Sirt7<sup>-/-</sup> cells, which is restored after removal of one Sirt1 allele. (B-C) The relative weights of WAT (B) and relative mRNA levels of PPAR $\gamma$ , Sirt7 and Sirt1 (C) in WT, Sirt7 KO, Sirt7 KO/Sirt1<sup>+/-</sup> and Sirt1<sup>+/-</sup> mice. The mRNA levels were determined by quantitative RT-PCR (Taqman probe method) and normalized to GAPDH. Results represent average from several mice per group and were calculated as a fold difference to wild-type, WT control as 1. All values are average  $\pm$  SD. Significance was determined by Student's t test. \* P < 0.05; \*\* P < 0.01.

### 3.3 Sirt7 can inhibit Sirt1 activity by interfering with its auto-deacetylation

#### 3.3.1 Sirt7 does not deacetylate Sirt1 but increases the acetylation of Sirt1 and inhibits its activity

Taken together, our data imply that Sirt7 normally ensures efficient adipocytes differentiation by inhibition of Sirt1 activity and/or by destabilization of Sirt1 protein. Moreover, Sirt7 deficient hepatocytes have the disturbed response to fasting/refeeding and fail to stimulate the rDNA transcription by insulin. These changes might be also caused by a high protein amount and/or high activity of Sirt1. We exclude an influence of Sirt7 on Sirt1 transcription since there were no significant changes in Sirt1 transcripts levels in Sirt7 KO WAT or MEFs (Fig 3.11A and B). In contrast, the protein levels were significantly higher in Sirt7 KO MEFs or Sirt7 knock down cells (Fig 3.7E, Fig 3.10D, Fig 3.11C and D). We further asked whether Sirt1 protein might interact with and be regulated by Sirt7 via post-translation-modification. In fact, in cells overexpressing Sirt1-CFP fusion protein, endogenous Sirt7 peptides could be identified by mass-spectrometry among proteins precipitated with anti-(CGY)FP antibody and vice versa endogenous Sirt1 peptides were found in cell precipitates from the Sirt7-YFP overexpressing cells. The interaction between Sirt1 and Sirt7 was further confirmed in immunoprecipitation experiments (Fig 3.15A Smolka, unpublished data). The Sirt1/Sirt7 interaction was dependent on the intact Sirt7 deacetylation core domain because point mutation of two critical residues (N169 and H188) in its catalytic domain or expression of amino acids 1-210 of 5'-N-terminus without an intact catalytic domain both abolished binding of Sirt1 to Sirt7 (Fig 3.15A Smolka, unpublished). The inability of Sirt7 inactivating mutations to bind Sirt1 suggested that Sirt1 might be a substrate for Sirt7 dependent deacetylation. However, co-expression of Sirt7 with Sirt1 resulted in increased Sirt1 acetylation level whereas the Sirt1 acetylation was very low when it was expressed alone (Fig 3.15B). Moreover, when wildtype Sirt7, but not its catalytic inactive H188Y mutant was co-expressed with Flag-tagged Sirt1, a higher Sirt1 acetylation was observed (Fig 3.15C). Therefore, we hypothesized that Sirt7 does not

directly deacetylate Sirt1, but promotes certain acetyltransferase(s) to acetylate Sirt1 or inhibits other deacetylation enzyme(s). Since Sirt1 is a deacetylase we speculated that Sirt1 might deacetylate itself and that Sirt7 prevents its auto-deacetylation activity. Importantly, mapping of the acetylation sites of Sirt1 by liquid chromatography-tandem mass spectrometry analysis (LC-MS/MS) identified 4 acetyl-modified lysine residues in Sirt1 in the presence of Sirt7 (Fig 3.15D), while no acetylated residues were detected in the absence of Sirt7.

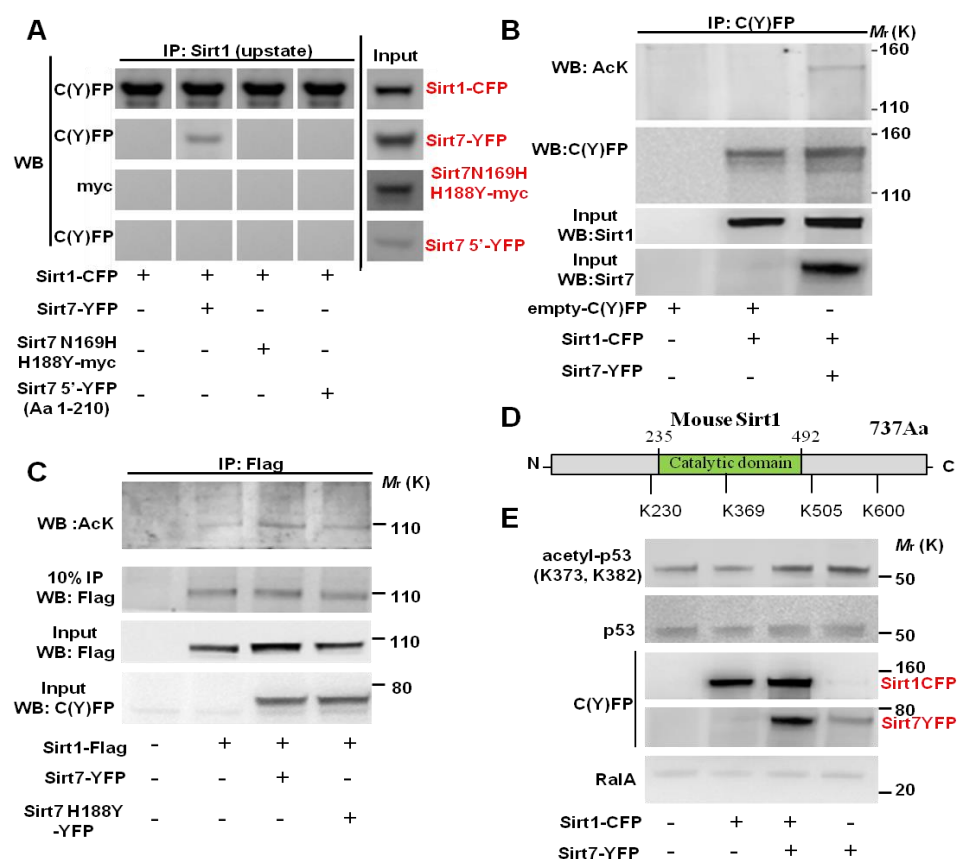


**Figure 3.15 Sirt7 physically interacts with Sirt1 and increases the acetylation of Sirt1.** (A) Wildtype Sirt7, but not Sirt7 bearing point mutation in the deacetylase domain nor the Sirt7 N-terminally truncated protein can interact with Sirt1 (data from Christian Smolka). (B) Increased acetylation of Sirt1 after co-expression with Sirt7. (C) The increased Sirt1 acetylation was only detected in cells expressing Sirt1 together with WT Sirt7 but not with a Sirt7 H188Y inactive mutant. (D) Overview of the localization of acetylated lysines in the mouse Sirt1, which were found in the presence of Sirt7 by mass-spectrometry analysis. (E) Acetylation of p53 in HEK293T cells expressing Sirt1 and Sirt7 alone or in combination was detected by Western blot. RalA was used as loading control.

To determine whether the increased acetylation of Sirt1 could alter its activity, we tested the Sirt1 deacetylation activity by estimating the acetylation status of its cellular target p53. The results showed that the acetylation inhibits Sirt1 activity, as demonstrated by

---

an increased acetylation levels of p53 in cells expressing Sirt1 together with Sirt7 and in contrast to low acetylation of p53 in cells overexpressing Sirt1 without Sirt7 (Fig 3.15E). High p53 acetylation was also observed in cells only overexpressing Sirt7 suggesting that Sirt7 increases acetylation of p53 through inhibition of endogenous Sirt1 activity and/or by other ways (Fig 3.15E).

### 3.3.2 Sirt1 has an auto-deacetylase activity *in vivo* and *in vitro*

To investigate whether Sirt1 is an auto-deacetylase, Sirt1-specific inhibitor Ex527 was used to block the activity of Sirt1 *in vivo* and acetylation of Sirt1 was measured using Sirt1 immunoprecipitation and anti-acetyl-lysine antibody in a western blot analysis. Fig 3.16A and B demonstrate that, indeed, Ex527 treatment leads to higher level of Sirt1 acetylation in cell culture. *In vitro* deacetylation assays using acetylated Sirt1 derived peptides and recombinant Sirt1 protein were also performed to detect the auto-deacetylation of Sirt1. These experiments were kindly supervised and analysed by Dr. Marcus Krüger and his group. Notably, Sirt1 showed highly efficient deacetylation activity on peptide containing acetylated lysine 230 (K230), the efficiency of the K230 auto-deacetylation was quantified by mass-spectrometry employing stable isotope labelled peptides (Fig 3.16C). These data indicate that Sirt1 can deacetylate itself both *in vivo* and *in vitro*.

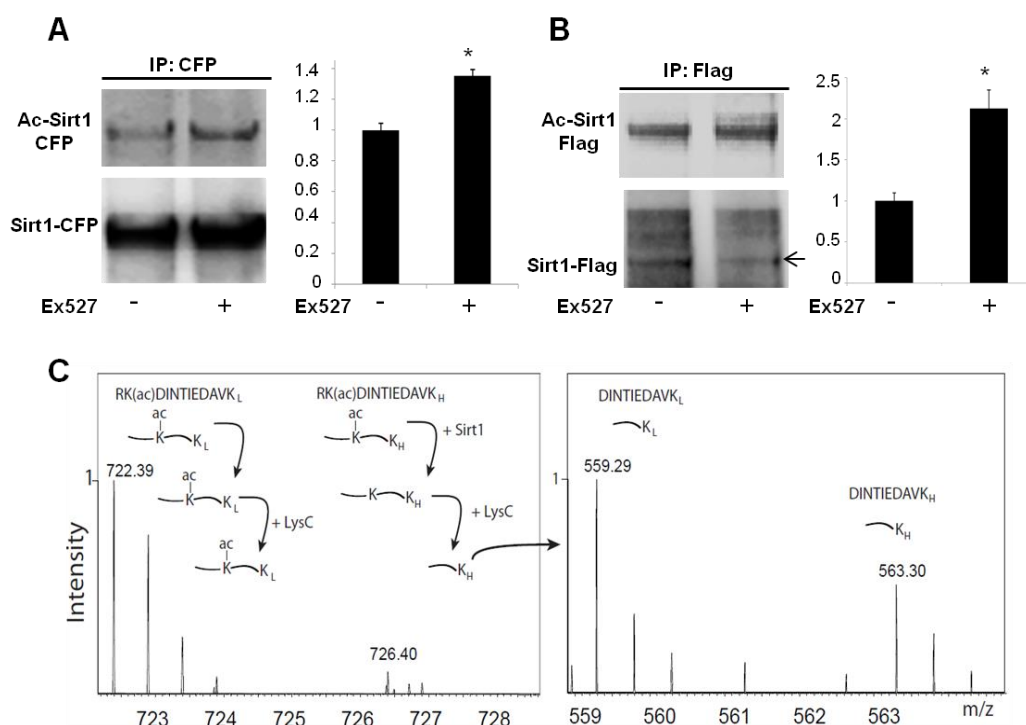


**Figure 3.16 Sirt1 is self-deacetylated *in vivo* and *in vitro*.** (A-B) Increased acetylation of Sirt1 was observed after specific inhibition of Sirt1 deacetylase activity by Ex527 in cell culture. Two different Sirt1 expressing constructs, Sirt1-CFP (A) and Sirt1-Flag (B) were used for transfections. Cell lysates were immunoprecipitated with CFP and Flag antibodies, respectively, followed by Western Blot analysis using Anti-CFP, anti-Flag and anti-Acetyl lysine (AcK) antibodies. Relative intensities of acetylated Sirt1 proteins were quantified and are shown in histograms. All values are average  $\pm$  SD for triplicate measurements. Significance was determined by Student's t test. \*  $P < 0.05$ ; \*\*  $P < 0.01$ . (C) Quantitative mass spectrometry analysis of deacetylation of Sirt1-derived peptides containing acetylated K230 residues by recombinant Sirt1. The acetylated K230 Sirt1 peptides were synthesized and labelled with the natural isotope for lysine (labelled with L (0)) and with the  $^{13}\text{C}_6^{15}\text{N}_2$  lysine isotope (labelled with H (8)) respectively using the SILAC technique (Guarani et al.).

### 3.3.3 The acetyltransferase MOF acetylates and decreases the activity of Sirt1

It was reported that Sirt1 can interact with some acetyltransferases including p300/CBP (Bouras et al., 2005), PCAF (Pediconi et al., 2009), TIP60 (Wang and Chen, 2010), MOF (Lu et al., 2011) and modulates their catalytic activity through deacetylation. Therefore, further investigations were performed to examine whether these acetyltransferases can acetylate Sirt1. HEK cells were transfected with Sirt1 in the presence or absence of p300 (CBP), MOF, PCAF respectively, and the acetylation levels of immunoprecipitated Sirt1 were detected by anti-acetyl-lysine immunoblotting. The level of Sirt1 acetylation was only increased in the presence of MOF and was similar to the increase of Sirt1 acetylation after addition of WT Sirt7 (Fig 3.17A, B). Next, the effect of Sirt1 acetylation by MOF on its enzymatic activity to deacetylate

H3K9 was examined in cell culture experiments. Deacetylation of H3K9 by Sirt1 was significantly reduced when cotransfected with MOF acetyltransferase (Fig 3.17C). Thus, the MYST acetyltransferases family member, MOF, can acetylate and repress the deacetylase activity of Sirt1. Surprisingly, MOF acetyltransferase increased acetylation of WT Sirt1 much stronger than of Sirt1 enzymatic inactive mutant, Sirt1H355Y (Fig 3.17D).

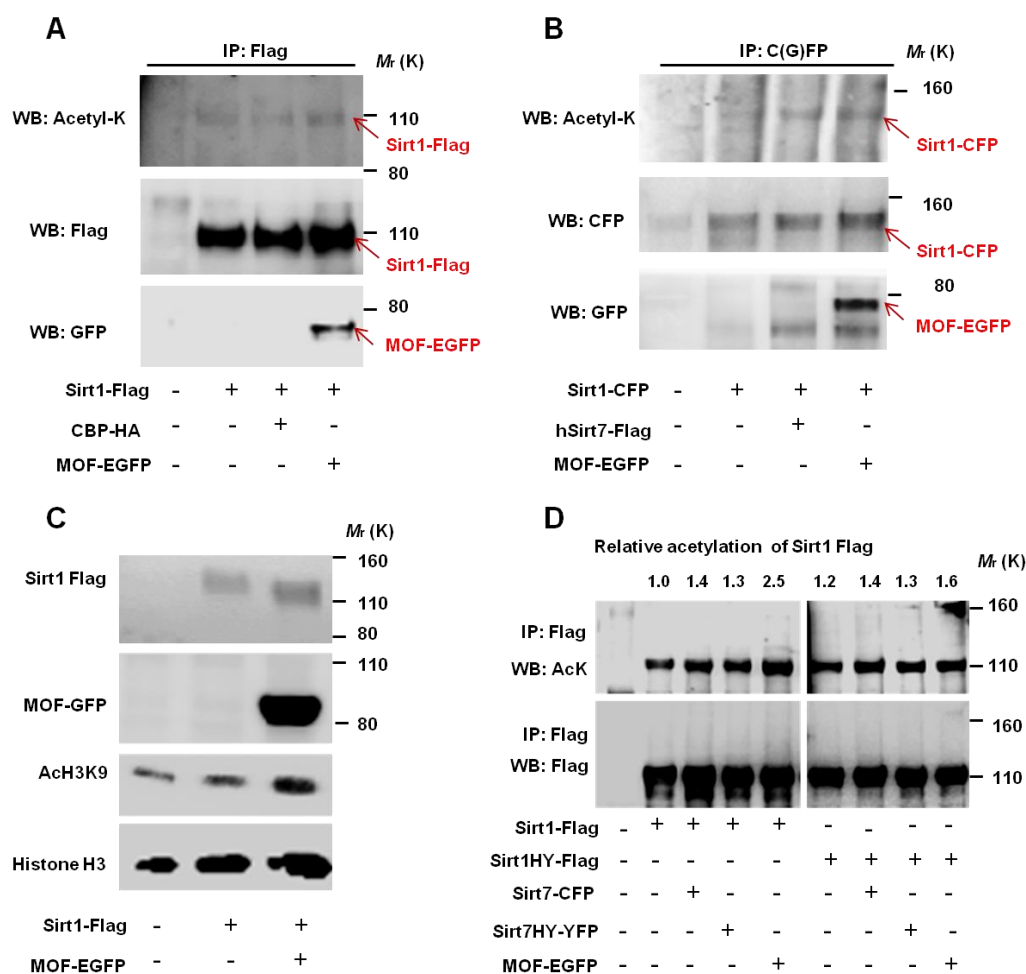


**Figure 3.17 Acetyltransferase MOF acetylates Sirt1 and attenuates its deacetylase activity.** (A) HEK 293T cells were transfected with Sirt1-Flag and acetyltransferases CBP-HA or MOF-EGFP as indicated. Acetylation of Sirt1 was examined by immunoblotting using anti-acetyl-lysine antibody (AcK) after immunoprecipitation. (B) Sirt1-CFP was transfected into HEK 293T cells in the presence of hSirt7-Flag or MOF-EGFP. Sirt1-CFP was immunoprecipitated with anti-GFP antibody and the acetylation detected by immunoblotting with anti AcK antibody. (C) HEK 293T cells were transfected with Sirt1-Flag alone or together with MOF-EGFP. The activity of Sirt1 was examined by the levels of acetylated H3K9 (AcH3K9) on the Western Blot using anti-acH3K9 antibody. The levels of histone H3 were used as loading control. (D) HEK 293T cells were transfected with WT Sirt1-Flag or inactive mutant Sirt1H355Y-Flag expression vectors together with WT Sirt7-CFP, inactive Sirt7H188Y-YFP and MOF-EGFP plasmids as indicated. The cell lysates were immunoprecipitated with anti-G(CY)FP antibody. The acetylation signals of precipitated products were analyzed by Western blot with anti-AcK antibody.

However, it was reported previously, that Sirt1 can deacetylate MOF and increase its activity and recruitment on the chromatin (Lu et al., 2011). The lower acetylation level of Sirt1H355Y mutant in the presence of MOF may thus reflect the lack of positive feedback regulation of MOF activity by Sirt1. The exact molecular mechanism of the regulatory loop existing among Sirt1, MOF, and Sirt7 has yet to be elucidated.

### 3.3.4 A combination of acetylation and deacetylation at specific lysine residues is responsible for Sirt1 activation

To further test the impact of the acetylation at specific lysine site(s) of Sirt1 on its enzymatic activity, a series of Sirt1 point-mutants in which the lysine residues at positions 230, 369, 505 and 600 were separately replaced with arginine to prevent acetylation were generated and assessed for their deacetylation activity on endogenous p53. Interestingly, only the K230R mutant showed increased catalytic activity on p53 as the acetylated p53 signal was significantly decreased when compared with the WT Sirt1 while none of the other mutants decreased p53 acetylation (Fig 3.18A). Together with the finding that Sirt1 efficiently auto-deacetylated lysine 230 *in vitro*, these results strongly suggest that K230 residue is a critical site of Sirt1 auto-deacetylation and the autodeacetylation of this site enhances the enzymatic activity of Sirt1. However, mutation of all four lysines converted to arginines (4KR) failed to decrease p53 acetylation (Fig 3.18B). This result indicates that Sirt1 activity is enhanced not only by deacetylation of K230, but the acetylation at one or more remaining lysines is also required for the catalytic activity of Sirt1. To test this hypothesis, several 3KR mutants, in which 3 of the four identified lysine residues were mutated to arginine while the fourth remaining lysine could still be acetylated, were constructed and analysed for their enzymatic activity on endogenous p53. The results showed that the increased deacetylation activity was only seen with the 3KR2 mutant (in which K369 remained unchanged) but not with the other 3 KR mutants (Fig 3.18C). Furthermore, ectopic over-expression of WT Sirt7 or MOF not only repressed the deacetylase activity of WT Sirt1 on endogenous p53, but they also inhibited the activity of Sirt1 3KR2 (without K369) mutant (Fig 3.18B and C), suggesting that the specific acetylation at K369 site,

which enhance the activity of Sirt1, is not possibly modified by the acetyltransferase MOF. Taken together, these findings demonstrate that the modification of Sirt1 at specific lysine residues, which can affect the function of Sirt1 is more complex: In addition to the deacetylation of K230, an acetylation at K369 may be responsible for the activation of Sirt1.

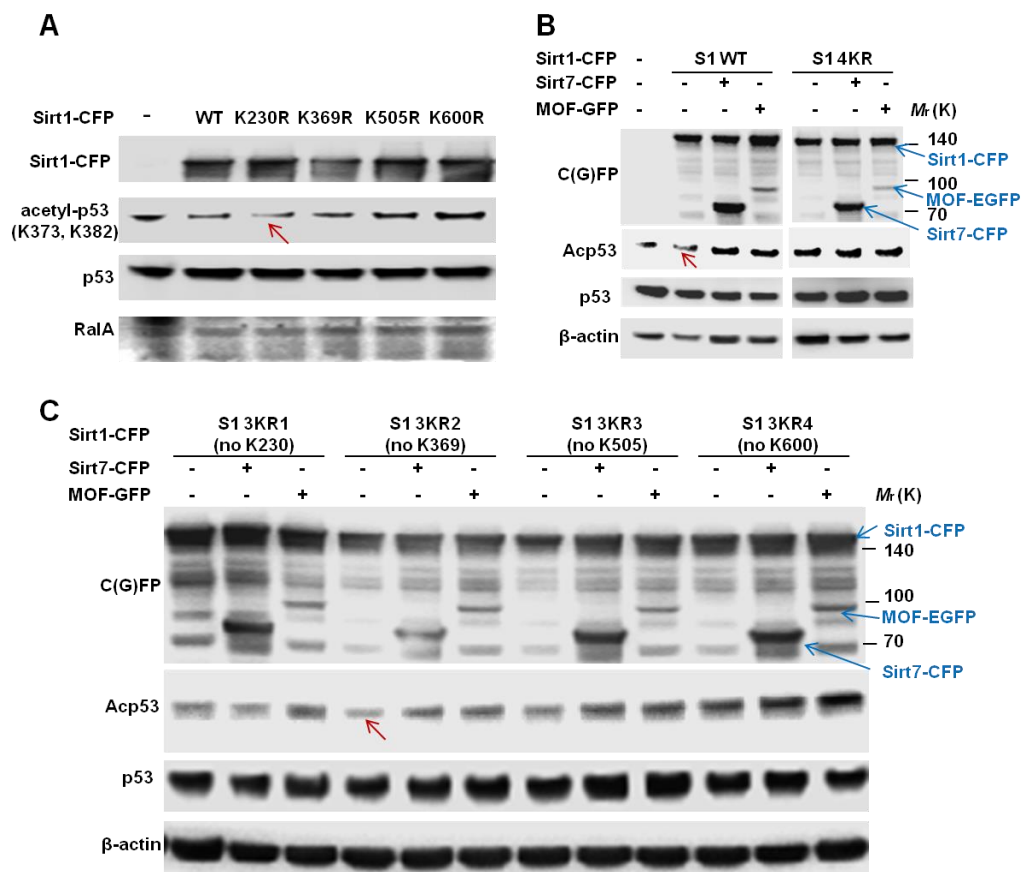


**Figure 3.18 Autodeacetylation of Sirt1 occurs mainly at K230. The combination of acetylation at K369 and deacetylation at other lysines may be responsible for the promotion of Sirt1 deacetylase activity.** (A) WT Sirt1-CFP and a series of Sirt1-CFP single KR mutation expression plasmids were transfected into HEK 293T cells as indicated. The acetylated p53 levels were detected by Western blot with anti-acetyl-p53 (K373, K382) antibody. RalA was used as loading control. Red arrow indicated the lowest acetylated p53 (the highest Sirt1 activity). (B-C) HEK 293T cells were transfected with WT Sirt1-CFP or 4KR mutants (B) or a series of 3KR mutants (C) together with Sirt7-YFP or MOF-EGFP. The acetylation level of p53 was detected by acp53 antibody in WB. β-actin was the loading control. Red arrows indicated the lowest acetyl-p53 in each picture.

### 3.4 Generation and initial characterization of Sirt1 conditional KO mice and Sirt1/Sirt7 double knock-out mice

Since we have found that Sirt7 inhibits Sirt1 expression and its activity, the disturbed hepatic response to fasting/refeeding and the diminished induction of transcription of hepatic rDNA by insulin as well as the impaired adipogenesis of white adipose tissue in Sirt7 deficient mice might be due to a higher expression and/or excess activation of Sirt1. To further study the *in vivo* roles of Sirt1 together with Sirt7 in the cross regulatory circuits important in the metabolic homeostasis, conditional Sirt1 knockouts and double knockout heterozygotes Sirt1<sup>+/-</sup> Sirt7<sup>-/-</sup> or Sirt1<sup>-/-</sup> Sirt7<sup>+/-</sup> in the whole body or in the special organ were generated.

#### 3.4.1 Constructing of targeting vectors for conditional Sirt1 knockouts

Two targeting strategies were employed to create conditional Sirt1 knockouts (Sirt1 CKO). The first one was designed to conditionally delete Sirt1 exon4, which encodes 51 amino acids of the conserved Sirt1 catalytic domain. This targeting vector Sirt1 CKOS(short) was utilized to introduce one loxP site upstream of the exon4 in mouse Sirt1 locus, and a FRT neomycin-resistance (neo) cassette followed by the second loxP site downstream of exon4 (Fig 3.19A). Because the aberrant Sirt1 $\Delta$ ex4 protein might retain partial function or have dominant-negative activity, a second targeting construct Sirt1 CKOL(long) was designed to conditionally delete the exon2, exon3 and exon4 of Sirt1, which completely abolishes Sirt1 protein expression. The neo cassette and the 2nd loxP site was the same as in the first strategy, but the 1st loxP site was inserted into the genomic sequence between exon1 and exon2 (Fig 3.19B). The protocols to generate the conditional target vectors followed the published methods (Liu et al., 2003) with some modifications. The strategy and workflow of the recombineering-based method for generating the Sirt1 conditional knockout targeting vectors was illustrated in Fig 3.20

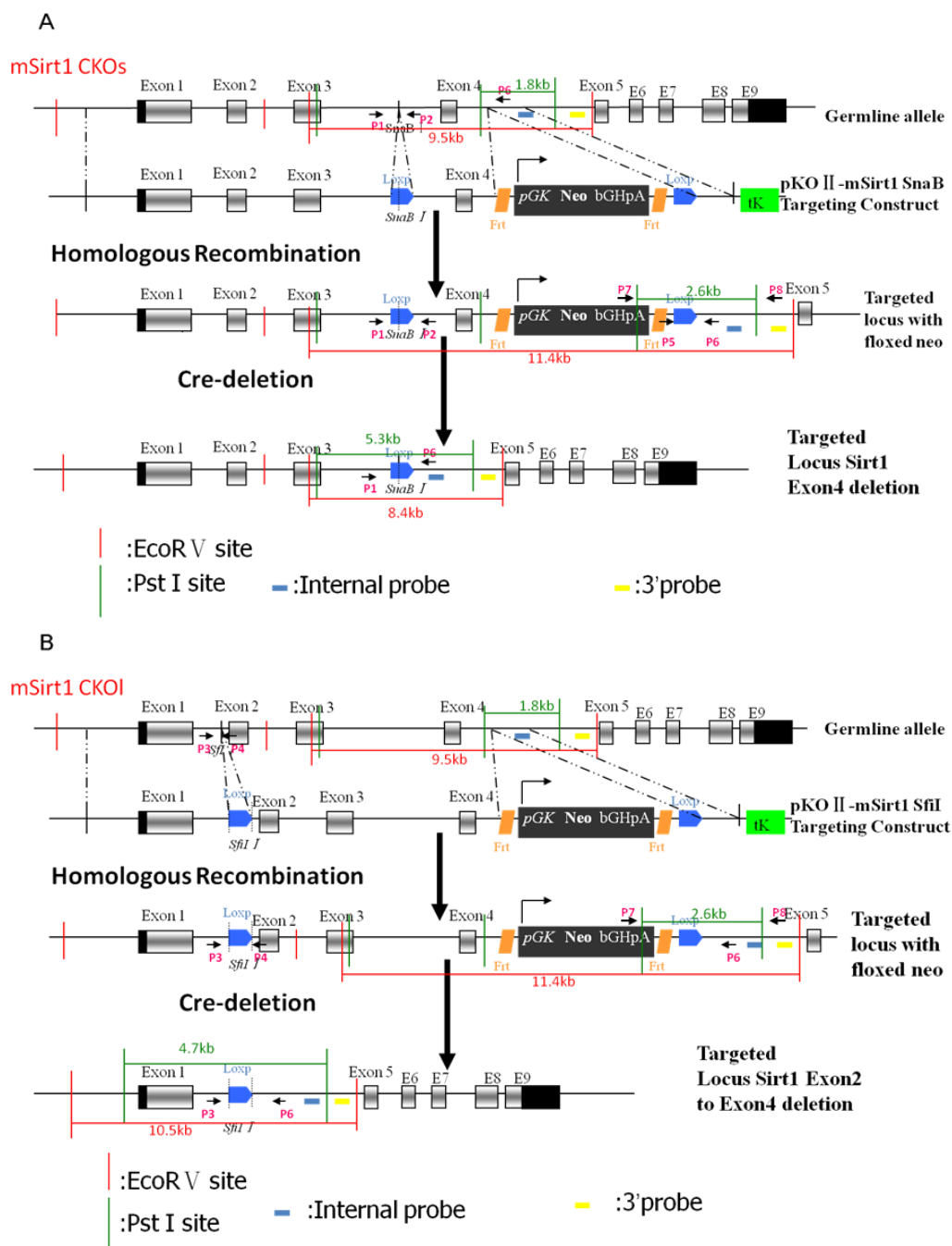


**Figure 3.19 Generation of two *Sirt1* conditional knockout constructs.** (A) A schematic diagram of the *Sirt1* germline locus, pKOII-*Sirt1* *SnaB* targeting vector, target locus with floxp and neomycin cassette and *Sirt1* locus after Exon4 deletion. *Sirt1* exons, the relative locations of the internal probe, 3'probe for Southern blot and primers for genotyping and relevant restriction enzymes sites are indicated. (B) A schematic diagram of the *Sirt1* germline locus, pKOII-*Sirt1* *SfiI* targeting vector, target locus with floxp and neomycin cassette and *Sirt1* locus after Exon2, Exon3 and Exon4 deletion. *Sirt1* exons, the relative locations of the internal probe, 3'probe for Southern blot and primers for genotyping and relevant restriction enzymes sites are indicated.

The targeting vectors were made using homologous recombination to introduce the mouse *Sirt1* genomic DNA sequence including 5'UTR, Ex1, Ex2, Ex3, Ex4, Ex5 and the corresponding introns from BAC DNA into pKOII (Fig 3.20). At first, two homologous arms 1 RP-5' and 1 RP-3' were amplified by PCR from BAC DNA as a template. 1 RP-5' arm is located in 5'UTR of *Sirt1* genomic DNA and contains *Sma*I and *Pme*I sites at its 5' end and *Hind*III site at the 3' end, while 1 RP-3' arm is located in the intron between exon4 and exon5 of the genomic DNA and contains *Bgl*II and *Eco*RI sites at its 5' and 3' ends. The two fragments were inserted into *Sma*I *Hind*III sites and *Bgl*II *Eco*RI sites of the pKOII plasmid, respectively. Subsequently, the neomycin cassette was deleted by *Sac*II and *Xho*I digestion, the linearized vector fragment containing the two homologous arms was gel extracted and transformed into recombination-competent cells carrying the BAC DNA. After the 1st retrieving, the targeting vector pKOII containing the 18kb DNA sequence spanning exon1 to exon4 of mouse *Sirt1* has been produced. The next step in creating the cko-targeting vector was introduction of a loxP site and a FRT floxed neomycin resistance cassette from pL451 plasmid into the subcloned DNA. To introduce the floxed Neo gene at the correct location in the target DNA vector, it was first flanked with two approximately 500bp long arms that are homologous to the targeting BAC DNA: 1MT-5' and 1MT-3'. These homologous arms were generated by PCR amplification of the BAC DNA including *Xho*I and *Eco*RI or *Bam*HI and *Sac*II restriction sites and inserted into the *Xho*I *Eco*RI and *Bam*HI *Sac*II restriction sites of pL451 plasmid, respectively (Fig. 3.20). Then, DNA fragment containing FRT neo and loxP sites was excised by *Xho*I and *Sac*II digestion, purified and electroporated along with the subcloned target DNA vector into EL350 cells for recombination. After the 2nd retrieving, the target vector contained a FRT floxed neo and one loxP site (Fig 3.20). The final step in the construction of the cko-targeting vector was the introduction of a second loxP site into the subcloned DNA, downstream of exon3 (*Sirt1*CKOS) or downstream of exon1 (*Sirt1*CKOL). A single loxP site with short extension sequence, favorable for genotyping by PCR, was inserted into the unique *Sfi*I or *Sna*BI site of each cko-targeting vector. For confirmation of homologous recombination, 3' probe and the internal probe, 540bp and 771bp in length

respectively, were prepared by PCR using BAC DNA template (Fig 3.19).

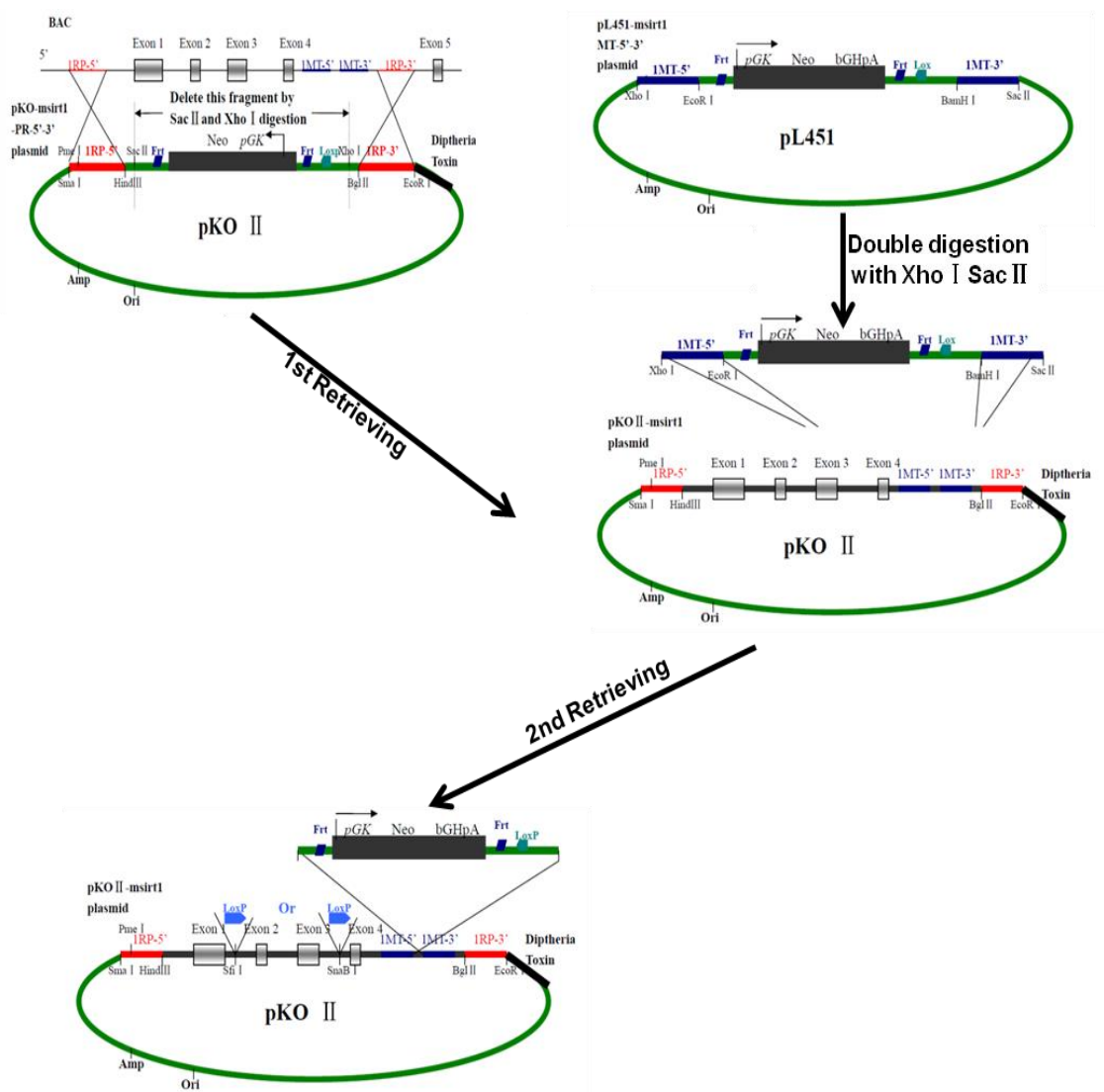
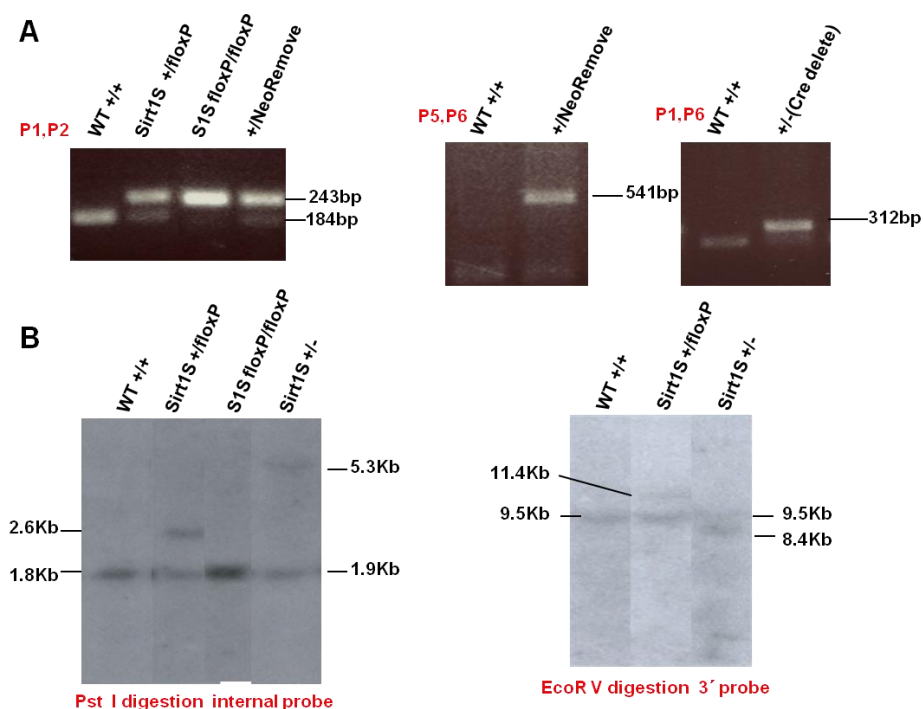


**Figure 3.20 Strategy and work flow chart used in generating the Sirt1 conditional knockout targeting vector by recombination.**

### 3.4.2 Production of targeted ES cell clones and chimera formation

The two constructed CKO targeting vectors were subsequently linearized at the unique PmeI site and electroporated into mouse embryonic stem (ES) cells derived from a hybrid line (SV129/C57BL6). For Sirt1 CKOS, from two electroporations, about 95 colonies with good morphology were isolated after 250µg/ml G418 selection. Targeted clones were identified by PCR using a 5' primer (neoP7), specific to the neo cassette, and 3' primer (neoP8) corresponding to the genomic sequence outside the vector (see

Figure 3.18). To ensure that a single loxP site upstream of exon4 did exist, PCR using primers *SnaBloxP P1* and *SnaBloxP P2* was performed to selectively amplify this loxP sequence (Fig 3.21A). 80% of colonies were positive and they were subsequently verified by Southern blot analysis with both 3' and internal probes as shown in Fig. 3.21B. A novel longer band of 2.6 Kb after *Pst*I digestion and of 11.4kb after *Eco*RV digestion corresponding to the targeted allele appeared as expected after hybridization with each probe, confirming homologous recombination of both arms (Fig 3.21B). After Southern blot verification, a total of 8 clones were positive. For *Sirt1* CKOL, 170 positive colonies were isolated and analyzed by PCR using primers *P7* and *P8* to confirm the neo cassette, and the *SfiloxP P3* and *SfiloxP P4* primers to confirm the loxP site (Fig3.21C). Then 122 candidate positive clones were verified by Southern hybridization with both internal and 3' end probes (Fig 3.21D). At last, a total of 11 positive clones were confirmed for homologous recombination after Southern blot.



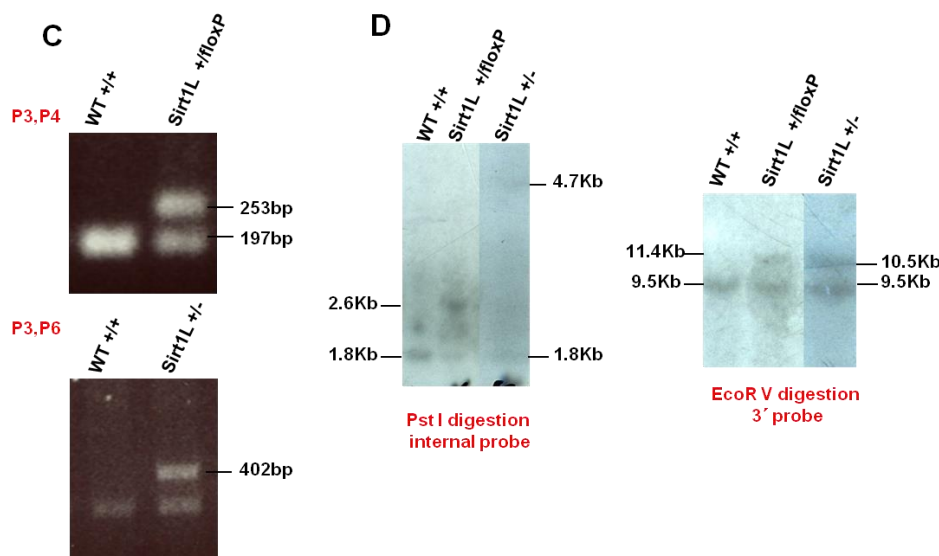


**Figure 3.21 Genotyping of two Sirt1 conditional knockout ES cells or mice tails by PCR and Southern blot.** (A) PCR genotyping of Sirt1 CKOS (short) ES cells. The first loxP site located between exon3 and exon4 was detected by P1 and P2 primers; the second loxP site located 3' to the Neo cassette was detected by P5 and P6; the allele generated by Cre recombinase deletion was detected by P1 and P6 primers. (B) Southern blot of PstI and EcoRV digested DNA isolated from Sirt1S +/+, Sirt1S +/- floxP and Sirt1S +/- (Cre deletion) mice tails and hybridized with the internal probe and 3'probe, respectively. (C) PCR genotyping of Sirt1 CKOL (Nin et al.) ES cells. The first loxP site located between exon1 and exon2 was detected by P3 and P4; the allele generated by Cre recombinase deletion was detected by by Cre recombinase was detected by P3 and P6. (D) Southern blot of PstI and EcoRV digested DNA isolated from Sirt1L +/+, Sirt1L +/- floxP and Sirt1L +/- (Cre deletion) mice tails and hybridized with the internal probe and 3'probe, respectively. All the relative locations of the internal probe and 3'probe for Southern blot and primers for PCR were indicated in Fig 3.19

### 3.4.3 Generation and genotypic verification of Sirt1 conditional KO mice

Two targeted ES cell clones carrying the Sirt1CKOS targeting vector were chosen for injection experiments. Using micromanipulator and dissecting microscope, 10-15 ES cells of each clone carrying the intergrated targeting vector were injected into C57BL/6 blastocysts. The injected blastocysts were implanted into the uteri of pseudopregnant NMRI foster mothers, each mouse was implanted with 8-10 blastocysts. A total of 15 chimeric mice with different degree of ES cell contribution in coat color were obtained and verified by Southern blot. The Sirt1 CKOS mice were backcrossed to WT C57Bl6 mice for at least 6 times. They were then bred with mice expressing Flp recombinase to delete the neo cassette and generate floxed Sirt1 exon4 (Sirt1SNeo) mice. Then these mice (Sirt1 Ex4 floxp/floxP, Flp negative) were crossed to CMV Cre

transgenic mice (expressing the Cre recombinase driven by CMV promoter) or to liver specific Cre mice (expressing the Cre recombinase driven by albumin promoter) to generate the constitutive Sirt1 knockout mice (Sirt1 CMVKOS) and liver-specific Sirt1 knockout mice (Sirt1sLiKO), respectively. RT-PCR analysis demonstrated the presence of a short length Sirt1 mRNA (without exon4) in the liver of Sirt1sLiKO mice (Fig 3.22A). The successful removal of exon4 was also confirmed at the protein level: In the liver of albumin Cre expressing Sirt1sLiKO mice only a truncated, smaller Sirt1 protein band could be detected on the WB while normal size Sirt1 protein band was present in the other tissues (Fig 3.22B). The heterozygote Sirt1S CMVKO (Sirt1<sup>+/-</sup> CMVCre negative) mice were bred with Sirt7<sup>-/-</sup> mice to generate Sirt1/Sirt7 double knockout mice, and the homozygous Sirt1SLiKO (Sirt1s floxP/floxP Liver-Cre<sup>+/-</sup>) mice were crossed to Sirt7<sup>-/-</sup> mice to generate Sirt7/Liver Sirt1S double knockout mice for the further investigation.

For generation of mice with a longer Sirt1 deletion, one Sirt1CKOL positive ES clone was injected into the blastocysts. 10 chimeras were obtained and verified by Southern blot. Similar to strains generated with the short Sirt1 deletion, the Sirt1LNeo mice carrying the floxed Sirt1 exon2-4 (Sirt1 Ex2-Ex4 floxp/floxp, Flp negative) were bred with CMV Cre and albumin-Cre transgenic mice to generate Sirt1LCMVKO and Sirt1LiLiKO mice, respectively. RT-PCR and Western blot analyses confirmed that Sirt1 expression was eliminated at mRNA level and protein levels exclusively in the liver of Sirt1 LiLiKO mice, with no detectable decrease in the other tissues (Fig 3.22C and D). Furthermore, the homozygous Sirt1LLiKO (Sirt1l floxP/floxP Liver-Cre<sup>+/-</sup>) mice were bred with Sirt7<sup>-/-</sup> mice to generate Sirt7/Liver Sirt1L double knockout mice for the further investigation.

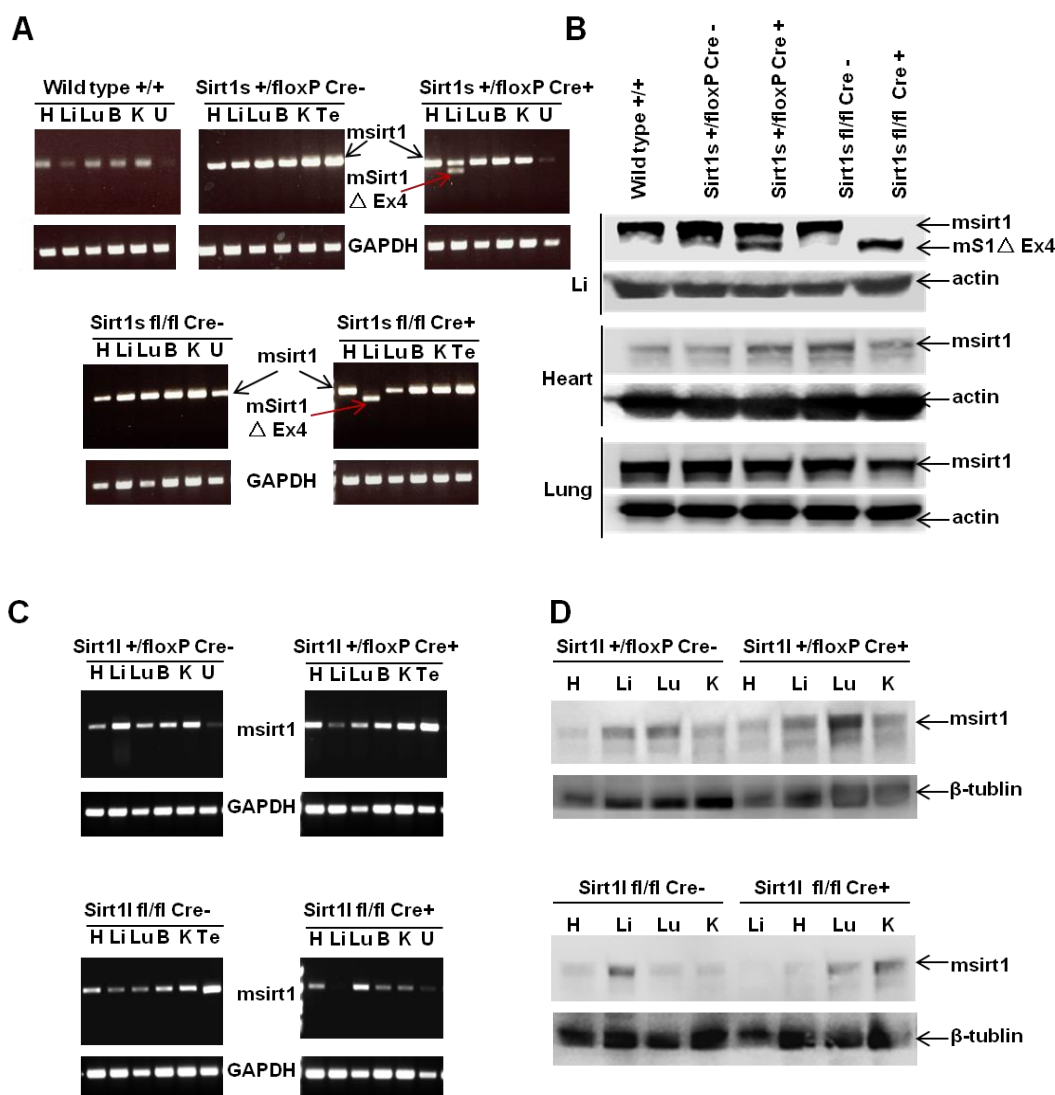


**Figure 3.22 Sirt1 is specifically knocked out in the livers of Sirt1sLiKO and Sirt1lLiKO mice.** (A-B) Expression of Sirt1 mRNA and proteins in different tissues of Sirt1sLiKO mice detected by RT-PCR (A) and Western blot (B), GAPDH or pan-actin was used as internal control in RT-PCR or loading control in Western blot, respectively. (C-D) Expression of Sirt1 mRNA and proteins in different tissues of Sirt1lLiKO mice detected by RT-PCR (C) and Western blot (D), GAPDH or  $\beta$ -tubulin was used as internal control in RT-PCR or loading control in Western blot, respectively. H, heart; Li, liver; Lu, lung; B, brain; K, kidney; Te, testis; U, uterus.

### 3.4.4 Confirmation of embryonic lethality of Sirt1 deficiency by Sirt1 CMVKO mice

Previous reports showed that Sirt1 constitutive KO mice died at perinatal stages or later at the age up to several months into adulthood, depending on the genetic background (Cheng et al., 2003; McBurney et al., 2003; Wang et al., 2008). After analyzing of 142 Sirt1CMVKOS offsprings, it was found that only 8 mice of Sirt1S<sup>-/-</sup> survived after birth (Table 3.1). Among which, 2 of the surviving Sirt1S<sup>-/-</sup> mice had

reduced life span and died in less than 1 month. In contrast to their WT or heterozygous littermates, the Sirt1S  $-/-$  mice were smaller in size after birth and their postnatal growth was inhibited. In addition, some of the Sirt1S  $-/-$  mice showed morphological eye defects as already described for constitutive Sirt1 KO mice (Cheng et al., 2003; McBurney et al., 2003). For the second Sirt1 knockout mouse carrying the longer deletion, Sirt1CMVKOL, no surviving homozygous deficient mice were found after birth (Table 3.1).

**Table 3.1 Genotypes of offsprings from crosses between heterozygous parents of Sirt1 CMVKOS and Sirt1 CMVKOL**

		Genotypes of offsprings		
<b>Sirt1 CMVKOS</b>	<b>Total of pups</b>	<b>WT +/+</b>	<b>Sirt1s +/-</b>	<b>Sirt1s -/-</b>
	142	44	90	8
<b>Sirt1 CMVKOL</b>	<b>Total of pups</b>	<b>WT +/+</b>	<b>Sirt1l +/-</b>	<b>Sirt1l -/-</b>
	39	19	20	0

To investigate whether embryonic lethality of Sirt1 deficiency was the cause of low number of surviving Sirt1  $-/-$  mice, embryos were isolated from Sirt1CMVKOS mice at E13.5. Indeed, among of 17 embryos analyzed, homozygous deficient embryos were present at approximately Mendelian ratio (4 of 17). Sirt1S  $-/-$  embryos were smaller than littermate controls, and often exhibited morphological malformations, lordosis and eye abnormalities (Fig 3.23A). The most often observed eye defect was the abnormal closure of the optic fissure (arrow in the Fig 3.23B). These observations are consistent with the findings of Cheng's study (Cheng et al., 2003).

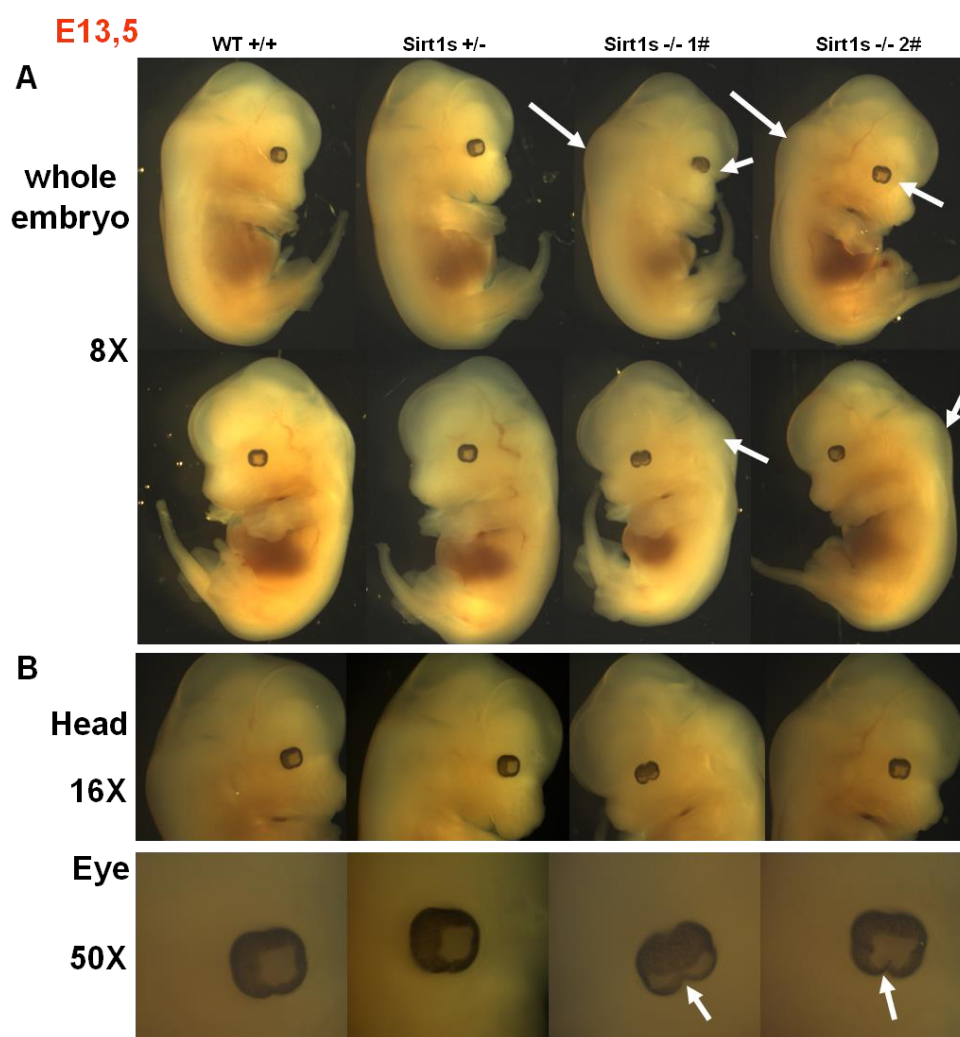


**Figure 3.23 Developmental abnormalities in Sirt1 deficient embryos.** (A) WT, Sirt1S +/- and Sirt1S -/- E13.5 embryos, arrows indicate developmental abnormalities in Sirt1 deficient embryos. (B) The enlargements of heads and eyes from the E13.5 WT and Sirt1 deficient embryos, arrows point at the abnormal optic fissure in Sirt1S -/- embryos.

Summing up, I demonstrated a successful generation of two Sirt1 targeting mouse strains, which allow conditional inactivation of the Sirt1 gene. These lines provide a valuable tool for further investigation of Sirt1 specific function. Considering the novel finding of regulation of Sirt1 through Sirt7, generation of double knockouts will help to further evaluate the sirtuin functions.

## 4. Discussion

Mammalian sirtuins constitute a family of cellular regulators that are involved in preservation of organ functions during stress response and aging. A variety of specific mouse models to knock out the members of sirtuin family have been created recently. The disruption of energy metabolism, genome stability and stress response in these sirtuin-deficient mice demonstrated that mammalian sirtuins are major contributors to maintain the balance between metabolism and aging. However, a few studies have shown the roles of the nucleolar Sirt7 in the metabolic homeostasis and aging so far. We generated the Sirt7 deficient mice. Mice lacking Sirt7 were born at the expected Mendelian ratio and did not show any significant phenotypical abnormalities during the first months of life, but Sirt7  $-/-$  mice had a reduced lifespan, most animals died between 10 and 13 months of age. Moreover, the knockout mice were smaller and leaner compared to WT mice, which became apparent at around five months of age. Sirt7  $-/-$  mice were very sensitive to cold and starvation stress. They were not able to keep a constant body temperature and normal blood glucose concentration under combined cold and starvation stress (Vakhrusheva et al., unpublished data). The impaired cold resistance has been described in several mouse mutants with defects in energy and/or fat metabolism (Exil et al., 2006; Goetzman et al., 2005). The leanness of the Sirt7 $-/-$  animals cannot be attributed to a restricted energy intake since the food consumption of Sirt7  $-/-$  mice was even slightly increased. These data suggest that the Sirt7 deficient mice suffer from severe metabolic dysfunction. This dissertation predominately focuses on the role of Sirt7 in maintenance of metabolic homeostasis in the liver and the adipocytes differentiation in white adipose tissue.

### 4.1 The role of Sirt7 in the fasting/refeeding adaptation of liver

In response to nutrient deprivation stress, the metabolic genes in the liver have to be precisely regulated to maintain glucose and lipid metabolic homeostasis. This regulation is accomplished by a network of transcription factors and coactivators, which functions are heavily dependent on the response to hormonal and nutrient signals.

PGC-1 $\alpha$  is a key coactivator of this network that has been shown to play several important roles in the metabolic adaptation in response to nutrient stresses, through regulation of gluconeogenic and fatty acid  $\beta$ -oxidation gene expression (Lin et al., 2005; Puigserver and Spiegelman, 2003). Interestingly, PGC-1 $\alpha$  knockout animals exhibited some phenotypic changes similar to those seen in Sirt7 knockouts such as cold sensitivity and leanness (Lin et al., 2004). In fact, a significant reduction of the expression of PGC-1 $\alpha$  was detected in the liver of Sirt7  $-/-$  mice (Fig 3.1A). PGC-1 $\alpha$  deficient mice developed mild hypoglycemia after 24hr of fasting due to the inefficient hormone-stimulated gluconeogenesis (Lin et al., 2004). In contrast to the defect in hormone-stimulated gluconeogenesis after short-term fasting, PGC-1 $\alpha$  deficient mice had constitutively activated gluconeogenic gene expression in the liver independent of feeding conditions (Lin et al., 2004). The increased C/EBP $\beta$  expression in the liver, which activates gluconeogenic genes in a PGC-1 $\alpha$  independent manner, might compensate for the lack of PGC-1 $\alpha$  (Lin et al., 2004). Despite the decreased PGC-1 $\alpha$  expression, Sirt7  $-/-$  mice showed even exaggerated response to fasting: transcripts levels of genes regulating gluconeogenesis and lipogenesis were more strongly induced or repressed, respectively, as compared to WT controls (Fig 3.2A). It is possible that, similar to the compensatory increase of C/EBP $\beta$  in PGC-1 $\alpha$  KO mice, changes in other metabolic regulators may play compensative roles to maintain or even exaggerate the hepatic metabolic adaptations in Sirt7 deficient mice. Other phenotypes observed in Sirt7 KO mice, such as the impaired cold resistance may still be caused by the lower expression of PGC-1 $\alpha$ , the critical regulator of adaptive thermogenesis. Further investigation should focus on the role of Sirt7 in the regulation of PGC-1 $\alpha$  transcription in brown adipose tissue, the main regulatory tissue of thermogenesis.

One of factors possibly responsible for the stronger changes of gluconeogenic and lipogenic genes detected in the fasting liver of Sirt7 KO mice might be the higher Sirt1 expression. Sirt1 is induced in the fasted liver and deacetylates PGC-1 $\alpha$  to activate gluconeogenic and fatty acid oxidation genes and thus regulates hepatic glucose and lipid metabolism response to fasting (Rodgers et al., 2005; Rodgers and Puigserver, 2007). In the Sirt7 deficient mice, despite the fact that PGC-1 $\alpha$  mRNA level is lower,

the high expression of Sirt1 upon fasting and its potentially higher activity (see below) may lead to the higher activation of PGC-1 $\alpha$  and, consequently, result in the stronger fasting response in the Sirt7  $-/-$  liver than WT mice. The status of acetylation of PGC-1 $\alpha$  should be checked in the future investigation. The Sirt7/liver specific Sirt1 double knockout mouse will be a valuable model to investigate the potential cross-regulatory interrelationships between the two sirtuins.

Another difference observed in metabolic adaptation in Sirt7 deficient mice was the inability to revert the fasting-induced inactivation of fatty acid synthesis and activation of gluconeogenesis under the refeeding state (Fig 3.2A). This effect might depend on the endogenous insulin resistance. In fact, the inactivation of PEPCCK and activation of FAS by insulin were severely impaired in primary Sirt7  $-/-$  hepatocytes (Christian Smolka, unpublished data). Moreover, without Sirt7, insulin was unable to activate its primary signaling targets in hepatocytes as indicated by low levels of Akt- and SAPK/JNK phosphorylation (Christian Smolka, unpublished data). Many insulin resistance mouse models including ob/ob mice (Lindstrom, 2007), db/db mice (Friedman et al., 1997; Kobayashi et al., 2000) and high-fat-diet mice (Winzell and Ahren, 2004) exhibit significant fasting hyperglycemia and hyperinsulinemia. These studies further demonstrated that the unbridled activity in promoting gluconeogenesis correlating with the pathogenesis of fasting hyperglycemia might be caused by the deregulated transcription factors such as forkhead transcription factor FoxO1 (Altomonte et al., 2003), FoxO6 (Kim et al., 2011a), hepatocyte nuclear factor 4 $\alpha$  (HNF4 $\alpha$ ) (Hirota et al., 2003), PGC-1 $\alpha$  (Koo et al., 2004), CREB coactivator TROC2 (Koo et al., 2005) and others. The disturbed hepatic adaptation in response to fasting/refeeding might be at least partly explained by the certain degree of insulin resistance in Sirt7 deficient liver. What is the role of Sirt7 in regulating insulin signaling pathway and the status of post-translational modification of the other transcription factors/coactivators in Sirt7 deficient hepatocytes should be further investigated.

## 4.2 Sirt7 is necessary for induction of hepatic ribosomal RNA transcription by insulin

Ribosome biogenesis is a process that consumes a considerable amount of energy, so it is important for the cells to regulate ribosome production in response to the intracellular availability of nutrients and energy (Rudra and Warner, 2004). This is very well illustrated in the liver, where fasting leads not only to a decrease in ribosome production, but also to the degradation of ribosomes through autophagy in order to save the amino acids and nucleotides during the nutrient shortage. Conversely, refeeding quickly stimulates ribosome biogenesis and suppresses degradation resulting in increasing the rate of protein synthesis and reestablishing an adequate content of ribosomes for the cells to perform their metabolic functions (Conde and Franze-Fernandez, 1980; Hutson and Mortimore, 1982). Furthermore, the synthesis of rRNA, the rate-limiting step in ribosome production, is regulated by nutritional conditions and energy status. Unexpectedly, the hepatic pre-rRNA transcription levels were increased upon fasting in WT mice. The increase of hepatic pre-rRNA levels in Sirt7 KO mice in response to fasting was significantly higher than in WT controls. Moreover, and interestingly, the pre-rRNA levels could not be restored to normal after refeeding in Sirt7 KO mice as observed in WT mice (Fig 3.2B). This pattern resembles other adaption changes in response to fasting/refeeding in the Sirt7 deficient liver as discussed above. The increased pre-rRNA levels after fasting in the liver seemed to be contradictory to the decrease in ribosome production caused by fasting as demonstrated in some previous reports (Conde and Franze-Fernandez, 1980; Enwonwu et al., 1971; Hutson and Mortimore, 1982; Sidransky and Verney, 1971). However, in the previous studies, fasting was mainly achieved by deprivation of protein (Sidransky and Verney 1971; Conde and Franze-Fernandez 1980; Hutson and Mortimore 1982). Moreover, the fasting time was extended to 48hrs and even longer (Enwonwu, Stambaugh et al. 1971; Anand and Gruppuso, 2005). No data indicated that pre-rRNA levels were decreased under fasting for 24hrs, although it was found that the yield of polyribosomal RNA decreased dramatically after 42- to 66-hours starvation (Princen et al., 1983). Yet the

level of mRNA assembled with polyribosomes may not necessarily match that of rRNA. In fact, one investigation indicated that serum albumin, H-ferritin, and ribosomal RNA nuclear transcripts were not decreased by fasting for 72hrs (Hayden et al., 1994). Despite the observed increase in liver rRNA levels during fasting, the ribosome synthesis may still be impaired. Since the cell needs precisely equimolar amounts of rRNA and each of the 79 ribosomal proteins (RPs), insufficiency of any one of the 79 RPs will lead to aberrant processing and insufficient ribosomal production despite of the excess of the rRNA (Rudra and Warner, 2004). Finally, the primers for pre-rRNA detection used in my experiments were located at the 5'-external transcribed spacer (5'-EST) sequence, which would be cleaved and degraded during the process of making the mature ribosomal RNAs (Eichler and Craig, 1994). The pre-rRNA level measured by QRT-PCR represented the relative dynamic level, reflecting the balance between the rate of transcription by RNA Pol I and the efficiency of cleavage to mature rRNAs. Thus the increased level of pre-rRNA detected in my experiments might correspond to the lower level of the cleavage process than that of the transcription. These results suggest that the inhibition of cleaving the pre-rRNA to mature rRNA might play a more important role than the suppression of Pol I mediated transcription in the early phase of fasting, because the former mechanism would be more efficient and quicker than the latter. Further experiments will be necessary to explore changes in RNA Pol I activity and the efficiency of cleavage of pre-rRNA during the response to fasting in Sirt7 KO and WT mice.

Recently, a new mechanism connecting the rDNA transcription to the energy status *in vitro* has been proposed. A regulatory complex, eNoSC, comprising Sirt1, histone methyl-transferase SUV39H1, and a novel nucleolar regulatory protein nucleomethylin NML, present at the rDNA promoter, can sense the energy starvation and induce transcriptional repression through histone deacetylation and H3K9 methylation, thus protecting cells from energy deprivation (Grummt and Ladurner, 2008; Murayama et al., 2008). However, no significant changes of the pre-rRNA levels had been found in the primary hepatocytes isolated from either WT or Sirt7 KO mice and cultured in different glucose concentrations, while glucose reduction significantly

decreased the pre-rRNA levels in HeLa cells (Fig 3.3). These results indicate that eNoSC may play its critical role only in some specific cells/tissues. Many cells need this mechanism to decrease the intercellular energy expenditure by rDNA silencing in response to the energy starvation since they cannot maintain the energy homeostasis by themselves. But, unlike these cells, hepatocytes can automatically regulate the homeostasis in the glucose, lipid and energy metabolism *in vitro* when the necessary hormone and cellular factors are present in the medium. When the glucose concentration is reduced, the hepatocytes stimulate gluconeogenesis to maintain the intracellular energy balance.

Insulin is one of the key factors controlling the hepatic regulation in metabolic homeostasis. Most studies demonstrated that insulin elevates the rRNA content of primary rat hepatocytes by stimulating rDNA transcription rather than by altering rates of processing or stability of the rRNA (Antonetti et al., 1993). As expected, the increased pre-rRNA levels were observed in the primary hepatocytes from WT mice cultured in high insulin medium (Fig 3.4A). However, in hepatocytes from aged mice (more than 18 months) no significant increase in pre-rRNA was observed (Fig 3.4B). This result suggests that insulin resistance develops in the aged hepatocytes. In contrast to wild-type hepatocytes, insulin failed to stimulate the rRNA transcription in young and old Sirt7 deficient hepatocytes even when the insulin concentration had been increased to 20nM. In the aged Sirt7 KO hepatocytes, insulin indeed down regulated the transcription of pre-rRNA (Fig 3.4A and B). Previous studies have examined the molecular mechanisms of insulin stimulated rRNA transcription (Hannan et al., 1998). By using 3T6 mouse fibroblasts and H4-II-E-C3 rat hepatoma cells, they found that insulin was capable of stimulating rDNA transcription by increasing the nuclear content of components, UBF and PAF53, required for assembly of RNA polymerase I at rDNA promoter. Such response was not associated with a change of the cellular content of RNA Pol I. Although Western blot for determining the content of RNA Pol I and UBF was not performed in my experiments, the recruitment of Pol I and UBF to the rDNA promoter had been detected using Chromatin Immunoprecipitation (ChIP) assay. Sirt7 has been described to interact with Pol I and UBF and to be a positive regulator of

rDNA transcription (Ford et al., 2006; Grob et al., 2009). It was not surprising that the binding of Pol I and UBF was significantly lower in Sirt7 deficient hepatocytes no matter with or without insulin. After insulin stimulation, increase in the nuclear UBF and PAF53 would favor their association at the rDNA promoter (Hannan et al., 1998), thus promoting the recruitment of RNA Pol I to rDNA promoter and increasing transcription. It was demonstrated that acetylation of UBF played a positive role in the regulation of pre-rRNA transcription (Hirschler-Laszkiewicz et al., 2001; Meraner et al., 2006; Pelletier et al., 2000). Furthermore, UBF1 acetylation at Lys (K) 352 by CREB binding protein (CBP) increases its occupancy at the rDNA promoter and stimulates the transcription of pre-rRNA (Lee et al., 2011). Moreover, the HAT activity of CBP can be stimulated by phosphorylation (Ait-Si-Ali et al., 1999). CBP phosphorylation by insulin-dependent pathway promotes its nuclear localization (Zhou et al., 2004). The posttranslational modifications of UBF or PAF53 may be another mechanism for insulin stimulated rDNA transcription. Impairment in these mechanisms in Sirt7 deficient mice may cause the defects of the rDNA transcription in response to insulin. It is not clear whether Sirt7 plays a direct role in regulation of UBF/PAF53 in response to insulin stimulation. Further studies will be required to investigate the roles of Sirt7 in regulating insulin signaling pathway(s) and the acetylation/phosphorylation status of UBF or PAF53 in WT and Sirt7 KO hepatocytes after insulin treatment.

#### 4.3 Sirt7 is required for the PPAR $\gamma$ -mediated adipogenesis through repression of Sirt1

In this thesis, I have described the important roles of Sirt7 in maintaining the hepatic metabolic homeostasis during adaptation to the fasting/refeeding and its requirement for the insulin stimulated rDNA transcription in vitro. In addition to the impaired function in the liver, the Sirt7 deficient mice exhibited also a compromised adipose tissue phenotype. The finding that Sirt7 deficient mice displayed reduced adipocyte size, stunted adipogenic gene expression (Fig 3.6), resistance to high-fat-diet (HFD) induced liver steatosis and insulin resistance (Yoshizawa et al., unpublished data)

is reminiscent of the phenotype observed in PPAR $\gamma$  +/- mice (Kubota et al., 1999). This observation is consistent with the hypothesis that the phenotype observed in Sirt7 KO mice is due to the reduced PPAR $\gamma$  expression and/or activity. Quantitative RT-PCR demonstrated the significantly reduced expression level of PPAR $\gamma$  in the white adipose tissue (Fig 3.6) as well as in the liver (Smolka et al., unpublished data).

PPAR $\gamma$  is considered the most important regulator in adipogenesis (Rosen and MacDougald, 2006; Tontonoz and Spiegelman, 2008). The further investigation in this work attempted to elucidate how Sirt7 regulates adipocytes differentiation. The results presented in these studies showed that Sirt7 was required for PPAR $\gamma$  expression and an efficient adipogenesis. Firstly, the adipogenesis assay *in vitro* showed that Sirt7 was required for the adipocytes differentiation in all *in vitro* cell models which I have tested in this thesis: Deletion of Sirt7 in MEFs (primary or immortalized) or downregulation of Sirt7 by retrovirus-mediated RNA interference in 3T3L1 both impaired the adipocytes differentiation *in vitro* (Fig 3.7 and 3.8). Moreover, Sirt7 deficient primary white preadipocytes also displayed severe adipocytes differentiation defects (Fig 3.14A). However, ectopic overexpression of Sirt7 in MEFs or 3T3L1 preadipocytes did not rescue the adipocytes differentiation (data not shown). These results suggest that Sirt7 is required but not sufficient to perform a full program of adipogenesis. Concomitant with the impaired adipogenesis, significantly reduced expression of adipogenic marker genes including PPAR $\gamma$ , C/EBP $\alpha$  and aP2 at both mRNA and protein levels were detected by QRT-PCR and Western blot or immunofluorescence (Fig 3.7, 3.8 and 3.9). In the early phase of adipogenesis *in vitro*, medium supplements such as fetal bovine serum (FBS), dexamethasone, isobutylmethylxanthine, and insulin induce low-level expression of PPAR $\gamma$  and C/EBP $\alpha$ , which then stimulate each other's expression in a positive feedback loop. Then the high levels of PPAR $\gamma$  and C/EBP $\alpha$  activate adipocyte gene expression and lipid accumulation and ultimately lead to phenotypic conversion from fibroblasts to adipocytes (Rosen et al., 2002). A variety of signaling factors have been identified that act upstream of PPAR $\gamma$  as positive or negative regulators (Lowe et al., 2011). Sirt1 was reported to inhibit adipogenesis through its binding to PPAR $\gamma$  promoter and repressing PPAR $\gamma$  transcription (Picard et al., 2004). Our previous studies

found that Sirt7 can interact with Sirt1 and inhibit Sirt1 enzymatic deacetylase activity on histone H4K16 as a substrate *in vitro* (Smolka et al., unpublished data). The present results showed that the Sirt1 protein expression was indeed elevated in Sirt7 KO MEFs especially in the early stages of differentiation (Fig 3.7E, and Fig 3.11C). We speculate that the high accumulation and/or high activity of Sirt1 might directly contribute to the lower expression of PPAR $\gamma$  in Sirt7 deficient MEFs. In line with the inhibitory role of Sirt1, a significant increase of Sirt1 occupancy at the PPAR $\gamma$  promoter in differentiating Sirt7 KO MEFs and Sirt7 knockdown 3T3L1 cells was observed (Fig 3.12). As a deacetylase, Sirt1 was shown to deacetylate lysine (K) residue 9 of histone 3 (H3K9) and facilitate the formation of heterochromatin and transcription repression (Imai et al., 2000; Vaquero et al., 2004). Sirt1 also regulates SUV39H1 to increase the levels of the H3K9me3 modification during heterochromatin formation (Vaquero et al., 2007). During the process of muscle development, Sirt1 deacetylates H3K9 and H3K14 in the myogenin and MHC promoter to inhibit muscle gene expression resulting in the retardation of muscle differentiation (Fulco et al., 2003). Sirt1 was found to interact with BCL11A (B cell leukemia 11A protein) and to be recruited to the BCL11A target genes promoters in a BCL11A-dependent manner leading to transcriptional repression in hematopoietic cell development and malignancies (Senawong et al., 2005). Considerable evidence suggests that epigenetic mechanisms, including histone methylation, acetylation, phosphorylation, and ubiquitination are critical for gene expression in the cellular physiological process (Jenuwein and Allis, 2001). In particular, acetylation of histones H3 (K9 and K14) and H4 (K5 and K12), mediated by histone acetyltransferases (HATs) such as p300, CBP, and P/CAF, is associated with transcriptional activation (Ogryzko et al., 1996; Schiltz et al., 1999). Methylation of H3K4, H4R3 and phosphorylation of H3S10 also results in gene activation (Chen et al., 1999; Cheung et al., 2000; Wang et al., 2001). In contrast, methylation of histone H3K9 and H3K27 generally correlates with gene repression (Nakayama et al., 2001; Rea et al., 2000; Vakoc et al., 2006). Recent studies have demonstrated that the chromatin remodeling factors were involved in the differentiation of specific cell types including muscle, neurons, and T cells (Avni et al., 2002; de la Serna et al., 2001; Machida et al.,

2001). Furthermore, ChIP assays revealed that histones are dynamically modified at the promoter regions of adipocyte marker genes during adipogenesis. The degree of histone H3K9 acetylation at the promoters of C/EBP $\alpha$ , PPAR $\gamma$ , aP2, ADD1/SREBP1c, and adiponectin was increased upon differentiation whereas level of histone H3K9 methylation displayed opposite patterns (Yoo et al., 2006). The histone methylation regulator PTIP (pax transactivation domain-interaction proteins) directly regulates H3K4 methyltransferase and H3K27 demethylase to activate PPAR $\gamma$  expression during adipogenesis (Cho et al., 2009). My results of ChIP assays to detect the epigenetic changes at PPAR $\gamma$  promoter in the differentiating cells showed that the active epigenetic marker AcH3K9 was significantly lower and inactivating epigenetic marker H3K9me3 was at a high level at the PPAR $\gamma$  promoter in Sirt7 deficient MEFs or in Sirt7 knockdown 3T3L1 cells differentiated for 5 days (Fig 3.9F and G). In agreement with the increase of epigenetic marks characteristic for heterochromatin, the increased occupancy of Sirt1 at the PPAR $\gamma$  promoter was also observed in Sirt7 deficient cells (Fig 3.12). It was demonstrated previously, that Sirt1 knockdown enhances the adipogenesis in 3T3L1 preadipocytes (Picard et al., 2004). Thus, it is reasonable to ask whether Sirt1 knockdown could improve the differentiation in Sirt7 KO MEFs. Indeed, as shown in Fig 3.13, decreased Sirt1 expression through shRNA as well as inhibition of Sirt1 activity by nicotinamide partly restored the adipogenic potential of Sirt7 KO cells, without, however reaching the level of differentiation in WT cells. Together, these data strongly suggest that increased cellular accumulation of Sirt1 and its increased binding to PPAR $\gamma$  promoter might result in higher deacetylation and increased trimethylation of histone H3K9 at the PPAR $\gamma$  promoter and thus be, at least in part, responsible for the reduced expression of PPAR $\gamma$  and impaired adipogenesis in Sirt7 knockout.

Subcellular localization of Sirt1 was found to vary in different tissues of the adult mouse and to shuttle between the nucleus and cytoplasm during development and in response to physiological and pathological stimuli (Tanno et al., 2007). For example, Sirt1 was mainly expressed in the nucleus of C2C12 myoblast cells, and was excluded from the nucleus upon differentiation. Moreover, only overexpressed nuclear but not

cytoplasmic Sirt1 enhanced the deacetylation of histone H3 (Tanno et al., 2007). These data prompted me to investigate the Sirt1 cellular localization during the adipogenesis in WT and Sirt7 KO MEFs. As shown in Fig 3.11D, the Sirt1 protein showed higher accumulation in cytoplasm and nucleus at the early stages of differentiation in Sirt7 deficient MEFs. In addition to the higher protein level, the time course of Sirt1 subcellular distribution was also affected in Sirt7 KO cells. In the wildtype cells the initially cytoplasmic Sirt1 gradually accumulated in the nucleus during differentiation. In Sirt7 deficient cells, Sirt1 was not only present in higher amounts in the cytoplasm but was already detected in the nucleus of undifferentiated Sirt7 KO cells. In contrast to the high level of Sirt1 in the nucleus of Sirt7 KO cells at the early stage of differentiation, ChIP assays failed to detect higher Sirt1 occupancy at the PPAR $\gamma$ 2 promoter at this stage (day0 or day2) in Sirt7 KO MEFs or Sirt7 KD cells (data not shown). However, the increased Sirt1 binding to the PPAR $\gamma$ 2 promoter in Sirt7 KO MEFs was detected at day5 of differentiation. Although the nuclear Sirt1 level was slightly lower in the late stage of differentiation (day5 or day8) in Sirt7 KO MEFs, the recruitment to the PPAR $\gamma$  promoter was still higher as compared to WT MEFs. In addition to the binding to PPAR $\gamma$  promoter, previous studies also found that Sirt1 could interact with PPAR $\gamma$  protein as a repressor to inhibit its activity (Picard et al., 2004). So the higher nuclear Sirt1 may directly inhibit PPAR $\gamma$  activity at the early stage in Sirt7 KO cells. Of course, technical difficulties in the ChIP experiments cannot be ruled out. Further ChIP experiments under varying conditions such as increase the amounts of chromatin or antibody for immunoprecipitation should be performed to optimize the assay, especially for the cells on day2 of differentiation.

A recent report indicated that C/EBP $\alpha$  regulated Sirt1 expression in 3T3L1 cell line during adipogenesis: Sirt1 protein levels were dramatically upregulated in differentiated 3T3-L1 cells along with increased C/EBP $\alpha$  during adipocyte differentiation (Jin et al., 2010). Likewise, Picard et al. observed that Sirt1 protein levels increased and peaked at day 5 after hormonal stimulation (Picard et al., 2004). Consistent with these reports, Sirt1 protein level was slightly elevated during differentiation in WT MEFs (Fig 3.7E) and 3T3L1 cells (data not shown). Moreover,

cellular fractionation displayed that Sirt1 was translocated from cytoplasm to nucleus in WT cells during differentiation while it was excluded from the nucleus following the prolonged differentiation in Sirt7 KO MEFs (Fig 3.11D). In agreement with the inhibitory influence of Sirt1 on the PPAR $\gamma$  transcription, PPAR $\gamma$  mRNA level increases at the early stage and then decreases from middle stage on during adipogenesis. It is likely that in WT cells, C/EBP $\alpha$  might stimulate PPAR $\gamma$  expression to promote adipogenesis induction, meanwhile the gradually increased Sirt1 expression (possibly induced by C/EBP $\alpha$ ) and its accumulation in the nucleus leads to PPAR $\gamma$  repression and suppresses further adipogenesis. Thus, Sirt1 and C/EBP $\alpha$  control adipocyte differentiation at an appropriate degree to maintain the adipose tissue homeostasis *in vivo*. The elevated protein levels and/or higher activity of Sirt1 together with its increased nuclear accumulation before the beginning of differentiation in Sirt7 KO MEFs may result in a significantly lower PPAR $\gamma$  expression at the critical time point important for induction of adipogenesis and thus result in the severe adipogenesis defect. As mentioned above, silencing of Sirt1 expression or inhibition of Sirt1 activity in Sirt7 deficient MEFs partially rescued the impaired adipocytes differentiation concomitantly with the increased expression of PPAR $\gamma$  and aP2, which, however did not reach the normal adipogenesis level. These effects were observed by inhibition of Sirt1 expression by shRNA mediated knock down and by treatment with a sirtuin specific inhibitor nicotinamide (NAM). NAM is a noncompetitive inhibitor and may inhibit all the members of the sirtuin family (Bitterman et al., 2002). Interestingly, NAM treatment can promote adipocytes differentiation in mouse mesenchymal cell line C3H10T1/2 and in pig preadipocytes (Backesjo et al., 2006; Bai et al., 2008). The improvement of adipogenesis in Sirt7 KO MEFs was stronger after NAM treatment than in Sirt1 knockdown. It is possible that NAM inhibits another sirtuin suppressing adipogenesis, such as Sirt2. In fact, Sirt2 was demonstrated to inhibit adipocytes differentiation through regulation of FoxO1 (Jing et al., 2007; Wang and Tong, 2009).

In addition to the preadipogenic cell lines such as 3T3L1 and embryonic fibroblasts, primary cultures of adipose-derived stromal vascular precursor cells (primary preadipocytes) are also commonly used to study molecular and cellular events

and regulatory influences on adipocyte differentiation. This culture system has several distinct advantages over preadipose cell lines: Such primary cells more closely reflect the *in vivo* characteristics of the tissue from which they are derived (Armani et al., 2010; Gregoire et al., 1998). Cells can also be obtained from rodent genetic models of obesity, transgenic mice or from rats and/or mice subjected to nutritional or hormonal manipulation (Hausman et al., 2008). My results showed that deletion of *Sirt7* leads to severe defects in adipogenesis of primary white preadipocytes compared to their heterozygous littermates (*Sirt7*<sup>+/-</sup>). Most interestingly, primary preadipocytes isolated from *Sirt7* knockouts lacking one *Sirt1* allele (*Sirt7*<sup>-/-</sup>/*Sirt1*<sup>+/-</sup>) exhibited significantly improved adipogenesis with a differentiation degree similar to the wildtype or *Sirt7*<sup>+/-</sup> controls (Fig 3.14A). Moreover, a significantly lower amount of preadipocytes could be isolated from *Sirt7*<sup>-/-</sup> mice, while no significant difference in amount of preadipocytes was observed in *Sirt7*<sup>+/-</sup> and *Sirt7*<sup>-/-</sup>/*Sirt1*<sup>+/-</sup> mice (Fig 3.14A and data not shown). Why *Sirt1* knock down could not completely restore the adipogenesis in *Sirt7* KO MEFs in contrast to the obviously successful rescue of adipogenesis in *Sirt7*<sup>-/-</sup>/*Sirt1*<sup>+/-</sup> mice? Decreased *Sirt1* expression through *Sirt1* knock down in *Sirt7* KO MEFs augmented the expression of PPAR $\gamma$ , however, the level of PPAR $\gamma$  expression could not reach the normal level in WT MEFs (Fig 3.13A, C and data not shown). Thus, it was not surprising that knockdown of *Sirt1* only partly rescued the adipogenesis defect in *Sirt7* deficient cells. In contrast to an acute decrease of *Sirt1* expression using *Sirt1* knock down in cultured cells, a constitutively decreased *Sirt1* expression is present throughout the entire development of the *Sirt7*<sup>-/-</sup>/*Sirt1*<sup>+/-</sup> mice. Therefore, in these mice, the PPAR $\gamma$  expression can recover gradually during the development, allowing the adipogenesis of preadipocytes to reach the normal level (Fig 3.14).

Preadipocytes (or adipocyte precursor cells) reside within the heterogeneous adipose stromal vascular fraction (SVF), which also contains fibroblasts, erythrocytes, macrophages, endothelial cells and other cell types (Ailhaud et al., 1992). Using the PPAR $\gamma$ -reporter (PPAR $\gamma$ -R26R) bearing mice, it has been found that most adipocytes descend from a pool of the proliferating progenitors (PPAR $\gamma$  positive) which are already, either prenatally or early in postnatal life, committed to adipogenesis (Tang et al., 2008).

Later, using fluorescence-activated cell sorting (FACS) in combination with an *in vivo* transplantation scheme, a resident subpopulation of early adipocyte progenitor cells (Lin<sup>-</sup>:CD29<sup>+</sup>:CD34<sup>+</sup>:Sca-1<sup>+</sup>:CD24<sup>+</sup>) was identified in adult WAT (Rodeheffer et al., 2008). These cells could be induced to differentiate into mature adipocytes, they were also able to reconstitute a normal WAT depot when injected into the residual fat pads of A-Zip lipodystrophic mice (Rodeheffer et al., 2008). Thus, it is reasonable to ask whether Sirt7 is required for regulation of the adipocyte progenitor cells and whether such regulation requires inhibition of Sirt1. In fact, Sirt1 has been demonstrated to regulate many progenitor cells during development and differentiation into the target cells. For example, activation of Sirt1 suppressed proliferation of neural progenitor cells (NPCs) and redirected their differentiation towards the astroglial lineage, whereas Sirt1 inhibition had the opposite effect. (Prozorovski et al., 2008). Inhibition of Sirt1 increased Mash1 and Ngn2 levels, which promotes neural progenitors toward motoneuron differentiation (Zhang et al., 2011). Sirt1 has been shown to increase muscle precursor cell (MPC) proliferation (Rathbone et al., 2009) but inhibit muscle differentiation (Fulco et al., 2003). Sirt1 also promotes osteogenesis of human mesenchymal stem cells by upregulating RUNX2 gene expression via an enhanced FOXO3A protein expression (Tseng et al., 2011). The discovery that Sirt1<sup>-/-</sup> and Sirt1<sup>+/-</sup> adult bone marrow had decreased numbers of hematopoietic progenitors indicated the critical role of Sirt1 in mouse hematopoiesis (Ou et al., 2011). Further experiments should concentrate on the analysis of the adipocyte progenitors in WT and Sirt7 deficient SVF cells together with the role of Sirt1.

My present results showed that ectopic Sirt7 overexpression could not rescue the defect of adipogenesis in Sirt7 KO MEFs or Sirt7 KD 3T3L1 cells (Fig 3.10A and data not shown), although the mRNA levels of PPAR $\gamma$  were slightly increased after Sirt7 overexpression, but still significantly lower than the normal levels in WT MEFs or control 3T3L1 cells (Fig 3.10C and data not shown). However, the impaired adipogenesis in Sirt7 deficient MEFs could be fully rescued by overexpression of ectopic PPAR $\gamma$ 2. The inability of Sirt7 overexpression to rescue the impaired adipogenesis of Sirt7 KO MEFs could imply that this phenotype is caused by long-term

changes occurring in the context of the whole organism of Sirt7 knockout mouse. It is also possible, as mentioned above, that Sirt7 knockout results in an inhibition of adipocyte progenitor cells likely via the suppression of PPAR $\gamma$  or prevention of mesenchymal stem cells to commitment to preadipocytes. Indeed, ectopic PPAR $\gamma$ 2 overexpression has been found to rescue several adipogenic defects in certain genetically deficient cells. For example, adding PPAR $\gamma$ 2 to C/EBP $\alpha$   $-/-$  fibroblasts via a retroviral vector restores their capacity to accumulate lipids and to activate markers of adipogenesis (Wu et al., 1999). Furthermore, the adipogenic defect in Med23-deficient cells was rescued by ectopic expression of PPAR $\gamma$ 2 (Wang et al., 2009).

#### 4.4 Sirt7 regulates Sirt1 activity by interfering with its auto-deacetylation

The results discussed above have demonstrated that Sirt7 normally ensures cellular functions responsible for the efficient adipocytes differentiation by inhibition of Sirt1 activity during the cellular physiological process. The influence of Sirt7 on Sirt1 transcription has been excluded since the transcript levels of Sirt1 were not changed in Sirt7 KO cells. Significantly, a direct interaction between Sirt1 and Sirt7 was identified in our laboratory. This interaction was dependent on the intact Sirt7 core deacetylation domain (Fig 3.15A). We initially speculated that Sirt7 regulates Sirt1 via post-translational modification (PTM) most probably through the deacetylation of Sirt1 by Sirt7. Post-translational modifications of proteins determine their tertiary and quaternary structures and regulate their activities and functions (Seo and Lee, 2004). Various recent studies indicated the effects of PTMs on Sirt1 in many biological processes. One study identified a novel PTM of Sirt1 by sumoylation at Lys734, and such sumoylation increased Sirt1 deacetylase activity in response to genotoxic stress (Yang et al., 2007). Subsequently, using mass spectrometry, 13 residues in Sirt1 were identified to be phosphorylated *in vivo*, these residues were phosphorylated by cell cycle-dependent kinase cyclinB/Cdk1 to control Sirt1 level and function during the cell cycle (Sasaki et al., 2008). Another protein kinase, casein kinase 2 (CK2), was found to phosphorylate conserved residues Ser154, 649, 651 and 683 in the N- and C-terminal

domains of mouse Sirt1 after ionizing radiation (IR) and such phosphorylation increased Sirt1 substrate-binding affinity and deacetylation rate of p53 to protect cells from apoptosis after DNA damage (Kang et al., 2009). cJUN N-terminal kinase (JNK1) phosphorylated Ser27, Ser47, and Thr530 of human Sirt1 and this phosphorylation increased its nuclear localization and enzymatic activity (Nasrin et al., 2009). In contrast to the findings of JNK1, the phosphorylation of Ser47 by mTOR inhibited the deacetylase activity of Sirt1 (Back et al., 2011). Moreover, it was showed that human Sirt1 was stabilized via JNK2-dependent phosphorylation of Ser27, but not of Ser47 by JNK1 (Ford et al., 2008). However, mouse Sirt1 could be phosphorylated by JNK1 at Ser46 (Ser47 in human Sirt1) to induce mSirt1 degradation (Gao et al., 2011). In addition, Sirt1 is also modified by methylation. Four lysine sites (Lys233, Lys235, Lys236, and Lys238) at the N-terminus of human Sirt1 have been identified to be methylated by methyltransferase Set7/9. Methylation of these residues disrupts the interaction between Sirt1 and its substrate p53 but does not affect its deacetylase activity toward p53 (Liu et al., 2011b). A recent report suggested that oxidants, aldehydes, and cigarette smoke induced carbonyl modifications on cysteine residues of Sirt1 concomitant with decreasing enzymatic activity and marking the protein for proteasomal degradation, which was implicated in chronic inflammatory conditions in human lung epithelial cells (Caito et al., 2010). So far no acetylation of lysine residues was reported for the mammalian Sirt1. However, the Sirt1's homologue in fruit fly, *Drosophila* Sir2 (dSir2), has been reported to be acetylated by the histone acetyltransferase CREB-binding protein (CBP) in *in vitro* and *in vivo* acetylation assays (Zhao et al., 2009). Moreover, another mammalian sirtuin, Sirt2, can be acetylated by p300 resulting in down-regulation of Sirt2 deacetylation (Han et al., 2008). Thus, I was interested in the effects of acetylation on Sirt1 enzyme activity and whether Sirt7 regulates Sirt1 through deacetylation.

Unexpectedly, overexpression of Sirt7 together with Sirt1 resulted in an increased Sirt1 acetylation, whereas Sirt7H188Y inactive mutant failed to increase the Sirt1 acetylation level (Fig 3.15B and C). Obviously, Sirt7 as a deacetylase could not directly acetylate Sirt1. The possible explanation may be that Sirt7 deacetylates certain

---

acetyltransferase to increase its activity, thus promoting the acetylation of Sirt1. Another possibility is that Sirt7 may prevent the auto-deacetylation of Sirt1 through direct interaction and inhibition.

My results revealed that Sirt1 undergoes reversible auto-deacetylation to regulate its catalytic activity. Sirt7 restricts Sirt1 activity by inhibition of the auto-catalytic process. Autocatalytic modifications of regulatory factors are common and play important role in posttranslational regulation of their activity. Such autoregulation has been primarily described for kinases, phosphatases, acetyltransferases, and also for ADP-ribosyltransferases. For example, the autophosphorylation of the ataxia telangiectasia-mutated and Rad3-related (Patrick) kinases (Patrick) stimulates the ATR kinase activation after DNA damage and facilitates ATR substrate recognition (Liu et al., 2011a). The catalytic activity of p300 is also stimulated by autoacetylation (Thompson et al., 2004). Autoacetylation induces the dissociation of p300 from the chromatin to enhance TFIID binding and subsequent preinitiation complex formation (Black et al., 2006). Autoacetylation of P/CAF increases its histone acetyltransferase activity (Santos-Rosa et al., 2003) and controls its nuclear localization (Blanco-Garcia et al., 2009). TIP60 is autoacetylated in response to UV damage to elevate its activity (Wang and Chen, 2010). Moreover, automethylation of the histone methyltransferase G9a creates a binding site for the heterochromatin protein 1 (HP1) (Chin et al., 2007), and PARP-1 can be auto-ADP-ribosylated, resulting in the release of PARP1 from chromatin (Kim et al., 2004). Among the members of mammalian sirtuins, Sirt6 possesses an auto-ADP-ribosylation activity, although the site of this automodification and its functions are not clear so far (Liszt et al., 2005). My finding that control of Sirt1 auto-deacetylation is instrumental for regulation of its activity indicates that the autocatalytic modification does apply for deacetylases as well. Thus, my study shows that Sirt1 deacetylates itself and enhances its activity in a positive regulatory loop, and Sirt7 negatively regulates Sirt1 possibly to protect from cellular damage, which may be caused by the continuous activation of Sirt1.

Furthermore, my data indicate that the acetyltransferase MOF can acetylate Sirt1 and the acetylation of Sirt1 by MOF can inhibit its deacetylase activity on its

target substrate H3K9 and p53 (Fig 3.17 and Fig 3.18C). Indeed, deacetylases are also subject to post-translational modifications including acetylation, phosphorylation, ubiquitylation and sumoylation, which can determine their stability, localization, activity and protein–protein interactions (Brandl et al., 2009). Taken together with the findings that p300 acetylates HDAC1 and inhibits its enzymatic activity (Qiu et al., 2006) as well as that acetylation of Sirt2 reduces its activity (Han et al., 2008), it is not surprising that the acetylation of Sirt1 down-regulates its deacetylase activity. It has been reported that the *drosophila* homologue of Sirt1, dSir2, is acetylated by CBP and the *in vitro* synthesized murine Sir2 (mSirt1), is acetylated by recombinant p300 and p300/CBP (HAT) proteins in the *in vitro* acetylation assay (Zhao et al., 2009). However, I was not able to detect the acetylation of mSirt1 by CBP in IP experiments after co-transfection of Sirt1-CFP and CBP-HA plasmids. The difference between mammalian and fly proteins and the difference between *in vivo* and *in vitro* assay can be the explanation of these contradictory results. A novel report showed that Sirt1 deacetylated the autoacetylated hMOF to improve its robust binding to nucleosomes, accompanied with increase of AcH4K16 and activation of gene transcription (Lu et al., 2011). My results showed that MOF acetylated Sirt1 and repressed its deacetylase activity. This provides another possibility for the modulatory mechanism of Sirt1 auto-deacetylation activity: The auto-deacetylated Sirt1 has high activity, while the autoacetylated MOF have reduced activity. Sirt1 can deacetylate MOF and increase its acetylation activity. Then MOF acetylates Sirt1 and attenuates its activity to form a negative feed-back loop. More interestingly, the acetylation sites seemed not to be the lysines for the auto-deacetylation by Sirt1 (such as K230), since the acetylation level of inactive Sirt1H355Y mutant was even lower as compared to the WT Sirt1 in presence of MOF (Fig 3.17D) and the acetylation of Sirt1 by MOF was also increased in the Sirt1 K230R mutation (data not shown). Whether Sirt7 deacetylates MOF and increases its catalytic activity to repress Sirt1 by post-translational acetylation should be further explored.

The mutation analyses showed that the K230R mutation increased Sirt1 deacetylase activity. Indeed, Sirt1 efficiently deacetylated lysine 230 in *in vitro*

deacetylase assay using an acetylated Sirt1 derived peptide and recombinant Sirt1 protein. These data suggest that the auto-deacetylation of Sirt1 mainly occurs on the lysine 230 residue. Furthermore, the multiple sequence alignment of Sirt1 homologs from various species clearly showed that K230 is shared among species, which indicates that auto-decetylation of Sirt1 may be conserved in different species. Interestingly, K230 is not localized in the conserved catalytic domain but in the N-terminal part of Sirt1. The available data suggest that the N- and C-terminal regions of sirtuins beyond the catalytic domain play a role in regulation of sirtuin functions. Moreover, multiple PTMs including phosphorylation, methylation and sumoylation, have been identified to target these domains (Flick and Luscher, 2012). In addition, initial studies suggest that PTMs identified within the N- and C-terminal domains of sirtuins may control the properties of their catalytic activity, polymerization, substrate specificity, and subcellular localization (Flick and Luscher, 2012). Using a serial multiple KR mutation strategy, I could demonstrate that beside the increased activity of Sirt1K230R mutant, the 3KR2 (without K369) mutation greatly enhanced the Sirt1 deacetylation activity on the p53 target as well, while, the other 3KR mutants and 4KR mutant failed to activate Sirt1. These findings indicate that a combination of acetylation and deacetylation at specific lysine residues is responsible for Sirt1 activation. Besides that autodeacetylation of K230 increases Sirt1 activity, K369 has to be acetylated to preserve Sirt1 activity. Interestingly, the lysine 369 resides in the catalytic domain of Sirt1. As the acetylation of *Drosophila* Sir2 in the catalytic domain by dCBP was required for dSir2 activity (Zhao et al., 2009), the acetylation of lysines in the catalytic domain might indeed be necessary for the Sirt1 deacetylase activity. However, which acetyltransferase is responsible for this acetylation still remains elusive.

My results highlight the importance of cross-regulatory circuits between two individual members of the nuclear sirtuins in organismal homeostasis and emphasize the role of posttranslational acetylation in the modulation of Sirt1 activity. Furthermore, my data demonstrate that Sirt7 can interact with Sirt1 and inhibit the activity of Sirt1, although the precise mechanisms of this effect are still unknown and need to be elucidated in future. The importance of the Sirt1/Sirt7 cross-regulation was revealed to

be pivotal to establish a well-balanced signaling network required for maintenance of metabolic homeostasis *in vivo* including the fasting/refeeding adaptation in liver and the adipogenesis in white adipose tissue. Based on the analysis of the Sirt7 deficient model *in vivo* or *in vitro*, I propose that the lack or decrease of Sirt7 will disturb the balance of the regulatory network resulting in an increased activity of Sirt1. Aberrant or pathologically sustained activation of Sirt1 distorts principally beneficial effects such as fat mobilization and prevention of adipogenesis causing metabolic dysfunctions. In WT cells, the adipogenic stimuli induce C/EBP $\alpha$  expression followed by PPAR $\gamma$  expression, this central regulatory loop promotes adipogenic gene expression. C/EBP $\alpha$  also induces the Sirt1 expression (Jin et al., 2010), Sirt1 then deacetylates itself and elevates its activity; the activated Sirt1 is recruited to the PPAR $\gamma$  promoter and suppresses the transcription of PPAR $\gamma$  through the epigenetic modification. Thus, this gradual suppression mechanism is able to control adipocytes differentiation at an appropriate degree to maintain the adipose homeostasis *in vivo*. During the adipogenesis, Sirt7 is also slightly up-regulated (Fig 3.7E) and negatively restricts auto-deacetylation of Sirt1 to prevent the occurring of the continuous increase of Sirt1 activity. In the Sirt7 KO cells, because of the deficiency of Sirt7 inhibition, Sirt1 is highly activated and the auto-deacetylation leads to hyperactivation of Sirt1 and the repression PPAR $\gamma$  expression, thus the cells are prevented to enter the adipogenesis program upon the adipogenic induction resulting in the defect of differentiation. Further investigations will focus on the cross-talk between Sirt1 and Sirt7, and the double knockout mice may be the important tools, which will lead to a better understanding of these two sirtuins.

## 5. Summary

Sirtuins are  $\text{NAD}^+$ -dependent protein deacetylases or ADP-ribosyltransferases, which play decisive roles in chromatin silencing, cell cycle regulation, cellular differentiation, metabolism, stress resistance and tumorigenesis. In mammals, sirtuins emerged as key metabolic sensors in various tissues and play a prominent role in metabolic adaptation to energy/nutrient stress. Sirt1 and Sirt6 are believed to act synergistically to prevent liver steatosis, especially under high-fat diet. Sirt1 and Sirt2 inhibit adipogenesis, and Sirt1 promotes the brown remodeling of white adipose tissue to control the metabolic balance in adipose tissue. Sirt7 was postulated to regulate rDNA transcription by associating with RNA polymerase I (Pol I) and maintain oncogenic transformation through deacetylation of histone H3K18, but the role of Sirt7 in metabolic regulation has remained enigmatic. Here, using the Sirt7 knockout mice and Sirt7 knock down approaches, my results describe the role of Sirt7 in maintenance of metabolic homeostasis in liver and the adipocytes differentiation in white adipose tissue. In liver, Sirt7 is required for the stimulation of hepatic rDNA transcription in response to insulin and is necessary for the fasting/refeeding adaptation. The second part of the study demonstrates the essential role of Sirt7 in adipocytes differentiation and white adipose tissue homeostasis. Absence of Sirt7 resulted in increased protein accumulation and activity of Sirt1 and restricted formation of white adipose tissue. In addition, my thesis shows that Sirt7 interacts with Sirt1 and restricts Sirt1 activity by inhibition of Sirt1 auto-deacetylation. These data uncover a new level of complexity in regulation of sirtuin activity and identify autocatalytic posttranscriptional modification as a new principle for regulation of Sirt1 activity. The antagonistic interactions between the two nuclear sirtuins are crucial to establish a well-balanced signalling network required for the maintenance of metabolic homeostasis. In the last part of this thesis, two Sirt1 targeting mouse strains were generated, which allow conditional, tissue specific inactivation of the Sirt1 gene and double knock out Sirt1 and Sirt7 in mice. These mouse models will help to further evaluate the sirtuin functions and the cross-regulatory network between Sirt1 and Sirt7 in the whole body or in the individual tissues.

## 6. Zusammenfassung

Sirtuine sind  $\text{NAD}^+$ -abhängige Protein Deacetylasen und/oder ADP-Ribosyltransferasen, die entscheidende Rollen in einer Vielzahl von Prozessen spielen. Dazu gehören: Zellzyklusregulation, Differenzierung, metabolische Regulation, Stressresistenz sowie Tumorentstehung und Chromatin-Remodellierung. In Säugetieren nehmen Sirtuine eine Schlüsselrolle als metabolische Sensoren ein und regulieren die Adaptation auf Energie- und Nährstoffveränderungen. Synergistische Funktionen wurden für Sirt1 und Sirt6 in der Leber beschrieben. Beide Sirtuine wirken der Entwicklung von Lebersteatose, insbesondere bei fettreicher Ernährung, entgegen. Bei der Differenzierung von weißem Fettgewebe (Adipogenese) wurde eine hemmende Wirkung von Sirt1 und Sirt2 beobachtet. Des Weiteren, fördert Sirt1 die Entstehung von braunem Fettgewebe aus weißem Fett und kontrolliert somit die metabolische Balance im Fettgewebe. Für Sirt7 wurde bislang eine Funktion in der Regulation der rDNA Transkription durch die Interaktion mit der RNA-Polymerase I postuliert, eine Rolle in der Regulation metabolischer Prozesse konnte bis jetzt aber noch nicht nachgewiesen werden. In meiner Arbeit konnte ich mittels der Sirt7 Knock Out Maus bzw. verschiedener Sirt7 Knock Down Versuche belegen, dass Sirt7 eine Rolle in der Aufrechterhaltung der metabolischen Homöostase in der Leber und in der Differenzierung von Adipozyten in weißem Fettgewebe spielt. In der Leber ist Sirt7 für die Anregung der rDNA Transkription als Antwort auf eine Stimulation durch Insulin notwendig. Zudem konnte belegt werden, dass Sirt7 für eine Anpassung an Hungerphasen und anschließender Nahrungsaufnahme erforderlich ist. Im zweiten Teil meiner Arbeit konnte ich zeigen, dass die Funktion von Sirt7 in der Differenzierung von Adipozyten und in der Homöostase des weißen Fettgewebes essentiell ist. Hier resultiert der Verlust von Sirt7 in einer vermehrten Proteinakkumulation und einer erhöhten Aktivität von Sirt1, die der Fettgewebsentstehung entgegen wirkt. Hier konnte durch meine Arbeit eine Interaktion zwischen Sirt7 und Sirt1 belegt werden, welche mit einem Aktivitätsverlust von Sirt1 durch Inhibierung dessen Auto-Deacetylasefunktion einhergeht. Diese Ergebnisse decken eine neue Stufe der Komplexität der Aktivitätsanpassung der Sirtuine auf und

identifizieren eine posttranskriptionelle Modifizierung als einen neuen Weg der Sirt1 Regulation durch dessen autokatalytische Aktivität. Die antagonistische Interaktion zwischen diesen zwei nukleären Sirtuinen ist entscheidend um eine ausgewogene Verknüpfung einzelner Signalwege herzustellen, die für die Aufrechterhaltung der metabolischen Homöostase notwendig sind. Im letzten Teil meiner Arbeit wurden zwei konditionelle Sirt1 Knock Out Mausstämme generiert, welche einerseits eine gewebsspezifische Inaktivierung von Sirt1 und zum anderen die gleichzeitige Ausschaltung von Sirt1 und Sirt7 in Mäusen erlauben. Die entstandenen Mausmodelle können helfen, die Funktionen von Sirt1 und Sirt7 und deren gegenseitige Beeinflussung im gesamten Organismus oder speziell in einzelnen Organen genauer zu untersuchen.

## **7. List of abbreviations:**

A	Adenine
ACC	Acetyl-CoA carboxylase
ACLY	ATP citrate lyase
AceCS1	Acetyl-coenzyme A (acetyl-CoA) synthetase 1
ADP	Adenosine diphosphate
albCre	Albumin Cre
Akt/PKB	Protein Kinase B
ATP	Adenosine triphosphate
aP2	adipocyte protein 2
BAC	Bacterial artificial chromosom
BGH	Bovine growth hormone
BMP	Bone morphogenetic protein
bp	Base pairs
BSA	Bovine serum albumin
C	Cytosine
CBP	CREB-binding protein
cDNA	complementary DNA
C/EBP	CCAAT-enhancer-binding protein
CFP	Cyan fluorescent protein
ChREBP	Carbohydrate-responsive element-binding protein
ChIP	Chromatin immunoprecipitation
Cm	centimeter
CMV	Cytomegalovirus
Co-IP	Co-immunopräzipitation
CREB	cAMP response element-binding protein
DAPI	4',6-diamidino-2-phenylindole
DMEM	Dulbecco's Modified Eagle Medium
DMSO	Dimethyl sulfoxide

---

DNA	Deoxyribonucleic acid
DSB	Double-strand break
DTA	Diphtheria toxin A
DTT	Dithiothreitol
<i>E. coli</i>	<i>Escherichia coli</i>
EDTA	Ethylenediaminetetraacetic acid
eNoSC	Energy-dependent nucleolar silencing complex
ES	Embryonic stem cell
FAS	Fatty acid synthase
FCS	Fetal calf serum
FGF	Fibroblast growth factor
FOXO	Forkhead box protein O
g	Gram
<i>g</i>	Gravitational acceleration
G	Guanine
GAPDH	Glyceraldehyde 3-phosphate dehydrogenase
GFP	Green fluorescent protein
GLUT	Glucose transporter
h	Hour
HA	Hemagglutinin
HBS	HEPES Buffered Saline
HDAC	Histondeacetylase
HDL	High-density lipoprotein
HE	Hematoxylin and eosin
HEPES	4-(2-hydroxyethyl)-1-piperazineethanesulfonic acid
HIF	Hypoxia-inducible factor
HNF-4 $\alpha$	Hepatocyte nuclear factor 4 alpha
IF	Immunofluorescence
IP	Immunoprecipitation

JNK	c-Jun N-terminal kinases
kb	kilo-base pairs
kDa	kilodalton
kg	kilogram
KO	Knock Out
M	molar
MES	2-( <i>N</i> -morpholino)ethanesulfonic acid
MEF	Mouse embryonic fibroblast
min	Minute
ml	milliliter
mm	millimeter
mM	millimolar
MOPS	3-( <i>N</i> -morpholino)propanesulfonic acid
MPI	Max-Planck Institute
mRNA	messenger RNA
MS	Mass spectrometry
mTOR	Mammalian target of rapamycin
NAD <sup>+</sup>	Nicotinamide Adenine Dinucleotide
NAM	Nicotinamide
NB	Northern blot
Neo	Neomycin
Ng	Nanogram
NFκB	Nuclear factor kappa-light-chain-enhancer of activated B cells
nM	Nanomolar
NoRC	Nucleolar remodeling complex
OD600	Optical density measured at a wavelength of 600 nm
ORF	Open reading frame
P300	E1A binding protein p300
PAF53	Polymerase-associated factor 53

---

PBS	Phosphate Buffered Saline
PCAF	P300/CBP-associated factor
PCR	Polymerase chain reaction
PEPCK	Phosphoenolpyruvate carboxykinase
PFA	Paraformaldehyde
PGC-1	Peroxisome proliferator-activated receptor gamma coactivator 1
PGK	Phosphoglycerate kinase
PI3	Phosphorus triiodide
pM	Picomolar
PMSF	Phenyl methyl sulfonyl fluoride
Pol I	RNA Polymerase I
PPAR $\gamma$	Peroxisome proliferator-activated receptor gamma
Pre-rRNA	Preribosomal RNA
Q-PCR	quantitative PCR
rDNA	Ribosomal DNA
RNA	Ribonucleic acid
RPM	Rotations per minute
rRNA	Ribosomal RNA
RT	Room temperature
RT-PCR	Reverse transcription PCR
s	Second
SB	Southern blot
SDS	Sodium dodecyl sulfate
SDS-PAGE	Sodium dodecyl sulfate polyacrylamide gel electrophoresis
ShRNA	Small hairpin RNA
SILAC	Stable isotope labeling with amino acids in cell culture
SREBP	Sterol Regulatory Element-Binding Protein
SSC	Saline-sodium citrate buffer
STAT	Signal transducer and activator of transcription

T	Thymine
T3	Triiodothyronine
TBS	Tris-Buffered Saline
TIP60	HIV-1 Tat-inactive protein 60
TNF- $\alpha$	Tumor necrosis factor alpha
TORC	Targets of rapamycin complex
TSA	Trichostatin A
UBF	Upstream binding factor
UCP1	Uncoupling protein 1
UV	Ultraviolet
V	Volt
WT	Wild type
WAT	White adipose tissue
YFP	Yellow fluorescent protein
$\mu\text{g}$	micro gram
$\mu\text{l}$	micro liter
$\mu\text{M}$	micro molar
$\mu\text{m}$	micro meter

## **8. List of figures and tables**

Figure 1.1: Sirtuin enzymatic activities.

Figure 1.2: Schematic representation of seven mammalian sirtuins.

Figure 1.3: Substrates and biological functions of Sirt1.

Figure 1.4: Mouse knockout models as tools for exploring sirtuin function.

Figure 1.5: Scheme of hepatic signaling in fed state activating anabolic pathways in the liver.

Figure 1.6: Scheme of hepatic signalling events during fasting resulting in an increased glucose output from the liver.

Figure 1.7: A model for the epigenetic on/off switch regulating nucleolar dominance.

Figure 3.1: Dysregulation of key enzymes involved in hepatic fat metabolism and of PGC1 $\alpha$  expression.

Figure 3.2: Disturbed expression of genes encoding key enzymes involved in gluconeogenesis and lipid metabolism and of the pre-rRNA transcription in Sirt7 deficient mice liver in response to fasting/refeeding.

Figure 3.3: Different glucose concentration does not affect transcription of pre-rRNA in hepatocytes but in HeLa cells.

Figure 3.4: Insulin stimulates pre-rRNA transcription in WT but not in Sirt7 deficient hepatocytes.

Figure 3.5: The increased recruitment of Pol I and UBF to rDNA promoter and higher of acetylation of H3K9 at the rDNA can be seen in WT but not Sirt7 KO hepatocytes after insulin treatment.

Figure 3.6: Sirt7 knockout mice accumulate less subcutaneous and visceral fat with age.

Figure 3.7: Sirt7 is required for adipogenesis in primary MEFs.

Figure 3.8: Sirt7 is required for differentiation of 3T3-L1 preadipocytes.

Figure 3.9: Sirt7 is required for PPAR $\gamma$  expression in MEFs.

Figure 3.10: Ectopic PPAR $\gamma$  but not Sirt7 overexpression rescues the adipogenesis defect in Sirt7 deficient cells.

Figure 3.11: Higher accumulation of Sirt1 protein in Sirt7 deficient cells.

Figure 3.12: Increased occupancy of Sirt1 at the PPAR $\gamma$  promoter in Sirt7 deficient cells during adipogenesis.

Figure 3.13: Sirt1 knock down or inhibition of Sirt1 activity can partly rescue the impaired adipogenesis in Sirt7 KO immortalized MEFs.

Figure 3.14: Removal of a single Sirt1 allele improves the adipogenesis of primary Sirt7 deficient preadipocytes and increases the WAT mass and PPAR $\gamma$  expression of Sirt7 KO mice.

Figure 3.15: Sirt7 physically interacts with Sirt1 and increases the acetylation of Sirt1.

Figure 3.16: Sirt1 is self-deacetylated *in vivo* and *in vitro*.

Figure 3.17: Acetyltransferase MOF acetylates Sirt1 and attenuates its deacetylase activity.

Figure 3.18: Autodeacetylation of Sirt1 occurs mainly at K230. The combination of acetylation at K369 and deacetylation at other lysines may be responsible for the promotion of Sirt1 deacetylase activity.

Figure 3.19: Generation of two Sirt1 conditional knockout constructs.

Figure 3.20: Strategy and work flow chart used in generating the Sirt1 conditional knockout targeting vector by recombination.

Figure 3.21: Genotyping of two Sirt1 conditional knockout ES cells or mice tails by PCR and Southern blot.

Figure 3.22: Sirt1 is specifically knocked out in the livers of Sirt1sLiKO and Sirt1lLiKO mice.

Figure 3.23: Developmental abnormalities in Sirt1 deficient embryos.

Table 2.1: List of primary antibodies.

Table 2.2: List of secondary antibodies.

Table 2.3: List of primers for quantitative real-time-PCR (QRT-PCR).

Table 2.4: List of primers for semi-quantitative RT-PCR.

Table 2.5: List of primers for genotyping.

Table 2.6: List of primers for Northern blot probes.

Table 2.7: List of primers for Southern blot probes.

Table 2.8: List of primers for the construction of targeting vectors.

Table 2.9: List of primers for mutagenesis.

Table 2.10: List of primers for sequencing.

Table 2.11: List of probes for Northern blot.

Table 2.12: List of probes for Southern blot genotyping.

Table 2.13: List of vectors.

Table 2.14: List of bacterial strains.

Table 2.15: List of cell lines.

Table 2.16: List of media for cell culture.

Table 2.17: List of mouse strains.

Table 2.18: List of used kits.

Table 2.19: List of special equipment.

Table 2.20: List of used software.

Table 3.1: Genotypes of offsprings from crosses between heterozygous parents of Sirt1 CMVKOS and Sirt1 CMVKOL

## 9. References

- Ailhaud, G., Grimaldi, P., and Negrel, R. (1992). Cellular and molecular aspects of adipose tissue development. *Annu Rev Nutr* 12, 207-233.
- Ait-Si-Ali, S., Carlisi, D., Ramirez, S., Upegui-Gonzalez, L.C., Duquet, A., Robin, P., Rudkin, B., Harel-Bellan, A., and Trouche, D. (1999). Phosphorylation by p44 MAP Kinase/ERK1 stimulates CBP histone acetyl transferase activity in vitro. *Biochem Biophys Res Commun* 262, 157-162.
- Alcain, F.J., and Villalba, J.M. (2009). Sirtuin inhibitors. *Expert Opin Ther Pat* 19, 283-294.
- Altomonte, J., Richter, A., Harbaran, S., Suriawinata, J., Nakae, J., Thung, S.N., Meseck, M., Accili, D., and Dong, H. (2003). Inhibition of Foxo1 function is associated with improved fasting glycemia in diabetic mice. *Am J Physiol Endocrinol Metab* 285, E718-728.
- Anand, P., and Gruppuso, P.A. (2005). The regulation of hepatic protein synthesis during fasting in the rat. *J Biol Chem* 280, 16427-16436.
- Anderson, R.M., Bitterman, K.J., Wood, J.G., Medvedik, O., and Sinclair, D.A. (2003). Nicotinamide and PNC1 govern lifespan extension by calorie restriction in *Saccharomyces cerevisiae*. *Nature* 423, 181-185.
- Antonetti, D.A., Kimball, S.R., Horetsky, R.L., and Jefferson, L.S. (1993). Regulation of rDNA transcription by insulin in primary cultures of rat hepatocytes. *J Biol Chem* 268, 25277-25284.
- Aparicio, O.M., Billington, B.L., and Gottschling, D.E. (1991). Modifiers of position effect are shared between telomeric and silent mating-type loci in *S. cerevisiae*. *Cell* 66, 1279-1287.
- Aranda, A., and Pascual, A. (2001). Nuclear hormone receptors and gene expression. *Physiological reviews* 81, 1269-1304.
- Arany, Z., He, H., Lin, J., Hoyer, K., Handschin, C., Toka, O., Ahmad, F., Matsui, T., Chin, S., Wu, P.H., *et al.* (2005). Transcriptional coactivator PGC-1 alpha controls the energy state and contractile function of cardiac muscle. *Cell Metab* 1, 259-271.

- Armani, A., Mammi, C., Marzolla, V., Calanchini, M., Antelmi, A., Rosano, G.M., Fabbri, A., and Caprio, M. (2010). Cellular models for understanding adipogenesis, adipose dysfunction, and obesity. *J Cell Biochem* 110, 564-572.
- Ashraf, N., Zino, S., Macintyre, A., Kingsmore, D., Payne, A.P., George, W.D., and Shiels, P.G. (2006). Altered sirtuin expression is associated with node-positive breast cancer. *Br J Cancer* 95, 1056-1061.
- Avni, O., Lee, D., Macian, F., Szabo, S.J., Glimcher, L.H., and Rao, A. (2002). T(H) cell differentiation is accompanied by dynamic changes in histone acetylation of cytokine genes. *Nature immunology* 3, 643-651.
- Back, J.H., Rezvani, H.R., Zhu, Y., Guyonnet-Duperat, V., Athar, M., Ratner, D., and Kim, A.L. (2011). Cancer cell survival following DNA damage-mediated premature senescence is regulated by mammalian target of rapamycin (mTOR)-dependent inhibition of sirtuin 1. *J Biol Chem* 286, 19100-19108.
- Backesjo, C.M., Li, Y., Lindgren, U., and Haldosen, L.A. (2006). Activation of Sirt1 decreases adipocyte formation during osteoblast differentiation of mesenchymal stem cells. *Journal of bone and mineral research : the official journal of the American Society for Bone and Mineral Research* 21, 993-1002.
- Bai, L., Pang, W.J., Yang, Y.J., and Yang, G.S. (2008). Modulation of Sirt1 by resveratrol and nicotinamide alters proliferation and differentiation of pig preadipocytes. *Mol Cell Biochem* 307, 129-140.
- Banks, A.S., Kon, N., Knight, C., Matsumoto, M., Gutierrez-Juarez, R., Rossetti, L., Gu, W., and Accili, D. (2008). SirT1 gain of function increases energy efficiency and prevents diabetes in mice. *Cell metabolism* 8, 333-341.
- Barber, M.F., Michishita-Kioi, E., Xi, Y., Tasselli, L., Kioi, M., Moqtaderi, Z., Tennen, R.I., Paredes, S., Young, N.L., Chen, K., *et al.* (2012). SIRT7 links H3K18 deacetylation to maintenance of oncogenic transformation. *Nature* 487, 114-118.
- Baur, J.A., Pearson, K.J., Price, N.L., Jamieson, H.A., Lerin, C., Kalra, A., Prabhu, V.V., Allard, J.S., Lopez-Lluch, G., Lewis, K., *et al.* (2006). Resveratrol improves health and survival of mice on a high-calorie diet. *Nature* 444, 337-342.
- Bitterman, K.J., Anderson, R.M., Cohen, H.Y., Latorre-Esteves, M., and Sinclair, D.A.

- (2002). Inhibition of silencing and accelerated aging by nicotinamide, a putative negative regulator of yeast sir2 and human SIRT1. *J Biol Chem* 277, 45099-45107.
- Black, J.C., Choi, J.E., Lombardo, S.R., and Carey, M. (2006). A mechanism for coordinating chromatin modification and preinitiation complex assembly. *Mol Cell* 23, 809-818.
- Blanco-Garcia, N., Asensio-Juan, E., de la Cruz, X., and Martinez-Balbas, M.A. (2009). Autoacetylation regulates P/CAF nuclear localization. *J Biol Chem* 284, 1343-1352.
- Bobrowska, A., Donmez, G., Weiss, A., Guarente, L., and Bates, G. (2012). SIRT2 ablation has no effect on tubulin acetylation in brain, cholesterol biosynthesis or the progression of Huntington's disease phenotypes in vivo. *PLoS One* 7, e34805.
- Boden, G. (2004). Gluconeogenesis and glycogenolysis in health and diabetes. *J Investig Med* 52, 375-378.
- Boisvert, F.M., van Koningsbruggen, S., Navascues, J., and Lamond, A.I. (2007). The multifunctional nucleolus. *Nature reviews* 8, 574-585.
- Bollen, M., Keppens, S., and Stalmans, W. (1998). Specific features of glycogen metabolism in the liver. *The Biochemical journal* 336 ( Pt 1), 19-31.
- Bordone, L., Cohen, D., Robinson, A., Motta, M.C., van Veen, E., Czopik, A., Steele, A.D., Crowe, H., Marmor, S., Luo, J., *et al.* (2007). SIRT1 transgenic mice show phenotypes resembling calorie restriction. *Aging Cell* 6, 759-767.
- Bordone, L., Motta, M.C., Picard, F., Robinson, A., Jhala, U.S., Apfeld, J., McDonagh, T., Lemieux, M., McBurney, M., Szilvasi, A., *et al.* (2006). Sirt1 regulates insulin secretion by repressing UCP2 in pancreatic beta cells. *PLoS biology* 4, e31.
- Bosch-Presegue, L., and Vaquero, A. (2011). The dual role of sirtuins in cancer. *Genes & cancer* 2, 648-662.
- Bouras, T., Fu, M., Sauve, A.A., Wang, F., Quong, A.A., Perkins, N.D., Hay, R.T., Gu, W., and Pestell, R.G. (2005). SIRT1 deacetylation and repression of p300 involves lysine residues 1020/1024 within the cell cycle regulatory domain 1. *J Biol Chem* 280, 10264-10276.
- Brandl, A., Heinzl, T., and Kramer, O.H. (2009). Histone deacetylases: salesmen and customers in the post-translational modification market. *Biology of the cell / under the*

- auspices of the European Cell Biology Organization *101*, 193-205.
- Braunstein, M., Rose, A.B., Holmes, S.G., Allis, C.D., and Broach, J.R. (1993). Transcriptional silencing in yeast is associated with reduced nucleosome acetylation. *Genes Dev* *7*, 592-604.
- Brunet, A., Sweeney, L.B., Sturgill, J.F., Chua, K.F., Greer, P.L., Lin, Y., Tran, H., Ross, S.E., Mostoslavsky, R., Cohen, H.Y., *et al.* (2004). Stress-dependent regulation of FOXO transcription factors by the SIRT1 deacetylase. *Science* *303*, 2011-2015.
- Burnett, C., Valentini, S., Cabreiro, F., Goss, M., Somogyvari, M., Piper, M.D., Hoddinott, M., Sutphin, G.L., Leko, V., McElwee, J.J., *et al.* (2011). Absence of effects of Sir2 overexpression on lifespan in *C. elegans* and *Drosophila*. *Nature* *477*, 482-485.
- Caito, S., Rajendrasozhan, S., Cook, S., Chung, S., Yao, H., Friedman, A.E., Brookes, P.S., and Rahman, I. (2010). SIRT1 is a redox-sensitive deacetylase that is post-translationally modified by oxidants and carbonyl stress. *Faseb J* *24*, 3145-3159.
- Cannon, B., and Nedergaard, J. (2004). Brown adipose tissue: function and physiological significance. *Physiological reviews* *84*, 277-359.
- Chalkiadaki, A., and Guarente, L. (2012). High-Fat Diet Triggers Inflammation-Induced Cleavage of SIRT1 in Adipose Tissue To Promote Metabolic Dysfunction. *Cell metabolism* *16*, 180-188.
- Chandramouli, V., Ekberg, K., Schumann, W.C., Kalhan, S.C., Wahren, J., and Landau, B.R. (1997). Quantifying gluconeogenesis during fasting. *The American journal of physiology* *273*, E1209-1215.
- Chaudhuri, S., and Lieberman, I. (1968). Control of ribosome synthesis in normal and regenerating liver. *J Biol Chem* *243*, 29-33.
- Chen, H., Lin, R.J., Xie, W., Wilpitz, D., and Evans, R.M. (1999). Regulation of hormone-induced histone hyperacetylation and gene activation via acetylation of an acetylase. *Cell* *98*, 675-686.
- Cheng, H.L., Mostoslavsky, R., Saito, S., Manis, J.P., Gu, Y., Patel, P., Bronson, R., Appella, E., Alt, F.W., and Chua, K.F. (2003). Developmental defects and p53 hyperacetylation in Sir2 homolog (SIRT1)-deficient mice. *Proc Natl Acad Sci U S A* *100*, 10794-10799.

- Cheung, P., Tanner, K.G., Cheung, W.L., Sassone-Corsi, P., Denu, J.M., and Allis, C.D. (2000). Synergistic coupling of histone H3 phosphorylation and acetylation in response to epidermal growth factor stimulation. *Mol Cell* 5, 905-915.
- Chin, H.G., Esteve, P.O., Pradhan, M., Benner, J., Patnaik, D., Carey, M.F., and Pradhan, S. (2007). Automethylation of G9a and its implication in wider substrate specificity and HP1 binding. *Nucleic Acids Res* 35, 7313-7323.
- Cho, Y.W., Hong, S., Jin, Q., Wang, L., Lee, J.E., Gavrilova, O., and Ge, K. (2009). Histone methylation regulator PTIP is required for PPARgamma and C/EBPalpha expression and adipogenesis. *Cell Metab* 10, 27-39.
- Conde, R.D., and Franze-Fernandez, M.T. (1980). Increased transcription and decreased degradation control and recovery of liver ribosomes after a period of protein starvation. *The Biochemical journal* 192, 935-940.
- Dali-Youcef, N., Lagouge, M., Froelich, S., Koehl, C., Schoonjans, K., and Auwerx, J. (2007). Sirtuins: the 'magnificent seven', function, metabolism and longevity. *Ann Med* 39, 335-345.
- Darlington, G.J., Ross, S.E., and MacDougald, O.A. (1998). The role of C/EBP genes in adipocyte differentiation. *J Biol Chem* 273, 30057-30060.
- de la Serna, I.L., Carlson, K.A., and Imbalzano, A.N. (2001). Mammalian SWI/SNF complexes promote MyoD-mediated muscle differentiation. *Nature genetics* 27, 187-190.
- DePhilip, R.M., Chadwick, D.E., Ignatz, R.A., Lynch, W.E., and Lieberman, I. (1979). Rapid stimulation by insulin of ribosome synthesis in cultured chick embryo fibroblasts. *Biochemistry* 18, 4812-4817.
- Dioum, E.M., Chen, R., Alexander, M.S., Zhang, Q., Hogg, R.T., Gerard, R.D., and Garcia, J.A. (2009). Regulation of hypoxia-inducible factor 2alpha signaling by the stress-responsive deacetylase sirtuin 1. *Science (New York, N.Y)* 324, 1289-1293.
- Dominy, J.E., Jr., Lee, Y., Gerhart-Hines, Z., and Puigserver, P. Nutrient-dependent regulation of PGC-1alpha's acetylation state and metabolic function through the enzymatic activities of Sirt1/GCN5. *Biochimica et biophysica acta* 1804, 1676-1683.
- Dominy, J.E., Jr., Lee, Y., Gerhart-Hines, Z., and Puigserver, P. (2010).

- Nutrient-dependent regulation of PGC-1alpha's acetylation state and metabolic function through the enzymatic activities of Sirt1/GCN5. *Biochim Biophys Acta* 1804, 1676-1683.
- Du, J., Zhou, Y., Su, X., Yu, J.J., Khan, S., Jiang, H., Kim, J., Woo, J., Kim, J.H., Choi, B.H., *et al.* (2011). Sirt5 is a NAD-dependent protein lysine demalonylase and desuccinylase. *Science (New York, N.Y)* 334, 806-809.
- Eichler, D.C., and Craig, N. (1994). Processing of eukaryotic ribosomal RNA. *Progress in nucleic acid research and molecular biology* 49, 197-239.
- Enerback, S. (2009). The origins of brown adipose tissue. *The New England journal of medicine* 360, 2021-2023.
- Enwonwu, C.O., Stambaugh, R., and Sreebny, L. (1971). Synthesis and degradation of liver ribosomal RNA in fed and fasted rats. *J Nutr* 101, 337-345.
- Exil, V.J., Gardner, C.D., Rottman, J.N., Sims, H., Bartelds, B., Khuchua, Z., Sindhal, R., Ni, G., and Strauss, A.W. (2006). Abnormal mitochondrial bioenergetics and heart rate dysfunction in mice lacking very-long-chain acyl-CoA dehydrogenase. *Am J Physiol Heart Circ Physiol* 290, H1289-1297.
- Fajas, L., Schoonjans, K., Gelman, L., Kim, J.B., Najib, J., Martin, G., Fruchart, J.C., Briggs, M., Spiegelman, B.M., and Auwerx, J. (1999). Regulation of peroxisome proliferator-activated receptor gamma expression by adipocyte differentiation and determination factor 1/sterol regulatory element binding protein 1: implications for adipocyte differentiation and metabolism. *Molecular and cellular biology* 19, 5495-5503.
- Farmer, S.R. (2006). Transcriptional control of adipocyte formation. *Cell metabolism* 4, 263-273.
- Feige, J.N., Lagouge, M., Canto, C., Strehle, A., Houten, S.M., Milne, J.C., Lambert, P.D., Matakis, C., Elliott, P.J., and Auwerx, J. (2008). Specific SIRT1 activation mimics low energy levels and protects against diet-induced metabolic disorders by enhancing fat oxidation. *Cell metabolism* 8, 347-358.
- Finkel, T., Deng, C.X., and Mostoslavsky, R. (2009). Recent progress in the biology and physiology of sirtuins. *Nature* 460, 587-591.

- Flick, F., and Luscher, B. (2012). Regulation of sirtuin function by posttranslational modifications. *Frontiers in pharmacology* 3, 29.
- Ford, E., Voit, R., Liszt, G., Magin, C., Grummt, I., and Guarente, L. (2006). Mammalian Sir2 homolog SIRT7 is an activator of RNA polymerase I transcription. *Genes Dev* 20, 1075-1080.
- Ford, J., Ahmed, S., Allison, S., Jiang, M., and Milner, J. (2008). JNK2-dependent regulation of SIRT1 protein stability. *Cell Cycle* 7, 3091-3097.
- Friedman, J.E., Sun, Y., Ishizuka, T., Farrell, C.J., McCormack, S.E., Herron, L.M., Hakimi, P., Lechner, P., and Yun, J.S. (1997). Phosphoenolpyruvate carboxykinase (GTP) gene transcription and hyperglycemia are regulated by glucocorticoids in genetically obese db/db transgenic mice. *J Biol Chem* 272, 31475-31481.
- Fritsche, L., Weigert, C., Haring, H.U., and Lehmann, R. (2008). How insulin receptor substrate proteins regulate the metabolic capacity of the liver--implications for health and disease. *Current medicinal chemistry* 15, 1316-1329.
- Frye, R.A. (1999). Characterization of five human cDNAs with homology to the yeast SIR2 gene: Sir2-like proteins (sirtuins) metabolize NAD and may have protein ADP-ribosyltransferase activity. *Biochem Biophys Res Commun* 260, 273-279.
- Frye, R.A. (2000). Phylogenetic classification of prokaryotic and eukaryotic Sir2-like proteins. *Biochem Biophys Res Commun* 273, 793-798.
- Fulco, M., Schiltz, R.L., Iezzi, S., King, M.T., Zhao, P., Kashiwaya, Y., Hoffman, E., Veech, R.L., and Sartorelli, V. (2003). Sir2 regulates skeletal muscle differentiation as a potential sensor of the redox state. *Mol Cell* 12, 51-62.
- Gao, Z., Zhang, J., Kheterpal, I., Kennedy, N., Davis, R.J., and Ye, J. (2011). Sirtuin 1 (SIRT1) protein degradation in response to persistent c-Jun N-terminal kinase 1 (JNK1) activation contributes to hepatic steatosis in obesity. *J Biol Chem* 286, 22227-22234.
- Ge, K., Guermah, M., Yuan, C.X., Ito, M., Wallberg, A.E., Spiegelman, B.M., and Roeder, R.G. (2002). Transcription coactivator TRAP220 is required for PPAR gamma 2-stimulated adipogenesis. *Nature* 417, 563-567.
- Gesta, S., Tseng, Y.H., and Kahn, C.R. (2007). Developmental origin of fat: tracking obesity to its source. *Cell* 131, 242-256.

- Gillum, M.P., Kotas, M.E., Erion, D.M., Kursawe, R., Chatterjee, P., Nead, K.T., Muise, E.S., Hsiao, J.J., Frederick, D.W., Yonemitsu, S., *et al.* (2011). SirT1 regulates adipose tissue inflammation. *Diabetes* 60, 3235-3245.
- Goetzman, E.S., Tian, L., and Wood, P.A. (2005). Differential induction of genes in liver and brown adipose tissue regulated by peroxisome proliferator-activated receptor-alpha during fasting and cold exposure in acyl-CoA dehydrogenase-deficient mice. *Mol Genet Metab* 84, 39-47.
- Gottlieb, S., and Esposito, R.E. (1989). A new role for a yeast transcriptional silencer gene, SIR2, in regulation of recombination in ribosomal DNA. *Cell* 56, 771-776.
- Gregoire, F.M., Smas, C.M., and Sul, H.S. (1998). Understanding adipocyte differentiation. *Physiological reviews* 78, 783-809.
- Grob, A., Roussel, P., Wright, J.E., McStay, B., Hernandez-Verdun, D., and Sirri, V. (2009). Involvement of SIRT7 in resumption of rDNA transcription at the exit from mitosis. *J Cell Sci* 122, 489-498.
- Grummt, I. (2007). Different epigenetic layers engage in complex crosstalk to define the epigenetic state of mammalian rRNA genes. *Human molecular genetics* 16 Spec No 1, R21-27.
- Grummt, I., and Ladurner, A.G. (2008). A metabolic throttle regulates the epigenetic state of rDNA. *Cell* 133, 577-580.
- Grummt, I., and Pikaard, C.S. (2003). Epigenetic silencing of RNA polymerase I transcription. *Nature reviews* 4, 641-649.
- Guarani, V., Deflorian, G., Franco, C.A., Kruger, M., Phng, L.K., Bentley, K., Toussaint, L., Dequiedt, F., Mostoslavsky, R., Schmidt, M.H., *et al.* Acetylation-dependent regulation of endothelial Notch signalling by the SIRT1 deacetylase. *Nature* 473, 234-238.
- Haigis, M.C., Mostoslavsky, R., Haigis, K.M., Fahie, K., Christodoulou, D.C., Murphy, A.J., Valenzuela, D.M., Yancopoulos, G.D., Karow, M., Blander, G., *et al.* (2006). SIRT4 inhibits glutamate dehydrogenase and opposes the effects of calorie restriction in pancreatic beta cells. *Cell* 126, 941-954.
- Haigis, M.C., and Sinclair, D.A. Mammalian sirtuins: biological insights and disease

- relevance. *Annu Rev Pathol* 5, 253-295.
- Haigis, M.C., and Sinclair, D.A. (2010). Mammalian sirtuins: biological insights and disease relevance. *Annu Rev Pathol* 5, 253-295.
- Hammond, M.L., and Bowman, L.H. (1988). Insulin stimulates the translation of ribosomal proteins and the transcription of rDNA in mouse myoblasts. *J Biol Chem* 263, 17785-17791.
- Han, Y., Jin, Y.H., Kim, Y.J., Kang, B.Y., Choi, H.J., Kim, D.W., Yeo, C.Y., and Lee, K.Y. (2008). Acetylation of Sirt2 by p300 attenuates its deacetylase activity. *Biochem Biophys Res Commun* 375, 576-580.
- Hannan, K.M., Brandenburger, Y., Jenkins, A., Sharkey, K., Cavanaugh, A., Rothblum, L., Moss, T., Poortinga, G., McArthur, G.A., Pearson, R.B., *et al.* (2003). mTOR-dependent regulation of ribosomal gene transcription requires S6K1 and is mediated by phosphorylation of the carboxy-terminal activation domain of the nucleolar transcription factor UBF. *Molecular and cellular biology* 23, 8862-8877.
- Hannan, K.M., Rothblum, L.I., and Jefferson, L.S. (1998). Regulation of ribosomal DNA transcription by insulin. *The American journal of physiology* 275, C130-138.
- Haslam, D.W., and James, W.P. (2005). Obesity. *Lancet* 366, 1197-1209.
- Hausman, D.B., DiGirolamo, M., Bartness, T.J., Hausman, G.J., and Martin, R.J. (2001). The biology of white adipocyte proliferation. *Obes Rev* 2, 239-254.
- Hausman, D.B., Park, H.J., and Hausman, G.J. (2008). Isolation and culture of preadipocytes from rodent white adipose tissue. *Methods Mol Biol* 456, 201-219.
- Hay, N., and Sonenberg, N. (2004). Upstream and downstream of mTOR. *Genes Dev* 18, 1926-1945.
- Hayden, J.M., Marten, N.W., Burke, E.J., and Straus, D.S. (1994). The effect of fasting on insulin-like growth factor-I nuclear transcript abundance in rat liver. *Endocrinology* 134, 760-768.
- Heix, J., Vente, A., Voit, R., Budde, A., Michaelidis, T.M., and Grummt, I. (1998). Mitotic silencing of human rRNA synthesis: inactivation of the promoter selectivity factor SL1 by cdc2/cyclin B-mediated phosphorylation. *EMBO J* 17, 7373-7381.
- Hirota, K., Daitoku, H., Matsuzaki, H., Araya, N., Yamagata, K., Asada, S., Sugaya, T.,

- and Fukamizu, A. (2003). Hepatocyte nuclear factor-4 is a novel downstream target of insulin via FKHR as a signal-regulated transcriptional inhibitor. *J Biol Chem* 278, 13056-13060.
- Hirschler-Laszkiewicz, I., Cavanaugh, A., Hu, Q., Catania, J., Avantaggiati, M.L., and Rothblum, L.I. (2001). The role of acetylation in rDNA transcription. *Nucleic Acids Res* 29, 4114-4124.
- Howitz, K.T., Bitterman, K.J., Cohen, H.Y., Lamming, D.W., Lavu, S., Wood, J.G., Zipkin, R.E., Chung, P., Kisielewski, A., Zhang, L.L., *et al.* (2003). Small molecule activators of sirtuins extend *Saccharomyces cerevisiae* lifespan. *Nature* 425, 191-196.
- Hutson, N.J., and Mortimore, G.E. (1982). Suppression of cytoplasmic protein uptake by lysosomes as the mechanism of protein regain in livers of starved-refed mice. *J Biol Chem* 257, 9548-9554.
- Imai, S., Armstrong, C.M., Kaeberlein, M., and Guarente, L. (2000). Transcriptional silencing and longevity protein Sir2 is an NAD-dependent histone deacetylase. *Nature* 403, 795-800.
- Jenuwein, T., and Allis, C.D. (2001). Translating the histone code. *Science* 293, 1074-1080.
- Jeong, J., Juhn, K., Lee, H., Kim, S.H., Min, B.H., Lee, K.M., Cho, M.H., Park, G.H., and Lee, K.H. (2007). SIRT1 promotes DNA repair activity and deacetylation of Ku70. *Experimental & molecular medicine* 39, 8-13.
- Jin, Q., Zhang, F., Yan, T., Liu, Z., Wang, C., Ge, X., and Zhai, Q. (2010). C/EBPalpha regulates SIRT1 expression during adipogenesis. *Cell Res* 20, 470-479.
- Jing, E., Gesta, S., and Kahn, C.R. (2007). SIRT2 regulates adipocyte differentiation through FoxO1 acetylation/deacetylation. *Cell metabolism* 6, 105-114.
- Kaeberlein, M., McVey, M., and Guarente, L. (1999). The SIR2/3/4 complex and SIR2 alone promote longevity in *Saccharomyces cerevisiae* by two different mechanisms. *Genes Dev* 13, 2570-2580.
- Kaidi, A., Weinert, B.T., Choudhary, C., and Jackson, S.P. (2010). Human SIRT6 promotes DNA end resection through CtIP deacetylation. *Science (New York, N.Y)* 329, 1348-1353.

- Kang, H., Jung, J.W., Kim, M.K., and Chung, J.H. (2009). CK2 is the regulator of SIRT1 substrate-binding affinity, deacetylase activity and cellular response to DNA-damage. *PLoS One* 4, e6611.
- Kawahara, T.L., Michishita, E., Adler, A.S., Damian, M., Berber, E., Lin, M., McCord, R.A., Ongaigui, K.C., Boxer, L.D., Chang, H.Y., *et al.* (2009). SIRT6 links histone H3 lysine 9 deacetylation to NF-kappaB-dependent gene expression and organismal life span. *Cell* 136, 62-74.
- Kemper, J.K., Xiao, Z., Ponugoti, B., Miao, J., Fang, S., Kanamaluru, D., Tsang, S., Wu, S.Y., Chiang, C.M., and Veenstra, T.D. (2009). FXR acetylation is normally dynamically regulated by p300 and SIRT1 but constitutively elevated in metabolic disease states. *Cell metabolism* 10, 392-404.
- Kershaw, E.E., and Flier, J.S. (2004). Adipose tissue as an endocrine organ. *The Journal of clinical endocrinology and metabolism* 89, 2548-2556.
- Kim, D.H., Perdomo, G., Zhang, T., Slusher, S., Lee, S., Phillips, B.E., Fan, Y., Giannoukakis, N., Gramignoli, R., Strom, S., *et al.* (2011a). FoxO6 integrates insulin signaling with gluconeogenesis in the liver. *Diabetes* 60, 2763-2774.
- Kim, H.S., Xiao, C., Wang, R.H., Lahusen, T., Xu, X., Vassilopoulos, A., Vazquez-Ortiz, G., Jeong, W.I., Park, O., Ki, S.H., *et al.* (2010). Hepatic-specific disruption of SIRT6 in mice results in fatty liver formation due to enhanced glycolysis and triglyceride synthesis. *Cell metabolism* 12, 224-236.
- Kim, J.B., and Spiegelman, B.M. (1996). ADD1/SREBP1 promotes adipocyte differentiation and gene expression linked to fatty acid metabolism. *Genes Dev* 10, 1096-1107.
- Kim, J.B., Wright, H.M., Wright, M., and Spiegelman, B.M. (1998). ADD1/SREBP1 activates PPARgamma through the production of endogenous ligand. *Proc Natl Acad Sci U S A* 95, 4333-4337.
- Kim, J.K., Noh, J.H., Jung, K.H., Eun, J.W., Bae, H.J., Kim, M.G., Chang, Y.G., Shen, Q., Park, W.S., Lee, J.Y., *et al.* (2012). Sirtuin7 oncogenic potential in human hepatocellular carcinoma and its regulation by the tumor suppressors MiR-125a-5p and MiR-125b. *Hepatology*.

- Kim, M.Y., Mauro, S., Gevry, N., Lis, J.T., and Kraus, W.L. (2004). NAD<sup>+</sup>-dependent modulation of chromatin structure and transcription by nucleosome binding properties of PARP-1. *Cell* *119*, 803-814.
- Kim, S., Jin, Y., Choi, Y., and Park, T. (2011b). Resveratrol exerts anti-obesity effects via mechanisms involving down-regulation of adipogenic and inflammatory processes in mice. *Biochemical pharmacology* *81*, 1343-1351.
- Klein, J., and Grummt, I. (1999). Cell cycle-dependent regulation of RNA polymerase I transcription: the nucleolar transcription factor UBF is inactive in mitosis and early G1. *Proc Natl Acad Sci U S A* *96*, 6096-6101.
- Klover, P.J., and Mooney, R.A. (2004). Hepatocytes: critical for glucose homeostasis. *The international journal of biochemistry & cell biology* *36*, 753-758.
- Kobayashi, K., Forte, T.M., Taniguchi, S., Ishida, B.Y., Oka, K., and Chan, L. (2000). The db/db mouse, a model for diabetic dyslipidemia: molecular characterization and effects of Western diet feeding. *Metabolism* *49*, 22-31.
- Koo, S.H., Flechner, L., Qi, L., Zhang, X., Sreaton, R.A., Jeffries, S., Hedrick, S., Xu, W., Boussouar, F., Brindle, P., *et al.* (2005). The CREB coactivator TORC2 is a key regulator of fasting glucose metabolism. *Nature* *437*, 1109-1111.
- Koo, S.H., Satoh, H., Herzig, S., Lee, C.H., Hedrick, S., Kulkarni, R., Evans, R.M., Olefsky, J., and Montminy, M. (2004). PGC-1 promotes insulin resistance in liver through PPAR-alpha-dependent induction of TRB-3. *Nat Med* *10*, 530-534.
- Kopelman, P.G. (2000). Obesity as a medical problem. *Nature* *404*, 635-643.
- Kralisch, S., Bluher, M., Paschke, R., Stumvoll, M., and Fasshauer, M. (2007). Adipokines and adipocyte targets in the future management of obesity and the metabolic syndrome. *Mini reviews in medicinal chemistry* *7*, 39-45.
- Kubota, N., Terauchi, Y., Miki, H., Tamemoto, H., Yamauchi, T., Komeda, K., Satoh, S., Nakano, R., Ishii, C., Sugiyama, T., *et al.* (1999). PPAR gamma mediates high-fat diet-induced adipocyte hypertrophy and insulin resistance. *Mol Cell* *4*, 597-609.
- Lafontaine, D.L. (2010). A 'garbage can' for ribosomes: how eukaryotes degrade their ribosomes. *Trends in biochemical sciences* *35*, 267-277.
- Lagouge, M., Argmann, C., Gerhart-Hines, Z., Meziane, H., Lerin, C., Daussin, F.,

- Messadeq, N., Milne, J., Lambert, P., Elliott, P., *et al.* (2006). Resveratrol improves mitochondrial function and protects against metabolic disease by activating SIRT1 and PGC-1alpha. *Cell* 127, 1109-1122.
- Landry, J., Sutton, A., Tafrov, S.T., Heller, R.C., Stebbins, J., Pillus, L., and Sternglanz, R. (2000). The silencing protein SIR2 and its homologs are NAD-dependent protein deacetylases. *Proc Natl Acad Sci U S A* 97, 5807-5811.
- Lee, J., Hwang, Y.J., Boo, J.H., Han, D., Kwon, O.K., Todorova, K., Kowall, N.W., Kim, Y., and Ryu, H. (2011). Dysregulation of upstream binding factor-1 acetylation at K352 is linked to impaired ribosomal DNA transcription in Huntington's disease. *Cell Death Differ* 18, 1726-1735.
- Li, X., Zhang, S., Blander, G., Tse, J.G., Krieger, M., and Guarente, L. (2007). SIRT1 deacetylates and positively regulates the nuclear receptor LXR. *Mol Cell* 28, 91-106.
- Li, Y., Xu, S., Giles, A., Nakamura, K., Lee, J.W., Hou, X., Donmez, G., Li, J., Luo, Z., Walsh, K., *et al.* (2011). Hepatic overexpression of SIRT1 in mice attenuates endoplasmic reticulum stress and insulin resistance in the liver. *FASEB J* 25, 1664-1679.
- Lim, J.H., Lee, Y.M., Chun, Y.S., Chen, J., Kim, J.E., and Park, J.W. (2010). Sirtuin 1 modulates cellular responses to hypoxia by deacetylating hypoxia-inducible factor 1alpha. *Mol Cell* 38, 864-878.
- Lin, J., Handschin, C., and Spiegelman, B.M. (2005). Metabolic control through the PGC-1 family of transcription coactivators. *Cell Metab* 1, 361-370.
- Lin, J., Wu, P.H., Tarr, P.T., Lindenberg, K.S., St-Pierre, J., Zhang, C.Y., Mootha, V.K., Jager, S., Vianna, C.R., Reznick, R.M., *et al.* (2004). Defects in adaptive energy metabolism with CNS-linked hyperactivity in PGC-1alpha null mice. *Cell* 119, 121-135.
- Lindstrom, P. (2007). The physiology of obese-hyperglycemic mice [ob/ob mice]. *ScientificWorldJournal* 7, 666-685.
- Liszt, G., Ford, E., Kurtev, M., and Guarente, L. (2005). Mouse Sir2 homolog SIRT6 is a nuclear ADP-ribosyltransferase. *J Biol Chem* 280, 21313-21320.
- Liu, P., Jenkins, N.A., and Copeland, N.G. (2003). A highly efficient

- recombineering-based method for generating conditional knockout mutations. *Genome research* *13*, 476-484.
- Liu, S., Shiotani, B., Lahiri, M., Marechal, A., Tse, A., Leung, C.C., Glover, J.N., Yang, X.H., and Zou, L. (2011a). ATR autophosphorylation as a molecular switch for checkpoint activation. *Mol Cell* *43*, 192-202.
- Liu, T., Liu, P.Y., and Marshall, G.M. (2009). The critical role of the class III histone deacetylase SIRT1 in cancer. *Cancer research* *69*, 1702-1705.
- Liu, X., Wang, D., Zhao, Y., Tu, B., Zheng, Z., Wang, L., Wang, H., Gu, W., Roeder, R.G., and Zhu, W.G. (2011b). Methyltransferase Set7/9 regulates p53 activity by interacting with Sirtuin 1 (SIRT1). *Proc Natl Acad Sci U S A* *108*, 1925-1930.
- Liu, Y., Dentin, R., Chen, D., Hedrick, S., Ravnskjaer, K., Schenk, S., Milne, J., Meyers, D.J., Cole, P., Yates, J., 3rd, *et al.* (2008). A fasting inducible switch modulates gluconeogenesis via activator/coactivator exchange. *Nature* *456*, 269-273.
- Lombard, D.B., Alt, F.W., Cheng, H.L., Bunkenborg, J., Streeper, R.S., Mostoslavsky, R., Kim, J., Yancopoulos, G., Valenzuela, D., Murphy, A., *et al.* (2007). Mammalian Sir2 homolog SIRT3 regulates global mitochondrial lysine acetylation. *Molecular and cellular biology* *27*, 8807-8814.
- Lowe, C.E., O'Rahilly, S., and Rochford, J.J. (2011). Adipogenesis at a glance. *Journal of cell science* *124*, 2681-2686.
- Lowry, O.H., Rosebrough, N.J., Farr, A.L., and Randall, R.J. (1951). Protein measurement with the Folin phenol reagent. *J Biol Chem* *193*, 265-275.
- Lu, L., Li, L., Lv, X., Wu, X.S., Liu, D.P., and Liang, C.C. (2011). Modulations of hMOF autoacetylation by SIRT1 regulate hMOF recruitment and activities on the chromatin. *Cell Res* *21*, 1182-1195.
- Luo, J., Nikolaev, A.Y., Imai, S., Chen, D., Su, F., Shiloh, A., Guarente, L., and Gu, W. (2001). Negative control of p53 by Sir2alpha promotes cell survival under stress. *Cell* *107*, 137-148.
- Machida, Y., Murai, K., Miyake, K., and Iijima, S. (2001). Expression of chromatin remodeling factors during neural differentiation. *Journal of biochemistry* *129*, 43-49.
- Mayer, C., Zhao, J., Yuan, X., and Grummt, I. (2004). mTOR-dependent activation of

- the transcription factor TIF-IA links rRNA synthesis to nutrient availability. *Genes Dev* *18*, 423-434.
- McBurney, M.W., Yang, X., Jardine, K., Hixon, M., Boekelheide, K., Webb, J.R., Lansdorp, P.M., and Lemieux, M. (2003). The mammalian SIR2alpha protein has a role in embryogenesis and gametogenesis. *Mol Cell Biol* *23*, 38-54.
- McCord, R.A., Michishita, E., Hong, T., Berber, E., Boxer, L.D., Kusumoto, R., Guan, S., Shi, X., Gozani, O., Burlingame, A.L., *et al.* (2009). SIRT6 stabilizes DNA-dependent protein kinase at chromatin for DNA double-strand break repair. *Aging (Albany NY)* *1*, 109-121.
- McStay, B., and Grummt, I. (2008). The epigenetics of rRNA genes: from molecular to chromosome biology. *Annual review of cell and developmental biology* *24*, 131-157.
- Medina-Gomez, G., Virtue, S., Lelliott, C., Boiani, R., Campbell, M., Christodoulides, C., Perrin, C., Jimenez-Linan, M., Blount, M., Dixon, J., *et al.* (2005). The link between nutritional status and insulin sensitivity is dependent on the adipocyte-specific peroxisome proliferator-activated receptor-gamma2 isoform. *Diabetes* *54*, 1706-1716.
- Meraner, J., Lechner, M., Loidl, A., Goralik-Schramel, M., Voit, R., Grummt, I., and Loidl, P. (2006). Acetylation of UBF changes during the cell cycle and regulates the interaction of UBF with RNA polymerase I. *Nucleic Acids Res* *34*, 1798-1806.
- Michan, S., and Sinclair, D. (2007). Sirtuins in mammals: insights into their biological function. *The Biochemical journal* *404*, 1-13.
- Michishita, E., McCord, R.A., Berber, E., Kioi, M., Padilla-Nash, H., Damian, M., Cheung, P., Kusumoto, R., Kawahara, T.L., Barrett, J.C., *et al.* (2008). SIRT6 is a histone H3 lysine 9 deacetylase that modulates telomeric chromatin. *Nature* *452*, 492-496.
- Michishita, E., Park, J.Y., Burneskis, J.M., Barrett, J.C., and Horikawa, I. (2005). Evolutionarily conserved and nonconserved cellular localizations and functions of human SIRT proteins. *Mol Biol Cell* *16*, 4623-4635.
- Milne, J.C., Lambert, P.D., Schenk, S., Carney, D.P., Smith, J.J., Gagne, D.J., Jin, L., Boss, O., Perni, R.B., Vu, C.B., *et al.* (2007). Small molecule activators of SIRT1 as therapeutics for the treatment of type 2 diabetes. *Nature* *450*, 712-716.

- Moreno, M., Lombardi, A., Silvestri, E., Senese, R., Cioffi, F., Goglia, F., Lanni, A., and de Lange, P. (2010). PPARs: Nuclear Receptors Controlled by, and Controlling, Nutrient Handling through Nuclear and Cytosolic Signaling. *PPAR research* 2010.
- Mostoslavsky, R., Chua, K.F., Lombard, D.B., Pang, W.W., Fischer, M.R., Gellon, L., Liu, P., Mostoslavsky, G., Franco, S., Murphy, M.M., *et al.* (2006). Genomic instability and aging-like phenotype in the absence of mammalian SIRT6. *Cell* 124, 315-329.
- Moynihan, K.A., Grimm, A.A., Plueger, M.M., Bernal-Mizrachi, E., Ford, E., Cras-Meneur, C., Permutt, M.A., and Imai, S. (2005). Increased dosage of mammalian Sir2 in pancreatic beta cells enhances glucose-stimulated insulin secretion in mice. *Cell metabolism* 2, 105-117.
- Mueller, E., Drori, S., Aiyer, A., Yie, J., Sarraf, P., Chen, H., Hauser, S., Rosen, E.D., Ge, K., Roeder, R.G., *et al.* (2002). Genetic analysis of adipogenesis through peroxisome proliferator-activated receptor gamma isoforms. *J Biol Chem* 277, 41925-41930.
- Murayama, A., Ohmori, K., Fujimura, A., Minami, H., Yasuzawa-Tanaka, K., Kuroda, T., Oie, S., Daitoku, H., Okuwaki, M., Nagata, K., *et al.* (2008). Epigenetic control of rDNA loci in response to intracellular energy status. *Cell* 133, 627-639.
- Nakagawa, T., and Guarente, L. (2009). Urea cycle regulation by mitochondrial sirtuin, SIRT5. *Aging (Albany NY)* 1, 578-581.
- Nakagawa, T., and Guarente, L. (2011). Sirtuins at a glance. *Journal of cell science* 124, 833-838.
- Nakagawa, T., Lomb, D.J., Haigis, M.C., and Guarente, L. (2009). SIRT5 Deacetylates carbamoyl phosphate synthetase 1 and regulates the urea cycle. *Cell* 137, 560-570.
- Nakayama, J., Rice, J.C., Strahl, B.D., Allis, C.D., and Grewal, S.I. (2001). Role of histone H3 lysine 9 methylation in epigenetic control of heterochromatin assembly. *Science* 292, 110-113.
- Napper, A.D., Hixon, J., McDonagh, T., Keavey, K., Pons, J.F., Barker, J., Yau, W.T., Amouzegh, P., Flegg, A., Hamelin, E., *et al.* (2005). Discovery of indoles as potent and selective inhibitors of the deacetylase SIRT1. *Journal of medicinal chemistry* 48, 8045-8054.

- Nasrin, N., Kaushik, V.K., Fortier, E., Wall, D., Pearson, K.J., de Cabo, R., and Bordone, L. (2009). JNK1 phosphorylates SIRT1 and promotes its enzymatic activity. *PLoS One* 4, e8414.
- Nelson, L.R., and Bulun, S.E. (2001). Estrogen production and action. *Journal of the American Academy of Dermatology* 45, S116-124.
- Nie, Y., Erion, D.M., Yuan, Z., Dietrich, M., Shulman, G.I., Horvath, T.L., and Gao, Q. (2009). STAT3 inhibition of gluconeogenesis is downregulated by SirT1. *Nat Cell Biol* 11, 492-500.
- Nin, V., Escande, C., Chini, C.C., Giri, S., Camacho-Pereira, J., Matalonga, J., Lou, Z., and Chini, E.N. (2012). Role of Deleted in Breast Cancer 1 (DBC1) Protein in SIRT1 Deacetylase Activation Induced by Protein Kinase A and AMP-activated Protein Kinase. *J Biol Chem* 287, 23489-23501.
- North, B.J., Marshall, B.L., Borra, M.T., Denu, J.M., and Verdin, E. (2003). The human Sir2 ortholog, SIRT2, is an NAD<sup>+</sup>-dependent tubulin deacetylase. *Mol Cell* 11, 437-444.
- Ogryzko, V.V., Schiltz, R.L., Russanova, V., Howard, B.H., and Nakatani, Y. (1996). The transcriptional coactivators p300 and CBP are histone acetyltransferases. *Cell* 87, 953-959.
- Osborne, T.F., and Espenshade, P.J. (2009). Evolutionary conservation and adaptation in the mechanism that regulates SREBP action: what a long, strange tRIP it's been. *Genes Dev* 23, 2578-2591.
- Otto, T.C., and Lane, M.D. (2005). Adipose development: from stem cell to adipocyte. *Critical reviews in biochemistry and molecular biology* 40, 229-242.
- Ou, X., Chae, H.D., Wang, R.H., Shelley, W.C., Cooper, S., Taylor, T., Kim, Y.J., Deng, C.X., Yoder, M.C., and Broxmeyer, H.E. (2011). SIRT1 deficiency compromises mouse embryonic stem cell hematopoietic differentiation, and embryonic and adult hematopoiesis in the mouse. *Blood* 117, 440-450.
- Patrick, C.W. (2004). Breast tissue engineering. *Annual review of biomedical engineering* 6, 109-130.
- Pediconi, N., Guerrieri, F., Vossio, S., Bruno, T., Belloni, L., Schinzari, V., Scisciani,

- C., Fanciulli, M., and Levrero, M. (2009). hSirT1-dependent regulation of the PCAF-E2F1-p73 apoptotic pathway in response to DNA damage. *Molecular and cellular biology* 29, 1989-1998.
- Pelletier, G., Stefanovsky, V.Y., Faubladiet, M., Hirschler-Laszkiewicz, I., Savard, J., Rothblum, L.I., Cote, J., and Moss, T. (2000). Competitive recruitment of CBP and Rb-HDAC regulates UBF acetylation and ribosomal transcription. *Mol Cell* 6, 1059-1066.
- Pfluger, P.T., Herranz, D., Velasco-Miguel, S., Serrano, M., and Tschop, M.H. (2008). Sirt1 protects against high-fat diet-induced metabolic damage. *Proc Natl Acad Sci U S A* 105, 9793-9798.
- Picard, F., Kurtev, M., Chung, N., Topark-Ngarm, A., Senawong, T., Machado De Oliveira, R., Leid, M., McBurney, M.W., and Guarente, L. (2004). Sirt1 promotes fat mobilization in white adipocytes by repressing PPAR-gamma. *Nature* 429, 771-776.
- Preuss, S., and Pikaard, C.S. (2007). rRNA gene silencing and nucleolar dominance: insights into a chromosome-scale epigenetic on/off switch. *Biochimica et biophysica acta* 1769, 383-392.
- Princen, J.M., Mol-Backx, G.P., and Yap, S.H. (1983). Restoration effects of glucose refeeding on reduced synthesis of albumin and total protein and on disaggregated polyribosomes in liver of starved rats: evidence of a post-transcriptional control mechanism. *Annals of nutrition & metabolism* 27, 182-193.
- Prozorovski, T., Schulze-Topphoff, U., Glumm, R., Baumgart, J., Schroter, F., Ninnemann, O., Siegert, E., Bendix, I., Brustle, O., Nitsch, R., *et al.* (2008). Sirt1 contributes critically to the redox-dependent fate of neural progenitors. *Nat Cell Biol* 10, 385-394.
- Puigserver, P., and Spiegelman, B.M. (2003). Peroxisome proliferator-activated receptor-gamma coactivator 1 alpha (PGC-1 alpha): transcriptional coactivator and metabolic regulator. *Endocr Rev* 24, 78-90.
- Purushotham, A., Schug, T.T., Xu, Q., Surapureddi, S., Guo, X., and Li, X. (2009). Hepatocyte-specific deletion of SIRT1 alters fatty acid metabolism and results in hepatic steatosis and inflammation. *Cell metabolism* 9, 327-338.

- Qiang, L., Wang, L., Kon, N., Zhao, W., Lee, S., Zhang, Y., Rosenbaum, M., Zhao, Y., Gu, W., Farmer, S.R., *et al.* (2012). Brown remodeling of white adipose tissue by Sirt1-dependent deacetylation of Pparg. *Cell* 150, 620-632.
- Qiu, Y., Zhao, Y., Becker, M., John, S., Parekh, B.S., Huang, S., Hendarwanto, A., Martinez, E.D., Chen, Y., Lu, H., *et al.* (2006). HDAC1 acetylation is linked to progressive modulation of steroid receptor-induced gene transcription. *Mol Cell* 22, 669-679.
- Rajamohan, S.B., Pillai, V.B., Gupta, M., Sundaresan, N.R., Birukov, K.G., Samant, S., Hottiger, M.O., and Gupta, M.P. (2009). SIRT1 promotes cell survival under stress by deacetylation-dependent deactivation of poly(ADP-ribose) polymerase 1. *Molecular and cellular biology* 29, 4116-4129.
- Rathbone, C.R., Booth, F.W., and Lees, S.J. (2009). Sirt1 increases skeletal muscle precursor cell proliferation. *Eur J Cell Biol* 88, 35-44.
- Rea, S., Eisenhaber, F., O'Carroll, D., Strahl, B.D., Sun, Z.W., Schmid, M., Opravil, S., Mechtler, K., Ponting, C.P., Allis, C.D., *et al.* (2000). Regulation of chromatin structure by site-specific histone H3 methyltransferases. *Nature* 406, 593-599.
- Ren, D., Collingwood, T.N., Rebar, E.J., Wolffe, A.P., and Camp, H.S. (2002). PPARgamma knockdown by engineered transcription factors: exogenous PPARgamma2 but not PPARgamma1 reactivates adipogenesis. *Genes Dev* 16, 27-32.
- Rine, J., Strathern, J.N., Hicks, J.B., and Herskowitz, I. (1979). A suppressor of mating-type locus mutations in *Saccharomyces cerevisiae*: evidence for and identification of cryptic mating-type loci. *Genetics* 93, 877-901.
- Rodeheffer, M.S., Birsoy, K., and Friedman, J.M. (2008). Identification of white adipocyte progenitor cells in vivo. *Cell* 135, 240-249.
- Rodgers, J.T., Lerin, C., Gerhart-Hines, Z., and Puigserver, P. (2008). Metabolic adaptations through the PGC-1 alpha and SIRT1 pathways. *FEBS Lett* 582, 46-53.
- Rodgers, J.T., Lerin, C., Haas, W., Gygi, S.P., Spiegelman, B.M., and Puigserver, P. (2005). Nutrient control of glucose homeostasis through a complex of PGC-1alpha and SIRT1. *Nature* 434, 113-118.
- Rodgers, J.T., and Puigserver, P. (2007). Fasting-dependent glucose and lipid metabolic

- response through hepatic sirtuin 1. *Proc Natl Acad Sci U S A* *104*, 12861-12866.
- Rogina, B., and Helfand, S.L. (2004). Sir2 mediates longevity in the fly through a pathway related to calorie restriction. *Proc Natl Acad Sci U S A* *101*, 15998-16003.
- Rondinone, C.M. (2006). Adipocyte-derived hormones, cytokines, and mediators. *Endocrine* *29*, 81-90.
- Rosen, E.D., Hsu, C.H., Wang, X., Sakai, S., Freeman, M.W., Gonzalez, F.J., and Spiegelman, B.M. (2002). C/EBPalpha induces adipogenesis through PPARgamma: a unified pathway. *Genes Dev* *16*, 22-26.
- Rosen, E.D., and MacDougald, O.A. (2006). Adipocyte differentiation from the inside out. *Nature reviews* *7*, 885-896.
- Rudra, D., and Warner, J.R. (2004). What better measure than ribosome synthesis? *Genes Dev* *18*, 2431-2436.
- Russell, J., and Zomerdijk, J.C. (2005). RNA-polymerase-I-directed rDNA transcription, life and works. *Trends in biochemical sciences* *30*, 87-96.
- Saiki, R.K., Gelfand, D.H., Stoffel, S., Scharf, S.J., Higuchi, R., Horn, G.T., Mullis, K.B., and Erlich, H.A. (1988). Primer-directed enzymatic amplification of DNA with a thermostable DNA polymerase. *Science* *239*, 487-491.
- Salminen, A., and Kaarniranta, K. (2009). SIRT1 regulates the ribosomal DNA locus: epigenetic candles twinkle longevity in the Christmas tree. *Biochem Biophys Res Commun* *378*, 6-9.
- Santos-Rosa, H., Valls, E., Kouzarides, T., and Martinez-Balbas, M. (2003). Mechanisms of P/CAF auto-acetylation. *Nucleic Acids Res* *31*, 4285-4292.
- Sasaki, T., Maier, B., Koclega, K.D., Chruszcz, M., Gluba, W., Stukenberg, P.T., Minor, W., and Scrable, H. (2008). Phosphorylation regulates SIRT1 function. *PLoS One* *3*, e4020.
- Sauve, A.A. (2010). Sirtuin chemical mechanisms. *Biochimica et biophysica acta* *1804*, 1591-1603.
- Schiltz, R.L., Mizzen, C.A., Vassilev, A., Cook, R.G., Allis, C.D., and Nakatani, Y. (1999). Overlapping but distinct patterns of histone acetylation by the human coactivators p300 and PCAF within nucleosomal substrates. *J Biol Chem* *274*,

1189-1192.

Sebastian, C., Zwaans, B.M., Silberman, D.M., Gymrek, M., Goren, A., Zhong, L., Ram, O., Truelove, J., Guimaraes, A.R., Toiber, D., *et al.* (2012). The histone deacetylase SIRT6 is a tumor suppressor that controls cancer metabolism. *Cell* *151*, 1185-1199.

Seglen, P.O. (1976). Preparation of isolated rat liver cells. *Methods in cell biology* *13*, 29-83.

Senawong, T., Peterson, V.J., and Leid, M. (2005). BCL11A-dependent recruitment of SIRT1 to a promoter template in mammalian cells results in histone deacetylation and transcriptional repression. *Arch Biochem Biophys* *434*, 316-325.

Seo, J., and Lee, K.J. (2004). Post-translational modifications and their biological functions: proteomic analysis and systematic approaches. *Journal of biochemistry and molecular biology* *37*, 35-44.

Shi, T., Wang, F., Stieren, E., and Tong, Q. (2005). SIRT3, a mitochondrial sirtuin deacetylase, regulates mitochondrial function and thermogenesis in brown adipocytes. *J Biol Chem* *280*, 13560-13567.

Sidransky, H., and Verney, E. (1971). Studies on hepatic polyribosomes and protein synthesis in rats force-fed a protein-free diet. *J Nutr* *101*, 1153-1164.

Sinclair, D.A., and Guarente, L. (1997). Extrachromosomal rDNA circles--a cause of aging in yeast. *Cell* *91*, 1033-1042.

Sirri, V., Roussel, P., and Hernandez-Verdun, D. (1999). The mitotically phosphorylated form of the transcription termination factor TTF-1 is associated with the repressed rDNA transcription machinery. *Journal of cell science* *112* ( Pt 19), 3259-3268.

Smith, J.S., Brachmann, C.B., Celic, I., Kenna, M.A., Muhammad, S., Starai, V.J., Avalos, J.L., Escalante-Semerena, J.C., Grubmeyer, C., Wolberger, C., *et al.* (2000). A phylogenetically conserved NAD<sup>+</sup>-dependent protein deacetylase activity in the Sir2 protein family. *Proc Natl Acad Sci U S A* *97*, 6658-6663.

Spiegelman, B.M., and Flier, J.S. (2001). Obesity and the regulation of energy balance. *Cell* *104*, 531-543.

Suh, S.H., Paik, I.Y., and Jacobs, K. (2007). Regulation of blood glucose homeostasis

- during prolonged exercise. *Molecules and cells* 23, 272-279.
- Tang, Q.Q., and Lane, M.D. (1999). Activation and centromeric localization of CCAAT/enhancer-binding proteins during the mitotic clonal expansion of adipocyte differentiation. *Genes Dev* 13, 2231-2241.
- Tang, Q.Q., Otto, T.C., and Lane, M.D. (2004). Commitment of C3H10T1/2 pluripotent stem cells to the adipocyte lineage. *Proc Natl Acad Sci U S A* 101, 9607-9611.
- Tang, W., Zeve, D., Suh, J.M., Bosnakovski, D., Kyba, M., Hammer, R.E., Tallquist, M.D., and Graff, J.M. (2008). White fat progenitor cells reside in the adipose vasculature. *Science* 322, 583-586.
- Tanno, M., Sakamoto, J., Miura, T., Shimamoto, K., and Horio, Y. (2007). Nucleocytoplasmic shuttling of the NAD<sup>+</sup>-dependent histone deacetylase SIRT1. *J Biol Chem* 282, 6823-6832.
- Thompson, P.R., Wang, D., Wang, L., Fulco, M., Pediconi, N., Zhang, D., An, W., Ge, Q., Roeder, R.G., Wong, J., *et al.* (2004). Regulation of the p300 HAT domain via a novel activation loop. *Nature structural & molecular biology* 11, 308-315.
- Tissenbaum, H.A., and Guarente, L. (2001). Increased dosage of a sir-2 gene extends lifespan in *Caenorhabditis elegans*. *Nature* 410, 227-230.
- Tontonoz, P., and Spiegelman, B.M. (2008). Fat and beyond: the diverse biology of PPARgamma. *Annual review of biochemistry* 77, 289-312.
- Tsang, A.W., and Escalante-Semerena, J.C. (1998). CobB, a new member of the SIR2 family of eucaryotic regulatory proteins, is required to compensate for the lack of nicotinate mononucleotide:5,6-dimethylbenzimidazole phosphoribosyltransferase activity in cobT mutants during cobalamin biosynthesis in *Salmonella typhimurium* LT2. *J Biol Chem* 273, 31788-31794.
- Tseng, P.C., Hou, S.M., Chen, R.J., Peng, H.W., Hsieh, C.F., Kuo, M.L., and Yen, M.L. (2011). Resveratrol promotes osteogenesis of human mesenchymal stem cells by upregulating RUNX2 gene expression via the SIRT1/FOXO3A axis. *J Bone Miner Res* 26, 2552-2563.
- Vakhrusheva, O., Braeuer, D., Liu, Z., Braun, T., and Bober, E. (2008a). Sirt7-dependent inhibition of cell growth and proliferation might be instrumental to

- mediate tissue integrity during aging. *J Physiol Pharmacol* 59 *Suppl* 9, 201-212.
- Vakhrusheva, O., Smolka, C., Gajawada, P., Kostin, S., Boettger, T., Kubin, T., Braun, T., and Bober, E. (2008b). Sirt7 increases stress resistance of cardiomyocytes and prevents apoptosis and inflammatory cardiomyopathy in mice. *Circ Res* 102, 703-710.
- Vakoc, C.R., Sachdeva, M.M., Wang, H., and Blobel, G.A. (2006). Profile of histone lysine methylation across transcribed mammalian chromatin. *Mol Cell Biol* 26, 9185-9195.
- Van Gool, F., Galli, M., Gueydan, C., Kruys, V., Prevot, P.P., Bedalov, A., Mostoslavsky, R., Alt, F.W., De Smedt, T., and Leo, O. (2009). Intracellular NAD levels regulate tumor necrosis factor protein synthesis in a sirtuin-dependent manner. *Nat Med* 15, 206-210.
- Vaquero, A., Scher, M., Erdjument-Bromage, H., Tempst, P., Serrano, L., and Reinberg, D. (2007). SIRT1 regulates the histone methyl-transferase SUV39H1 during heterochromatin formation. *Nature* 450, 440-444.
- Vaquero, A., Scher, M., Lee, D., Erdjument-Bromage, H., Tempst, P., and Reinberg, D. (2004). Human SirT1 interacts with histone H1 and promotes formation of facultative heterochromatin. *Mol Cell* 16, 93-105.
- Vaziri, H., Dessain, S.K., Ng Eaton, E., Imai, S.I., Frye, R.A., Pandita, T.K., Guarente, L., and Weinberg, R.A. (2001). hSIR2(SIRT1) functions as an NAD-dependent p53 deacetylase. *Cell* 107, 149-159.
- Vidal-Puig, A., Jimenez-Linan, M., Lowell, B.B., Hamann, A., Hu, E., Spiegelman, B., Flier, J.S., and Moller, D.E. (1996). Regulation of PPAR gamma gene expression by nutrition and obesity in rodents. *The Journal of clinical investigation* 97, 2553-2561.
- Voelter-Mahlknecht, S., Letzel, S., and Mahlknecht, U. (2006). Fluorescence in situ hybridization and chromosomal organization of the human Sirtuin 7 gene. *Int J Oncol* 28, 899-908.
- Walker, A.K., Yang, F., Jiang, K., Ji, J.Y., Watts, J.L., Purushotham, A., Boss, O., Hirsch, M.L., Ribich, S., Smith, J.J., *et al.* (2010). Conserved role of SIRT1 orthologs in fasting-dependent inhibition of the lipid/cholesterol regulator SREBP. *Genes Dev* 24, 1403-1417.

- Wang, C., Chen, L., Hou, X., Li, Z., Kabra, N., Ma, Y., Nemoto, S., Finkel, T., Gu, W., Cress, W.D., *et al.* (2006). Interactions between E2F1 and SirT1 regulate apoptotic response to DNA damage. *Nature cell biology* 8, 1025-1031.
- Wang, F., and Tong, Q. (2009). SIRT2 suppresses adipocyte differentiation by deacetylating FOXO1 and enhancing FOXO1's repressive interaction with PPARgamma. *Mol Biol Cell* 20, 801-808.
- Wang, H., Huang, Z.Q., Xia, L., Feng, Q., Erdjument-Bromage, H., Strahl, B.D., Briggs, S.D., Allis, C.D., Wong, J., Tempst, P., *et al.* (2001). Methylation of histone H4 at arginine 3 facilitating transcriptional activation by nuclear hormone receptor. *Science* 293, 853-857.
- Wang, J., and Chen, J. (2010). SIRT1 regulates autoacetylation and histone acetyltransferase activity of TIP60. *J Biol Chem* 285, 11458-11464.
- Wang, R.H., Li, C., and Deng, C.X. (2010). Liver steatosis and increased ChREBP expression in mice carrying a liver specific SIRT1 null mutation under a normal feeding condition. *International journal of biological sciences* 6, 682-690.
- Wang, R.H., Sengupta, K., Li, C., Kim, H.S., Cao, L., Xiao, C., Kim, S., Xu, X., Zheng, Y., Chilton, B., *et al.* (2008). Impaired DNA damage response, genome instability, and tumorigenesis in SIRT1 mutant mice. *Cancer Cell* 14, 312-323.
- Wang, W., Huang, L., Huang, Y., Yin, J.W., Berk, A.J., Friedman, J.M., and Wang, G. (2009). Mediator MED23 links insulin signaling to the adipogenesis transcription cascade. *Dev Cell* 16, 764-771.
- Westerheide, S.D., Anckar, J., Stevens, S.M., Jr., Sistonen, L., and Morimoto, R.I. (2009). Stress-inducible regulation of heat shock factor 1 by the deacetylase SIRT1. *Science (New York, N.Y)* 323, 1063-1066.
- Winzell, M.S., and Ahren, B. (2004). The high-fat diet-fed mouse: a model for studying mechanisms and treatment of impaired glucose tolerance and type 2 diabetes. *Diabetes* 53 Suppl 3, S215-219.
- Wong, S., and Weber, J.D. (2007). Deacetylation of the retinoblastoma tumour suppressor protein by SIRT1. *Biochem J* 407, 451-460.
- Woodhouse, R. (2008). Obesity in art: a brief overview. *Frontiers of hormone research*

36, 271-286.

Wu, Z., Rosen, E.D., Brun, R., Hauser, S., Adelmant, G., Troy, A.E., McKeon, C., Darlington, G.J., and Spiegelman, B.M. (1999). Cross-regulation of C/EBP alpha and PPAR gamma controls the transcriptional pathway of adipogenesis and insulin sensitivity. *Mol Cell* 3, 151-158.

Xiao, C., Kim, H.S., Lahusen, T., Wang, R.H., Xu, X., Gavrilova, O., Jou, W., Gius, D., and Deng, C.X. (2010). SIRT6 deficiency results in severe hypoglycemia by enhancing both basal and insulin-stimulated glucose uptake in mice. *J Biol Chem* 285, 36776-36784.

Yang, B., Zwaans, B.M., Eckersdorff, M., and Lombard, D.B. (2009). The sirtuin SIRT6 deacetylates H3 K56Ac in vivo to promote genomic stability. *Cell Cycle* 8, 2662-2663.

Yang, Y., Fu, W., Chen, J., Olashaw, N., Zhang, X., Nicosia, S.V., Bhalla, K., and Bai, W. (2007). SIRT1 sumoylation regulates its deacetylase activity and cellular response to genotoxic stress. *Nat Cell Biol* 9, 1253-1262.

Yeung, F., Hoberg, J.E., Ramsey, C.S., Keller, M.D., Jones, D.R., Frye, R.A., and Mayo, M.W. (2004). Modulation of NF-kappaB-dependent transcription and cell survival by the SIRT1 deacetylase. *EMBO J* 23, 2369-2380.

Yoo, E.J., Chung, J.J., Choe, S.S., Kim, K.H., and Kim, J.B. (2006). Down-regulation of histone deacetylases stimulates adipocyte differentiation. *J Biol Chem* 281, 6608-6615.

Yoshizaki, T., Milne, J.C., Imamura, T., Schenk, S., Sonoda, N., Babendure, J.L., Lu, J.C., Smith, J.J., Jirousek, M.R., and Olefsky, J.M. (2009). SIRT1 exerts anti-inflammatory effects and improves insulin sensitivity in adipocytes. *Molecular and cellular biology* 29, 1363-1374.

You, M., Liang, X., Ajmo, J.M., and Ness, G.C. (2008). Involvement of mammalian sirtuin 1 in the action of ethanol in the liver. *Am J Physiol Gastrointest Liver Physiol* 294, G892-898.

Zakim, D., and Boyer, T.D. (2003). *Hepatology : a textbook of liver disease*, 4th edn (Philadelphia: Saunders).

- Zhang, J., Fu, M., Cui, T., Xiong, C., Xu, K., Zhong, W., Xiao, Y., Floyd, D., Liang, J., Li, E., *et al.* (2004). Selective disruption of PPARgamma 2 impairs the development of adipose tissue and insulin sensitivity. *Proc Natl Acad Sci U S A* *101*, 10703-10708.
- Zhang, Y., Wang, J., Chen, G., Fan, D., and Deng, M. (2011). Inhibition of Sirt1 promotes neural progenitors toward motoneuron differentiation from human embryonic stem cells. *Biochem Biophys Res Commun* *404*, 610-614.
- Zhao, Y., Takeyama, K., Sawatsubashi, S., Ito, S., Suzuki, E., Yamagata, K., Tanabe, M., Kimura, S., Fujiyama, S., Ueda, T., *et al.* (2009). Corepressive action of CBP on androgen receptor transactivation in pericentric heterochromatin in a *Drosophila* experimental model system. *Molecular and cellular biology* *29*, 1017-1034.
- Zhong, L., D'Urso, A., Toiber, D., Sebastian, C., Henry, R.E., Vadysirisack, D.D., Guimaraes, A., Marinelli, B., Wikstrom, J.D., Nir, T., *et al.* (2010). The histone deacetylase Sirt6 regulates glucose homeostasis via Hif1alpha. *Cell* *140*, 280-293.
- Zhou, X.Y., Shibusawa, N., Naik, K., Porras, D., Temple, K., Ou, H., Kaihara, K., Roe, M.W., Brady, M.J., and Wondisford, F.E. (2004). Insulin regulation of hepatic gluconeogenesis through phosphorylation of CREB-binding protein. *Nat Med* *10*, 633-637.

## 10. Erklärung zur Dissertation

„Hiermit erkläre ich, dass ich die vorliegende Arbeit selbständig und ohne unzulässige Hilfe oder Benutzung anderer als der angegebenen Hilfsmittel angefertigt habe. Alle Textstellen, die wörtlich oder sinngemäß aus veröffentlichten oder nichtveröffentlichten Schriften entnommen sind, und alle Angaben, die auf mündlichen Auskünften beruhen, sind als solche kenntlich gemacht. Bei den von mir durchgeführten und in der Dissertation erwähnten Untersuchungen habe ich die Grundsätze guter wissenschaftlicher Praxis, wie sie in der „Satzung der Justus-Liebig-Universität Gießen zur Sicherung guter wissenschaftlicher Praxis“ niedergelegt sind, eingehalten sowie ethische, datenschutzrechtliche und tierschutzrechtliche Grundsätze befolgt. Ich versichere, dass Dritte von mir weder unmittelbar noch mittelbar geldwerte Leistungen für Arbeiten erhalten haben, die im Zusammenhang mit dem Inhalt der vorgelegten Dissertation stehen, oder habe diese nachstehend spezifiziert. Die vorgelegte Arbeit wurde weder im Inland noch im Ausland in gleicher oder ähnlicher Form einer anderen Prüfungsbehörde zum Zweck einer Promotion oder eines anderen Prüfungsverfahrens vorgelegt. Alles aus anderen Quellen und von anderen Personen übernommene Material, das in der Arbeit verwendet wurde oder auf das direkt Bezug genommen wird, wurde als solches kenntlich gemacht. Insbesondere wurden alle Personen genannt, die direkt und indirekt an der Entstehung der vorliegenden Arbeit beteiligt waren. Mit der Überprüfung meiner Arbeit durch eine Plagiatserkennungssoftware bzw. ein internetbasiertes Softwareprogramm erkläre ich mich einverstanden.“

---

Ort, Datum

---

Unterschrift

## 11. Acknowledgements

My thesis could not have been accomplished without the support of many people. It is a pleasure to express my gratitude to them in my sincere acknowledgments.

First of all, I would like to thank Prof. Dr. Dr. Thomas Braun for providing me the opportunity to do the long-term research and pursue my doctor degree in his laboratory, I am also grateful for his strong scientific guidance throughout my project. His excellent knowledge, truly scientific attitude, invaluable suggestions and continuous support impressed me deeply and enabled me to develop a good understanding and performing of my project.

I am most grateful to my supervisor, Prof. Dr. Eva Bober, for guiding me these years. She was always a friend and a guide, provided me constant support, guidance, encouragement, and advice whenever I needed any help during my study. I am also indebted to her great patience and many useful suggestions while tutoring my scientific writing and reviewing my thesis. Her dedication to science and her pursuit of perfection will always inspire me to grow further not only in my scientific career but also my whole life in the future.

I sincerely thank Olesya Vakhrusheva for providing me the interesting Sirt7 KO mouse model and the initial technical guidance at the beginning of my study in our group. I would like to express my appreciation to Dr. Marcus Krüger and his group for performing and analyzing the *in vitro* deacetylation assays and mass spectrometry assay. I am also thankful to Dr. Johnny Kim for providing the constructs of Sirt7 shRNA, to Susanne, Marion, Moni, and Katja K for their technical assistance in my many experiments. In addition, I owe my gratitude to Dr. Yonggang Zhou and Dr. Xuejun Yuan, not only for providing some important plasmids and other materials, but also for sharing their valuable experimental experiences, precious advices and insightful discussions.

It is my great fortune to work in such a wonderful “Sirtuin group”. I would like to thank my lab mates-Christian, Alessandro, Danni, Sahar and Moni for their useful help, scientific discussions and fun. Their great companionship and selfless support

have made my research years more enjoyable and memorable! Especially, I would like to extend my gratitude to Christian for his time, patience and advice in proofreading my thesis. Additionally, I would like to appreciate the caretakers of the animal facility and thank them for their carefully breeding and caring for my mice.

I am also thankful to all the PhD students in the PhD office for their help in my work-related issues and the nice atmosphere in the office. I appreciate all my Chinese friends in Bad Nauheim, they made my life full of fun and activity beyond my studies and research work. With their kind help, I feel like it was a home in this beautiful city away from my home.

Finally, my most sincere acknowledgement goes to my parents for their enormous support, endless love, genuine understanding and constant encouragement through these years. I dedicate this dissertation to them.

**Der Lebenslauf wurde aus der elektronischen  
Version der Arbeit entfernt.**

**The curriculum vitae was removed from the  
electronic version of the paper.**